FINAL REPORT

STUDY OF EHF CONTROLLED-BEAM ANTENNAS FOR SATCOM

By: J.L. Yen, Department of Electrical Engineering
University of Toronto, Toronto M5S 1A4

For: Department of Communications, Ottawa, Ont.

Under: Department of Supplies and Services
Contract Serial No. OSU81-00336

Period: Covering up to May 31, 1982

(2)

STUDY OF EHF CONTROLLED-BEAM ANTENNAS FOR SATCOM

Final Report, May 31, 1982.

Principal Investigator: J.L. Yen (1)
Department of Electrical Engineering
University of Toronto

Submitted to: Department of Communications
Ottawa, Ontario.

Under DSS Contract OSU81-00336
For period ending May 31, 1982.

SUMMARY

A survey of three common classes of antennas namely, lens, reflector and microstrip array and a fourth, the less common reflector array for SATCOM at EHF is given. The optics and feeds for steerable multi-beam and phased-array antennas are discussed. A basic relation between antenna gain, size and scan angle or field of view is derived. Adaptive null steering for interference rejection is reviewed. The influence of antenna configuration on beam control performance is noted. An experimental study of an IF adaptive beam controller was undertaken. Advantages and disadvantages of IF analog implementation of beam control are discussed. Circuit components required for beam steering and control are also reviewed.

The conceptual designs of a microstrip phased array for the ground segment and a controlled-beam reflector antenna system with hybrid steering are presented to illustrate the influence of the major issues. Finally, recommendations on promising technologies for further investigation and development are identified.

STUDY OF EHF CONTROLLED-BEAM ANTENNAS FOR SATCOM.

Table of Contents

Chapter 1

INTRODUCTION

SATCOM systems operating at EHF are being vigorously developed in many countries for next generation implementation because of frequency and satellite congestion at lower frequencies and because of the larger bandwidths available. The higher frequency allows the use of smaller and lighter weight antennas to achieve a given communication objectives. It also means lower power is available for jamming because of physical limitations of electron devices. The increased bandwidth offers greater anti-jam protection and lower probability of intercept. However, at the present time concepts on complex and versatile systems fully exploiting these advantages are not well understood. In addition, device and component technologies for EHF are as yet inadequately developed for implementation of such advanced systems. The objectives of this Contract are to survey the current state of art on all aspects related to controlled-beam antennas for EHF SATCOM systems, and to identify in depth investigations necessary to arrive at realistic system specifications, overall design approaches and promising technologies for implementation.

Because of the many areas of technologies involved, the study is divided into two major parts in eight sections. The first half of the study deals with three major antenna classes, namely, lens, reflectors and microstrip array, as well as a fourth less common class the reflector array. The optics and feeds for steerable multi-beam and phased-array antennas are discussed for each class when applicable. A basic relation between antenna gain, size and scan angle or field of view is derived. Considerations on suitability of each class for the space and ground segments are given. The second part of the study is devoted to the concept and capabilities of beam control and its implementation. Adaptive null steering for interference rejection is reviewed. The influence of antenna configuration on beam control is noted. Advantages and disadvantages of IF analog beam control are studied in experiments and stringent requirements on device performance are noted. Devices and circuits required for phase and amplitude control are then reviewed. Lack of developments in EHF devices and circuit technology are found. Two sample designs are given, a ground segment microstrip array and a space segment controlled-beam reflector antenna system with hybrid steering. The Report concludes with recommendations of promising technologies for further investigation.

Each Section of the Final Report is prepared by a co-investigator as listed in the Table of Contents.

Chapter 2

EHF LENS ANTENNAS.

K.G. Balmain

1.

Review Material Available on Microwave Lenses.

The subject of lens optics for visible light comprises a very large body of useful reference material, the best example being the book by Born and Wolf [1]. A number of books contain extensive material specifically related to microwave lens antennas: they are by Silver [2], Brown [3], Jasik [4], Hansen [5], Collin and Zucker [6], Cornbleet [7], and Button and Wiltse [8]. In addition there is a brief review paper by Kay [9], and lenses are included in the review paper by Ricardi [10]. In the present report the emphasis is placed on large-aperture lenses for use on synchronous-orbit satellites.

2.

Comparison Between Lenses and Paraboloidal Reflectors.

Lenses have the advantages of no feed blockage and reduced sensitivity to mechanical inaccuracy. Lenses have two surfaces plus the medium between the surfaces, or in other words they have three major degrees of freedom for design compared to the one surface-shape factor for a reflector. These extra degrees of freedom permit lens designs to be optimized for special purposes such as beam scanning, by means of the imposition of appropriate constraints. One example of such a constraint is the 'Abbe sine condition' which for incident rays parallel to the axis can be stated as:

$$\frac{h}{\sin\theta} = f$$

where h is the distance of a ray from the axis, θ is the angle a focal ray makes with the axis, and f is a constant. In other words, any such incident ray and the corresponding focal ray are constrained to intersect in the same circle of radius f. This condition ensures that all parallel rays entering a lens at a small angle to the axis come to a focus in the focal plane, a result having obvious relevance to beam scanning.

On the debit side, lenses tend to be complicated, costly and heavy. The lens medium is often frequency sensitive, resulting in narrow bandwidth. Furthermore, the efficiency can be low due to power absorption in the lens medium, due to reflections at both surfaces and due to radiation into grating lobes when the lens medium is a periodic structure. In addition, most lens designs (and printed-circuit antennas as well) involve exposed dielectric surfaces which could lead to energetic-electron and ion charge accumulation and arc discharging in synchronous orbit.

3.

Beam Requirements and Lens System Examples.

The coverage of a large circular area by multiple circular spot beams arranged in a close-packed hexagonal pattern has been discussed by Cummings, et al. [11]. If β_0 is the angle subtended by the large circular area and β is the angle subtended by the illuminated spot, and further if D_0 and D are the apertures required to produce beams of angular widths β_0 and β, then

$$D_0 \approx \lambda / \beta_0 \quad \text{and} \quad D \approx \lambda / \beta$$

(the exact relations depend on the field taper toward the aperture edge). If N is the number of beams arranged in the close-packed hexagonal pattern with one central beam, then

$$N=3M^2+3M+1 \quad \text{and} \quad D=(2M+1)D_0$$

where M is an integer. The numbers of beams available in this pattern are as follows for the allowed values of the index M:

M	$2M+1$	N
0	1	1
1	3	7
2	5	19
3	7	37
4	9	61
5	11	91
6	13	127
7	15	169
8	17	217

Consider for example 91 beams distributed over the earth's disc as viewed from a satellite in synchronous orbit, the disc subtending an angle $\beta_0=17.3$ ° at the satellite. The spot beam angle is therefore

$$\beta=\frac{\beta_0}{2M+1}=\frac{17.3}{11}=1.57\ ^\circ$$

At a frequency of 43.5 *GHz*, $\lambda = 6.90mm$ and the required aperture diameter is

$$D=\frac{\lambda}{\beta}=\frac{0.69}{1.57/57.3}=25.2 \text{ cm or } 36.5\lambda$$

The required scanning angle is slightly less than ±9 ° from boresight. This spot-beam pattern could be produced by a lens illuminated with an array of approximately one-wavelength aperture horns located in the focal plane and having the same arrangement as the desired beam pattern. Such a system is sketched in Figure 1.

A quite different approach would be to have a feed-horn array with an aperture distribution that is the Fourier transform of the desired spot beam. In optical terms this would involve producing a real image of the feed array well within the Fresnel region of the system. One way to accomplish this is to place a 'field lens' at the focus of the 'objective lens' as shown in Fig. 2. In Fig. 2, the region between the two lenses contains rays which are parallel, which means that, ideally, the two lenses may be separated by any distance, not just the distance F shown in the figure. The separation distance f + F (the confocal arrangement) has been mentioned by Ricardi [10] who notes that, for plane wave incidence on the field lens, the scanning angle of the emergent plane wave is reduced by the ratio of the focal lengths.

4.

Solid-Dielectric Lenses.

A useful example of solid-dielectric lens design is given by Mayhan and Simmons [12] for a 61 *GHz* non-scanned 76 cm diameter plano-convex lens made of Rexolite ($\epsilon_r=2.55$), with the plane surface facing a corrugated-horn feed giving approximately a -17 *dB* illumination taper. The lens had an F/D of 0.83 and produced a 1.33 ° beam, with first sidelobes at -30 *dB*. A comparison prime-focus-fed paraboloid produced a 1.40 ° beam, with first sidelobes at -28 *dB* and significantly worse sidelobe performance further from the main beam, probably due to aperture blockage by the feed horn and supports.

The scanned-beam analysis by Kreutel [13] of a hyperboloidal plano-convex lens with the convex side facing a dipole feed shows that the primary coma of the lens must always be worse than that for a similar-sized paraboloid reflector by a factor of the order of 4. The paper concludes that lenses of this type are best suited to apertures of 20λ to 40λ and maximum fields of view of ±4 to ±5 beamwidths. The EHF SATCOM antennas for use in space would probably be at or over the stated upper limits on both aperture and field of view.

A 'bifocal' variant of the solid-dielectric lens is described in the book by Hansen [5], having two off-axis focal points. The basic two-dimensional design was 'rotated' to produce a circularly symmetric lens and the lens contours were determined by computer. The designs had off-axis focal angles of ±20 °, diameter 50 λ (16" to 18") at λ = 8.6 mm and a feed taper of 11 *dB* in both planes. Over a ±20 ° scan the beamwidths increased less than 10 percent and sidelobes stayed below -19 *dB*, for F/D = 2. For F/D = 0.96, a scan of ±10 °was achieved.

Holt and Mayer [14] give a detailed ray-tracing procedure for designing a three-dimensional, two-point-corrected, zoned scanning lens. However, Cloutier and Bekefi [15] point out that a microwave aplanatic lens (corrected for spherical aberration and coma) can perform just as well as a two-point-corrected lens. Cheston and Shinn [16] review scanning aberrations and conclude that for two-dimensional scanning with a thin lens, the maximum scanning angle is limited by astigmatic aberrations. Ramsay [17] derives a universal curve giving the loss of gain in scanning: for example, he shows that for $D=100\lambda$ (1 ° beamwidth), F/D = 1 and scan angle of ±9 °, the loss of gain on scanning can be kept to 0.5 *dB*. For situations such as on an aircraft where entirely mechanical scanning can be tolerated, Rotman and Lee [18] have built a two-frequency 20/44 *GHz* plano-convex Rexolite lens antenna with gains of 27/34 *dBi*.

Lee [19] has recently designed a specially-contoured 44 *GHz* lens to produce a broad main beam (3 °) with fast roll-off and very low sidelobes (-32 *dB* measured). This lens performed poorly as a scanner, but zoning in order to approximately satisfy the Abbe sine condition solved the problem [J.J. Lee: personal communication].

A very promising zoned scanning-lens for use at 44.5 *GHz* has been designed theoretically by Rotman [20]. It has F/D = 1.5, $D=90\lambda=24"$, $n=1.59$, minimum thickness of 1/4" and weight less than 10 pounds. The predicted boresight gain is 48.5 *dB* (beamwidth = 0.73 °) for a -10 *dB* illumination taper, and the predicted first sidelobe level is -22 *dB*. Scanning performance over ±9 ° is predicted to be very good but experimental verification remains to be carried out.

5.

Artificial Dielectric Lenses.

Artificial dielectrics are made using volumetric or planar distributions of metallic spheres, discs, strips, wires, dipoles, dielectric spheres and voids [4]. The main advantage is weight reduction in physically large lenses. The same principle can be used to achieve surface matching with solid-dielectric lenses. Recent work with a single-layer dipole lens at 6.75 *GHz* [13] reports -20 *dB* sidelobes over a 5 percent bandwidth for a design with F/D = 0.8; however, the lens exhibited an aperture efficiency of 50 percent compared to 65 percent to 70 percent for an equivalent paraboloidal reflector, and it is clear that any such single-layer distribution of scatterers would produce backlobes with magnitudes comparable to the main beam.

6.

Luneburg and Geodesic Lenses.

Relatively recent work on Luneburg lenses and other radially inhomogeneous spherical solid-dielectric designs can be found in the papers by Webster [22], Kay [23], Mathis [24], Schrank [25], and Rozenfeld [26]. Some of the types discussed are illustrated in Figure 3. The single-shell-plus-core approximation to the Luneburg lens is dealt with in depth by Ap Rhys [27] who reports theoretical and experimental work at 70 *GHz* on a 16 λ diameter quartz-

polystyrene design (ϵ_r=3.80, 2.46). The gain is 31.2 *dB* with the first sidelobe at -28 *dB*, and a Teflon matching layer is expected to give an additional 1.1 *dB* of gain. A 32 λ diameter design is expected to give a gain of 37.7 *dB* with sidelobes at -24 *dB*, and an 80 λ diameter design is predicted to give a gain of 50.7 *dB* with -23 *dB* sidelobes. Essentially, these designs permit very wide angle scanning, but they would be much heavier than lenses having an optical axis.

Geodesic lenses make use of the path-length variation in the space between two saucer-shaped metal surfaces, as shown in Fig. 4 [28]. In a folded geometry this design has been implemented at EHF [8]. However, this device scans in one plane only and it cannot be adapted easily to the EHF SATCOM application.

7.

Bootlace Lenses.

Bootlace lenses (Gent lenses, Rotman lenses) scan in one plane only but like 2-dimensional metal plate lenses they embody an important design principle, namely that of perfect off-axis focusing at a finite number of points as a substitute for (and improvement on) the use of the Abbe sine condition; see Rotman and Turner [29], Kales and Brown [30], Shelton [31]. The concept is illustrated in Fig. 5.

8.

Waveguide Lenses.

Up to about 10 *GHz* a number of waveguide lens designs have been developed over the last decade. An X-band design intended for synchronous-orbit application was described by Dion and Ricardi [32], consisting of a 30" diameter zoned circular-waveguide array with F/D = 1.0 and fed by a 19-horn array. It provides earth coverage with 30 *dB* gain spot beams and sidelobes at -20 *dB*. It has a bandwith of 10 percent for a 0.5 *dB* gain reduction and a 3 *dB* half-power beamwidth. A subsequent analysis was carried out by Lu [33]. The above articles indicate that the lens approach was decided on after considering competing reflector and phased-array designs.

An X-band version of the Dion and Ricardi [32] stepped waveguide lens design was described by Scott, et al. [34]. The lens had one spherical surface centered on the feed and one ellipsoidal surface; it had a diameter of 46" and F/D = 1, with 1528 square waveguides arranged in a square grid. The feed comprised 61 horns arranged on a spherical surface. Single-horn excitation produced a 2 ° beam, scanned over ±9 °, with a -20 *dB* sidelobe level, and excitation of all 61 horns produced an 18 ° nominally flat-topped beam (3 *dB* peak-to-peak ripple).

The usual narrow bandwidth of waveguide lenses has been increased by constraining the ray paths to have equal group delay [Ajioka and Ramsey [35]; Dion [36]]. In the Ajioka and Ramsey work, a 46" diameter circularly-polarized lens fed with a 7-horn cluster was demonstrated to function over 7 to 9 *GHz* with a maximum gain of 36 *dB*, 2 ° beamwidth, -20 *dB* sidelobes and a ±10 °scan (9 beams across) with sidelobes rising to −16 *dB* at the scan limits. This design includes: a) a spherical inner surface to satisfy the Abbe sine condition, b) an ellipsoidal outer surface (making the lens thickest on-axis in contrast to other types of waveguide lens), and c) 'half-wave-plate' phase shifters inside the 1573 waveguide sections. The evolution of the group-delay concept is illustrated in Fig. 6.

A 110λ diameter (24"), 55 GHz lens has been described by Dion [37], the lens having been machined from commercially available aluminum 'honeycomb' stock. The design had F/D = 1.5 and produced a 0.7 ° beamwidth as shown in Fig. 7. Random irregularities in the cell width were believed to be responsible for the low efficiency of 18 percent and the irregular patterns. Zoning was proposed as a curative measure although the machining technique used would surely produce ragged zone edges.

9.

Liquid Artificial Dielectrics.

Buscher [38] has described waveguide measurements at 35 *GHz* and 96 *GHz* on Kerr-effect phase shifters employing suspensions of aluminum flakes in low-loss dielectric liquids such as n-Heptane and FC-75 Fluorocarbon (with a surfactant to stabilize the suspension against settling). With cells 10 free-space wavelengths long phase shifts up to 180 ° were attained when a transverse voltage was applied, with the shifts being about 1 ° to 2 ° per rms volt in the 100 volt range. Losses ranged from 1 to 5 *dB* over the cell. The concept requires more development but ultimately it is claimed to be promising for voltage-controlled EHF lenses. The experimental difficulties include toxicity and flammability of the liquids used.

10.

Electronic Lens Control.

A beam-steering lens antenna derived from radome concepts (hence called RADANT) has been described by Chekroun, et al. [39], Park [40], and Pauchard [41]. The lens is made up of layers of parallel wires in which series-connected diodes have been inserted, as shown in Fig. 8. The diodes are used either 'on' or 'off', thus creating two phase-shift states. The addition of continuous wires of different diameter (Fig. 9) introduces a sufficient number of adjustable parameters to permit reduction of reflections to zero for both phase-shift states (normal incidence only). Lenses of this type have been built for frequencies up to 15 *GHz*, but performance data is not available. The RADANT appears to be useful only for linear polarization.

Wang, et al. [42] have recently built lenses consisting of PIN diode-controlled slot arrays and PIN diode loaded spiral arrays which are similar in concept to the RADANT, as shown in Fig. 10. They have carried out measurements up to 15 *GHz* but have achieved only marginal agreement with moment-method theoretical calculations. They point out that the PIN diodes are expensive, have forward bias properties which vary from diode to diode and are subject to damage from electrical discharges.

11.

The Problem of Charge Accumulation and Arc Discharge.

The region of synchronous orbit is characterized by the presence of energetic electrons (tens to hundreds of *keV*), and furthermore the population of energetic electrons increases during periods of solar activity ("magnetic storm" periods). These electrons will penetrate into exposed dielectrics such as lenses, thus building up a subsurface layer of negative electric charge. The outer surface can become positively charged due to secondary emission and ion accumulation, thus creating a high-field region near the dielectric surface. Breakdown can occur, followed by propagation of the breakdown arc through the charged region and ejection of both molten material and electrons. The total current of ejected electrons from laboratory simulations of such discharge has ranged up to hundreds of amperes depending on the size of the charged region which is drained during discharge (for references see the December issues of IEEE Trans. Nucl. Sci., for 1976 through 1981.).

The problems caused by these discharges are clearly: 1) physical surface damage, 2) electrical interference, 3) damage to electronic components such as phase-shifter diodes which are integral parts of lenses or lens feeds, and 4) increased attenuation in lens material due to electron-beam-induced conductivity. The ultimate solution will probably be the use of coatings or of additions to produce enough surface or volume conductivity to drain off the accumulated charge. The state of the art is that such curative techniques are not yet fully developed. It is worth pointing out that potential spacecraft charging problems have to be assessed even if lenses are not used, because discharges on nearby exposed dielectrics such as thermal blankets may damage antenna phase shifter diodes. Furthermore, there is reason to believe that

penetrating radiation (fractional-megavolt electrons) may be intense enought to cause discharge damage in shielded components, especially under conditons of nuclear-enhanced radiation from the β-decay of radioactive debris.

12.

A Design Example.

The most promising multi-beam EHF lens design identified so far is that of Rotman [20], which has already been discussed. A sketch and computed patterns are shown in Fig. 11. Its specifications for operation at 44.5 *GHz* are: $D=90\lambda_0=24"$, F/D = 1.5, minimum lens thickness = 0.25", refractive index = 1.59, weight less than 10 pounds. For -10 *dB* edge illumination it exhibits a boresight gain of 48.5 *dB*, bandwidth of ± 1 *GHz* and minimum gain of 47.0 *dB* at edge of band and maximum scan (8.6 ° from boresight). If full electrical scan could not be implemented, then a tilting plane mirror could provide mechanical scanning (W. Rotman: personal communication).

For a multi-beam antenna generating one beam per feed horn, with the horns in a close-packed array, it is clear that the horn aperture diameter determines the minimum angular steps in the scanned beam direction. For good coverage, the angular scanning steps would be approximately equal to the -3 *dB* beamwidth, or in other words, the scanned beams would exhibit -3 *dB* crossovers. To review this, we make the following definitions:

α = scan angle (in degrees).

$\Delta\alpha$ = minimum scan angle step (in degrees) determined by feed horn aperture diameter.

d = feed horn aperture diameter.

D = lens diameter.

F = lens focal length.

λ = wavelength.

θ = angle subtended at focus by lens radius (in degrees).

ϕ = -3 *dB* beamwidth of lens radiation pattern (in degrees).

From the geometry it is clear that

$$\tan\Delta\alpha = d/F$$

and

$$\tan\theta = D/2\,F$$

or, approximately for small angles,

$$\frac{\Delta\alpha}{57.3} = \frac{d}{F} \quad \text{and} \quad \frac{\theta}{57.3} = \frac{D}{2F}$$

It is well known that the -3 *dB* beamwidth of the lens can be expressed as

$$\phi = k\lambda/D$$

where k is of the order of one radian, dependent on the aperture illumination. The design of Rotman [20] assumes a -10 *dB* lens edge illumination (-10 *dB* taper), for which Rotman's data gives k = 66.0 °. For the feed horn, consider a corrugated horn with a small flare angle. For a 5 ° half-angle, the design data of Chan [43] gives the following for -3 *dB* and -10 *dB* pattern half-angles:

$$\theta(-3dB) = 37.0\lambda/d \quad \text{and} \quad \theta(-10dB) = 66.6\lambda/d$$

The numerical constants 37.0 and 66.6 would be somewhat larger for larger flare angles.

For -10 *dB* edge illumination, the above formulas give the following, which is independent of wavelength:

$$\frac{\Delta\alpha}{\phi} = 2\times\frac{66.6}{66.0} = 2.02$$

For -3 *dB* edge illumination, the same procedure gives

$$\frac{\Delta\alpha}{\phi} = 2\times\frac{37.0}{66.0} = 1.12$$

which should be corrected to a slightly larger value if the constant 66.0 ° were replaced by some value closer to 57.3 ° which would be more appropriate for a -3 *dB* taper. In general the above formulas make it clear that even to approach a -3 *dB* crossover level for the scanned beams, a -3 *dB* lens edge illumination would have to be used with a consequent high level of spillover. With a -10 *dB* edge illumination the scanned beams would be separated by a centre-to-centre angle of more than two beamwidths. Thus, it is clear that electronic scanning coverage is limited by feed horn diameter. Furthermore this approximate analysis shows why the X-band multi-beam lens of Dion and Ricardi [32] ended up with an inevitable compromise design of -5.2 *dB* lens edge illumination and -4.5 *dB* scanned-beam crossover levels. One would have to either tolerate such a compromise or try to design a feed horn producing the same pattern but having a smaller aperture diameter.

Two-lens EHF systems of the phased-array type illustrated in Fig. 2 could also be designed. A detailed design would be required in order to evaluate scanning beam coverage and sidelobe levels. To date, no detailed discussions of such systems have been found in the literature, so no information on matters such as scanning aberrations is available. Obvious disadvantages of such systems are the increased weight and increased system length, both associated with the presence of the additional lens.

13.

Conclusions.

Zoned dielectric lenses perform well and are light enough to be feasible in single-frequency multi-beam EHF antennas. Feed horn aperture size limits electronic scanning coverage and could necessitate partial mechanical scanning in some situations.

Other lens antenna types require further study to establish feasibility. Of these, the phased-array type consisting of two zoned dielectric lenses is deserving of particular attention. The diode-loaded-wire lens designs may be feasible eventually at EHF, but extensive development is required to overcome the drawbacks which have been identified.

All EHF lens designs which are presently feasible or potentially feasible involve large amounts of dielectric material exposed to the energetic electrons and ions which populate the synchronous-orbit region. The threat of material damage and electromagnetic interference due to charge accumulation and resultant arc discharge on these materials needs to be assessed, under both natural and nuclear-enhanced radiation conditions, before space implementation can be recommended.

References.

1. M. Born, and E. Wolf, "Principles of Optics." Pergamon Press, Inc. 1964.
2. S. Silver, "Microwave Antenna Theory and Design." (Chapter 11 on Dielectric and Metal-Plate Lenses, by J.R. Risser). McGraw-Hill Book Co. Inc., 1949. (see also Dover Publications, Inc., 1965).
3. J. Brown, "Microwave Lenses." Mathuen & Co., Ltd., and John Wiley & Sons, Inc., 1953.
4. H. Jasik, "Antenna Engineering Handbook." (Chapter 14 on Lens-Type Radiators by S.B. Cohn, and Chapter 15 on Scanning Antennas by K.S. Kelleher). McGraw-Hill Book Co., Inc., 1961.
5. R.C. Hansen, "Microwave Scanning Antennas." Vol. 1, Academic Press, Inc., 1964.
6. R.E. Collin and F.J. Zucker, "Antenna Theory, Part 2." (Chapter 18 on Lens Antennas by J. Brown). McGraw-Hill Book Co., Inc., 1969.
7. S. Cornbleet, "Microwave Optics." Academic Press, Inc., 1976.
8. K.J. Button and J.C. Wiltse, "Infrared and Millimeter Waves, Volume 4: Millimeter Systems." Academic Press, Inc., 1981.
9. A.F. Kay, "Millimeter wave antennas." *Proc. IEEE*, Vol. 54, No. 4, pp. 641-647, 1966.
10. L.J. Ricardi, "Communication Satellite Antennas." *Proc. IEEE,* Vol. 65, No. 3, pp. 356-369, 1977.
11. W.C. Cummings, P.C. Jain and L.J. Ricardi, "Fundamental performance characteristics that influence EHF MILSATCOM systems." *IEEE Trans., Communications*, Vol. COM-27, No. 10, pp. 1423-1434, 1979.
12. J.T. Mayhan and A.J. Simmons, "A low-sidelobe Ka-band antenna-radome study." *IEEE Trans. Antennas Propagat.*, Vol. AP-23, No. 4, pp. 569-572, 1975.
13. R.W. Kreutel, "The hyperboloidal lens with laterally displaced dipole feed." *IEEE Trans. Antennas Propagat.*, Vol. AP-28, No. 4, pp. 443-450, 1980.
21. R, Milne, "Dipole array lens antenna." *Digest of IEEE AP-S, Inter. Symp.*, Vol. 2, pp. 576-579, 1980.
14. F.S. Holt and A. Mayer, "A Design Procedure for Dielectric Microwave Lenses of Large Aperture Ratio and Large Scanning Angle." *IRE Trans. Antennas Propagat.*, Vol. AP-5, pp. 25-30, January 1957.
15. G.G. Cloutier and G. Bekefi, "Scanning Characteristics of Microwave Aplanatic Lenses." *IRE Trans. Antennas Propagat.*, Vol. AP-5, pp. 391-396, October 1957.
16. T.C. Cheston and D.H. Shinn, "Scanning Aberrations of Radio Lenses." *Marconi Review*, Vol. 15, pp. 174-184, 1952.
17. J.F. Ramsay, "A Universal Scanning Curve for Wide Angle Mirrors and Lenses." *Marconi Review*, Vol. 19, pp. 150-159, 1956.
18. W. Rotman and J.C. Lee, "Dielectric Lens Antenna for EHF Airborne Satellite Communication Terminals." MIT Lincoln Laboratory Technical Report 592, 16 February 1982.

19. J.J. Lee, "A Dielectric Lens Shaped for a Generalized Taylor Distribution." *Digest of the 1982 IEEE International Symposium on Antennas and Propagation.*

20. W. Rotman, "EHF Dielectric Lens Antenna for Multiple-Beam MIL-SATCOM Applications." *Digest of the 1982 IEEE International Symposium on Antennas and Propagation.*

22. R.E. Webster, "Radiation patterns of a spherical Luneberg lens with simple feeds." *IRE Trans. Antennas Propagat.*, Vol. AP-6, No. 4, pp. 301-302, 1958.

23. A.F. Kay, "Spherically symmetric lenses." *IRE Trans. Antennas Propagat.*, Vol. AP-7, No. 1, pp. 32-38, 1959.

24. H.F. Mathis, "Checking design of stepped Luneberg lens." *IRE Trans. Antennas Propagat.*, Vol. AP-8, No. 3, pp. 342-343, 1960.

25. H.E. Schrank, "Graphical construction of rays in an ideal Luneburg lens." *IRE Trans. Antennas Propagat.*, Vol. AP-9, No. 4, pp. 410-411, 1961.

26. P. Rozenfeld, "The electromagnetic theory of three-dimensional inhomogeneous lenses." *IEEE Trans. Antennas Propagat.*, Vol. AP-24, No. 3, pp. 365-370, 1976.

27. T.L. Ap Rhys, "The design of radially symmetric lenses." *IEEE Trans. Antennas Propagat.*, Vol. AP-18, No. 4, pp. 497-506, 1970.

28. R.C. Rudduck, C.E. Ryan and C.H. Walter, "Beam elevation positioning in geodesic lenses." *IEEE Trans. Antennas Propagat.*, Vol. AP-12, No. 6, pp. 678-684, 1964.

29. W. Rotman and R.F. Turner, "Wide-angle microwave lens for line-source applications." *IEEE Trans. Antennas Propagat.*, Vol. AP-11, No. 6, pp. 623-632, 1963.

30. M.L. Kales and R.M. Brown, "Design considerations for two-dimensional symmetric bootlace lenses." *IEEE Trans. Antennas Propagat.*, Vol. AP-13, No. 4, pp. 521-528, 1965.

31. J.P. Shelton, "Focusing characteristics of symmetrically configured bootlace lenses." *IEEE Trans. Antennas Propagat.*, Vol. AP-26, No. 4, pp. 513-578, 1978.

32. A.R. Dion and L.J. Ricardi, "A variable-coverage satellite antenna system." *Proc. IEEE*, Vol. 59, No. 2, pp. 252-262, 1971.

33. H.S. Lu, "On computation of the radiation pattern of a zoned waveguide lens." *IEEE Trans. Antennas Propagat.*, Vol. AP-22, No. 3, pp. 483-484, 1974.

34. W.G. Scott, H.S. Luh, T.M. Smith and R.H. Grace, "Development of multiple-beam lens antennas." *Progress in Astronautics and Aeronautics*, Vol. 55, pp. 257-270, 1976.

35. J.S. Ajioka and V.W. Ramsey, "An equal group delay waveguide lens." *IEEE Trans. Antennas Propagat.*, Vol. AP-26, No. 4, pp. 419-527, 1978.

36. A.R. Dion, "A broadband compound waveguide lens." *IEEE Trans. Antennas Propagat.*, Vol. AP-26, No. 5, pp. 751-755, 1978.

37. A.R. Dion, "An investigation of a 110-wavelength EHF waveguide lens." *IEEE Trans. Antennas Propagat.*, Vol. AP-20, No. 4, pp. 493-496, 1972.

38. H.T. Buscher, "Electrically controllable liquid artifical dielectric media." *IEEE Trans. Microwave Theory Tech.*, Vol. MTT-27, No. 5, pp. 540-545, 1979.

39. C. Chekroun, D. Herrick, Y. Michel, R. Pauchard, P. Vidal, "RADANT: New method of electronic scanning." *Microwave Journal*, pp. 45-53 (February), 1981.

40. R.H. Park, "RADANT Lens: Alternative to expensive phased arrays." *Microwave Journal*, pp. 101-105 (September), 1981.

41. R. Pauchard, "Rayonnement d'une grille plane de fils continus et discontinus." *Annales des Telecommunications*, Vol. 35, No. 9-10, pp. 303-312, 1980.

42. J.J.H. Wang, D.R. Blount, C.E. Ryan, Jr. and R.J. Puskar, "Diode-Switched Reflectors and Lenses." *Digest of the 1982 IEEE International Symposium on Antenna and Propagation.*

43. K.B. Chan, "Design Handbook for Conical Corrugated Horns." Report KBC/72/6, Department of Electrical Engineering, Queen Mary College, University of London, August 1972.

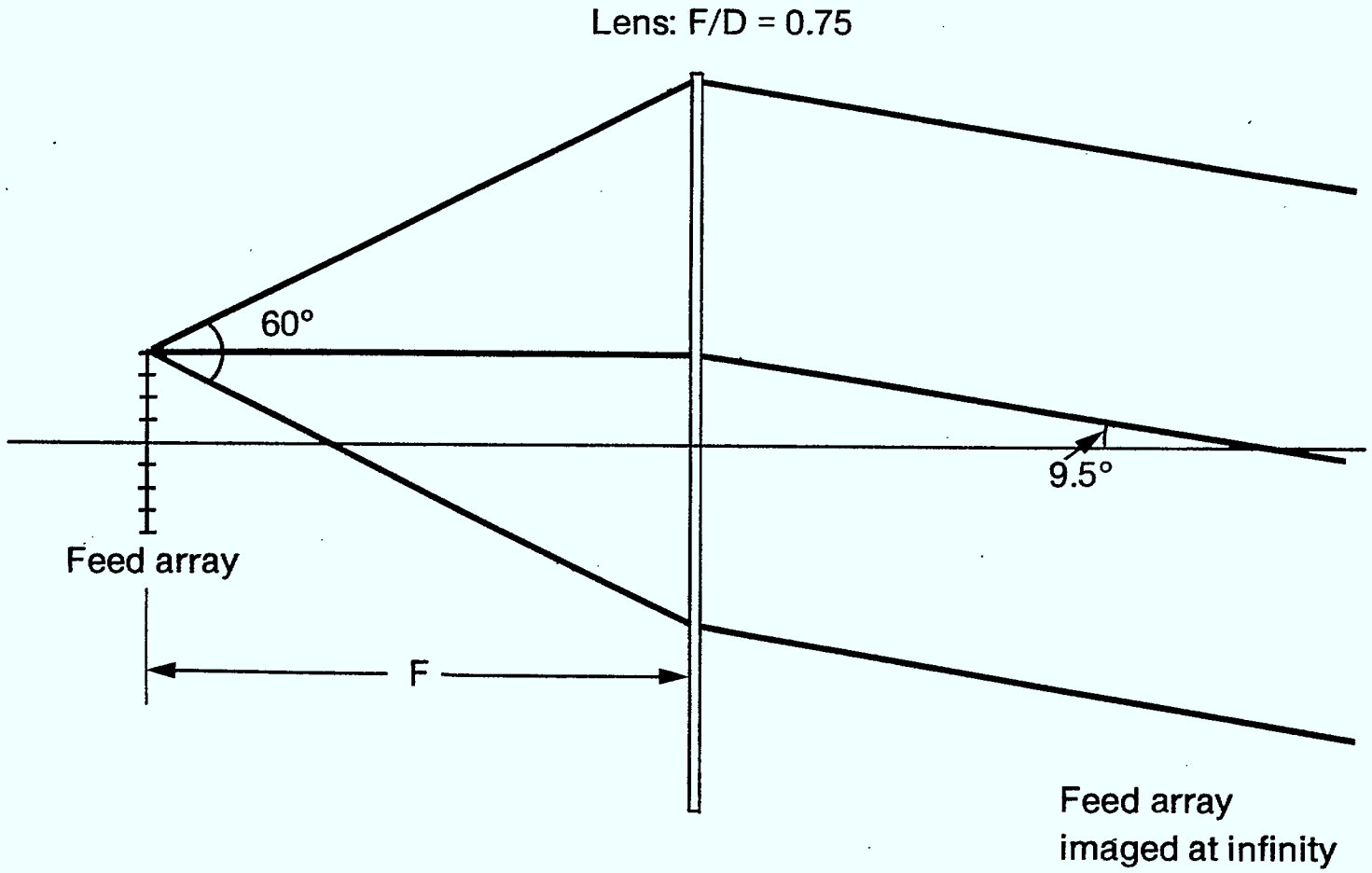

Fig. 1 Basic single-lens scanning arrangement with feed array located in the focal plane of the lens.

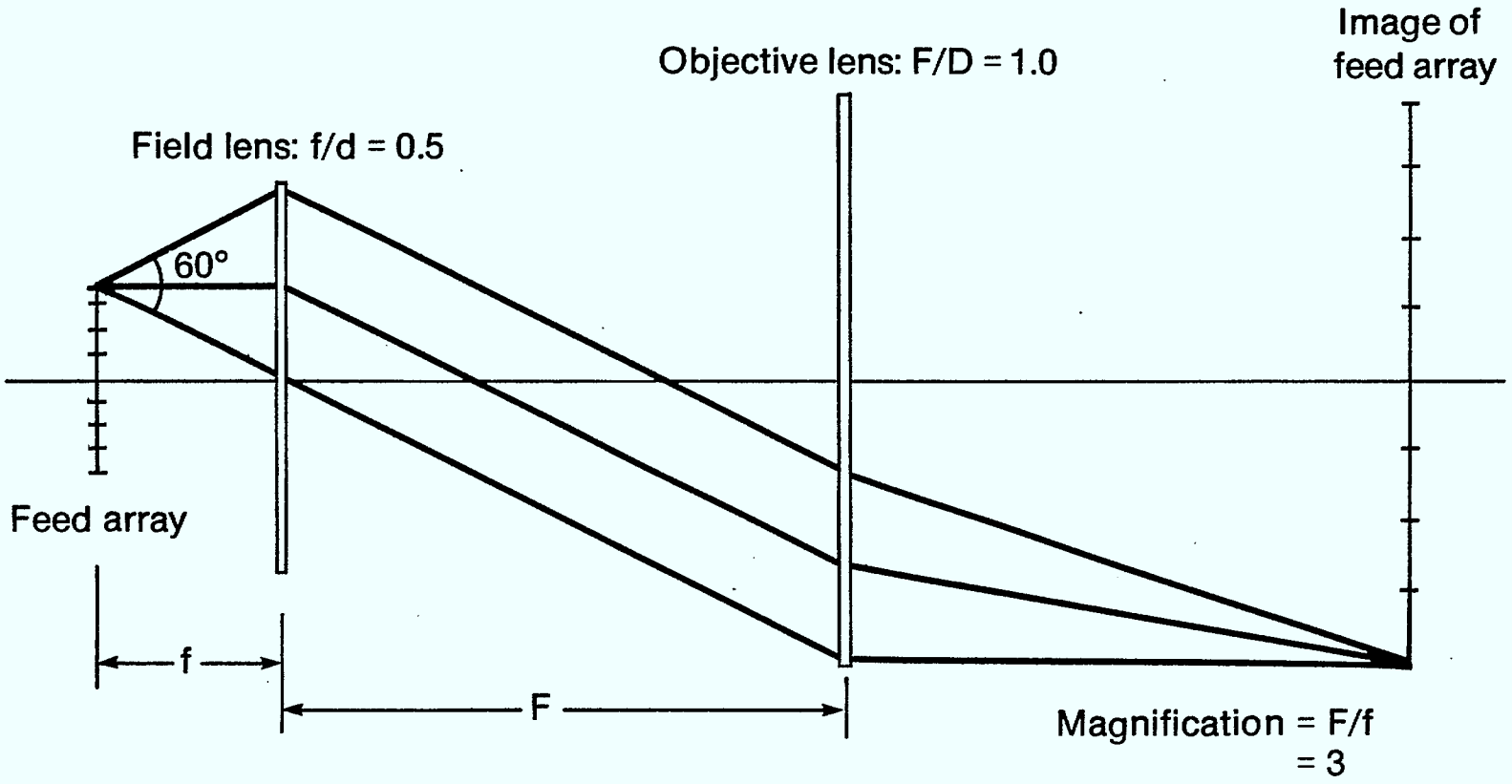

Fig. 2 A possible lens arrangement which images the feed array within the Fresnel region of the microwave-optical system.

Mathis(1960)

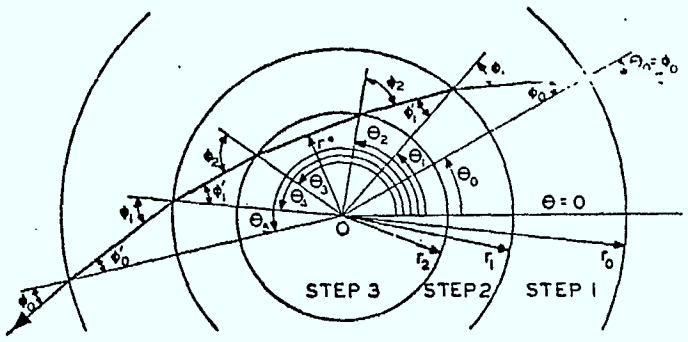

A stepped Luneberg lens.

Luneburg lens

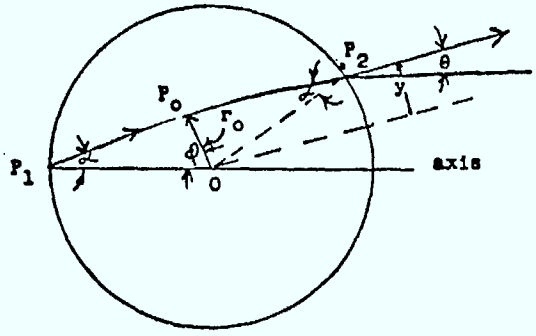

Type I

Luneburg reflector

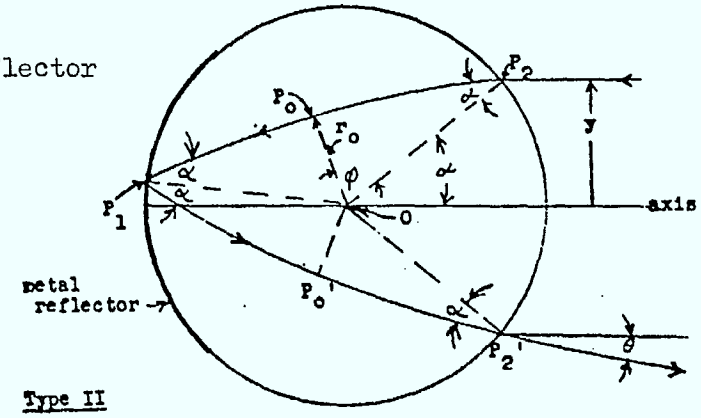

Type II

Eaton-Lippman lens

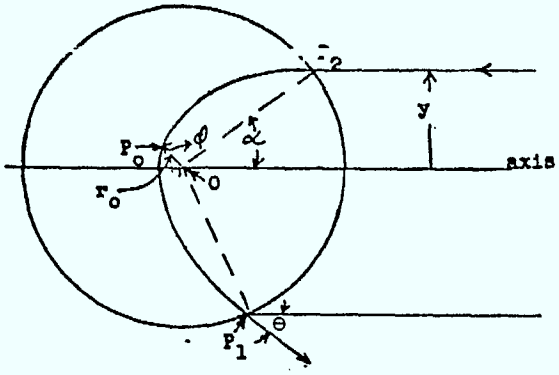

Type III

Kay(1959)

Fig. 3

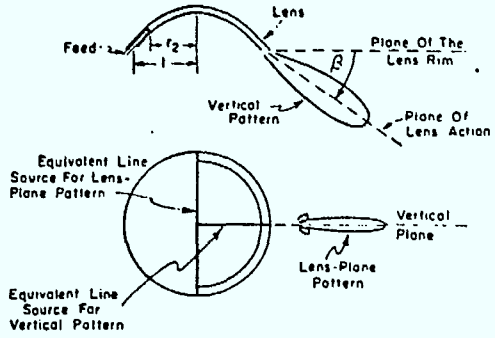

Description of lens patterns.

Geodesic Lens

Rudduck et al.(1964)

Fig. 4

Rotman & Turner (1963)

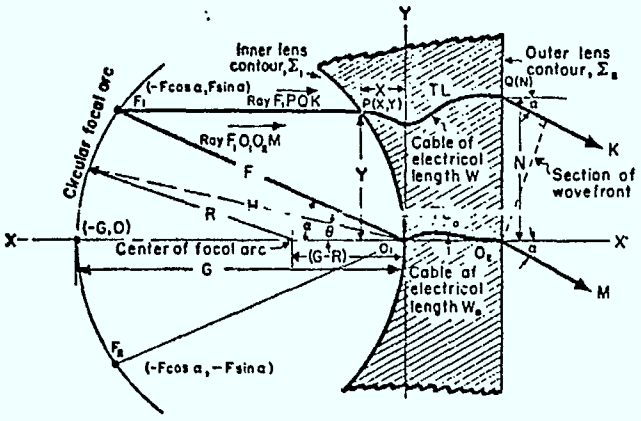

Microwave lens parameters.

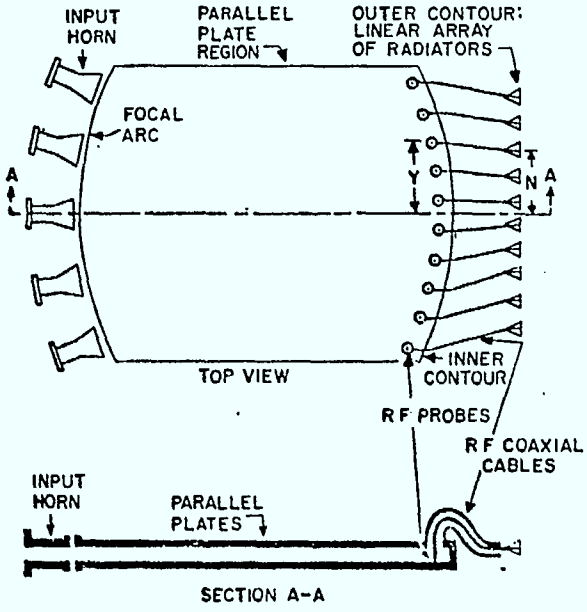

Parallel-plate microwave lens.

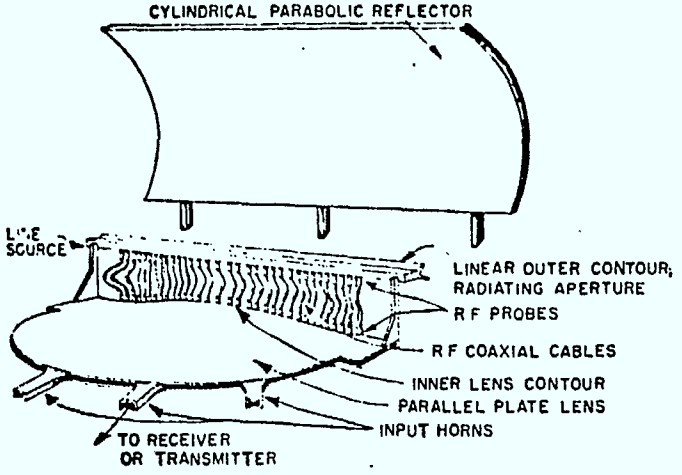

Parallel-plate lens and reflector.

Fig. 5

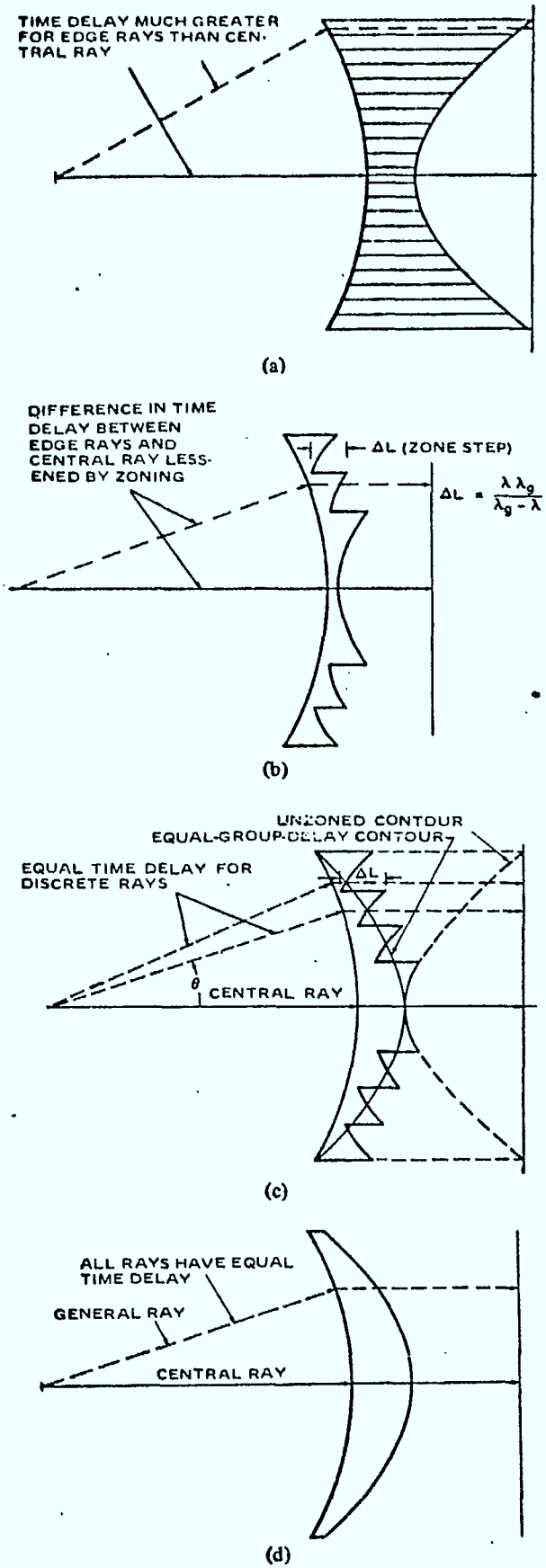

Unzoned waveguide lens deviates furthest from constant time delay. (b) Zoned waveguide lens deviates less from constant time delay. (c) Phase compensated (Coulbourn) zoned lens can be made to have equal time delay at discrete points. (d) Group delay waveguide lens has constant time delay for all rays.

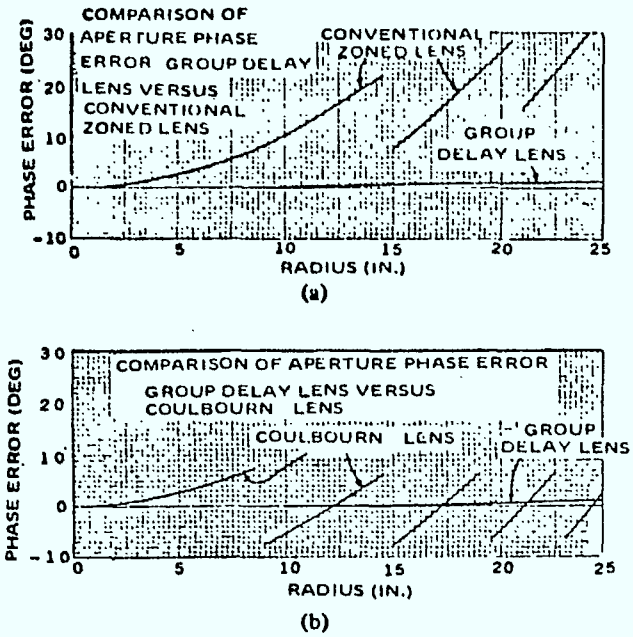

(a) Phase error as function of radial distance from center of lens for frequency two percent below design frequency. Here, conventional zoned lens is compared to equal group delay lens. (b) Phase error as function of radial distance from center of lens for frequency two percent below design frequency. Here, phase compensated (Coulbourn) lens is compared to equal group delay lens.

Ajioka & Ramsey (1978)

Fig. 6

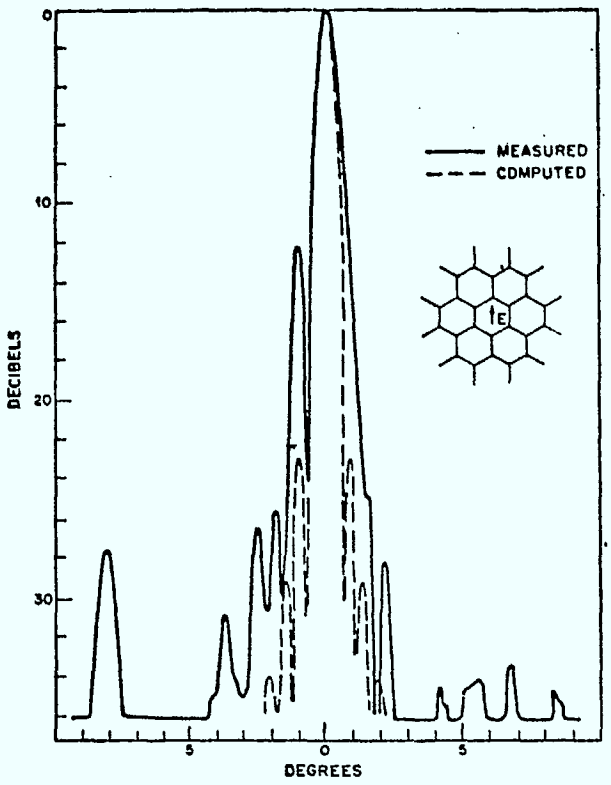

E-plane pattern of EHF lens antenna.

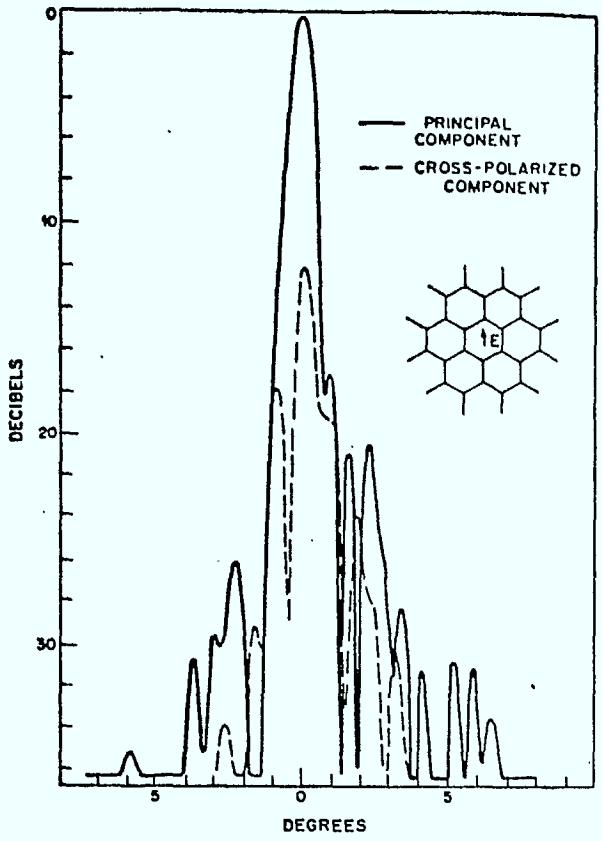

H-plane patterns of EHF lens antenna, Principal and cross-polarized components.

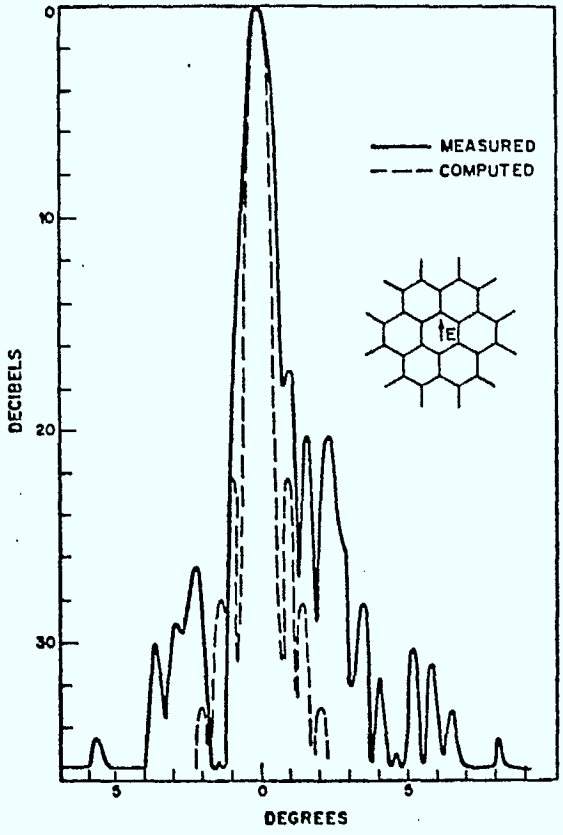

H-plane pattern of EHF lens antenna.

EHF Honeycomb Lens at 55 GHz

Dion (1972)

Fig. 7

" RADANT "

Chekroun et al.(1981)

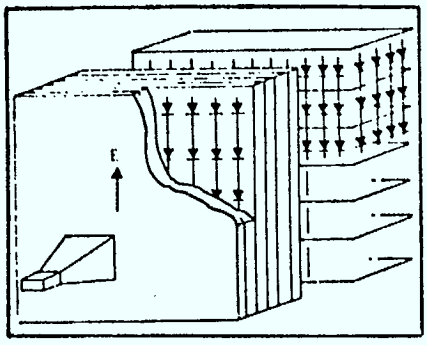

Radant antenna dual plane scanning.

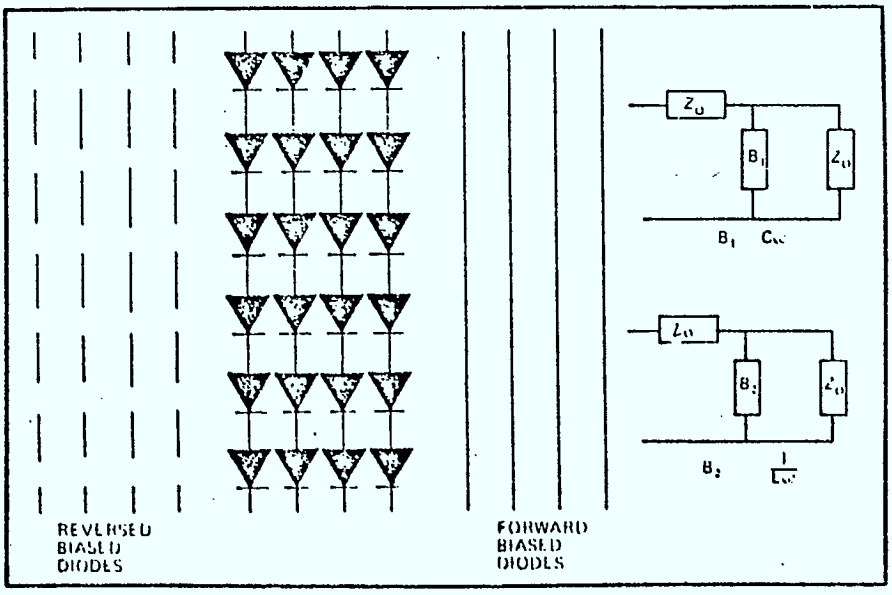

Wire-diode grid and equivalent circuits for both bias conditions.

Fig. 8 .

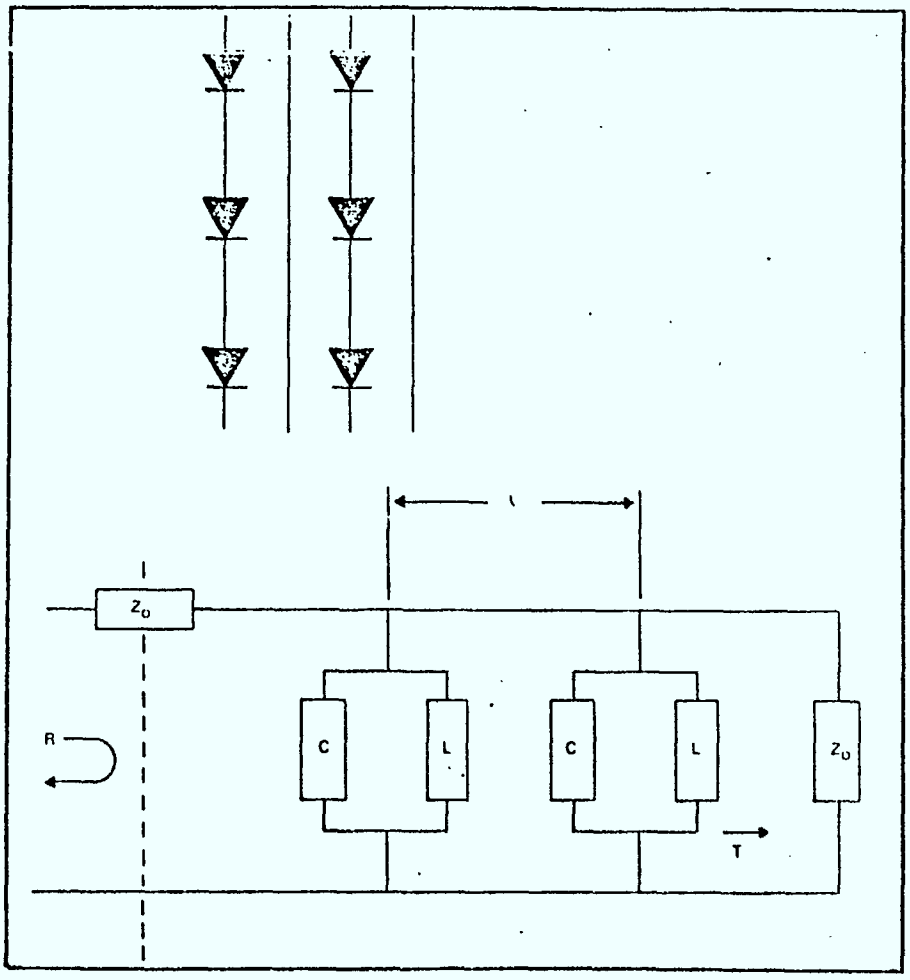

Phase shifting panel–equivalent circuit–diodes reverse biased.

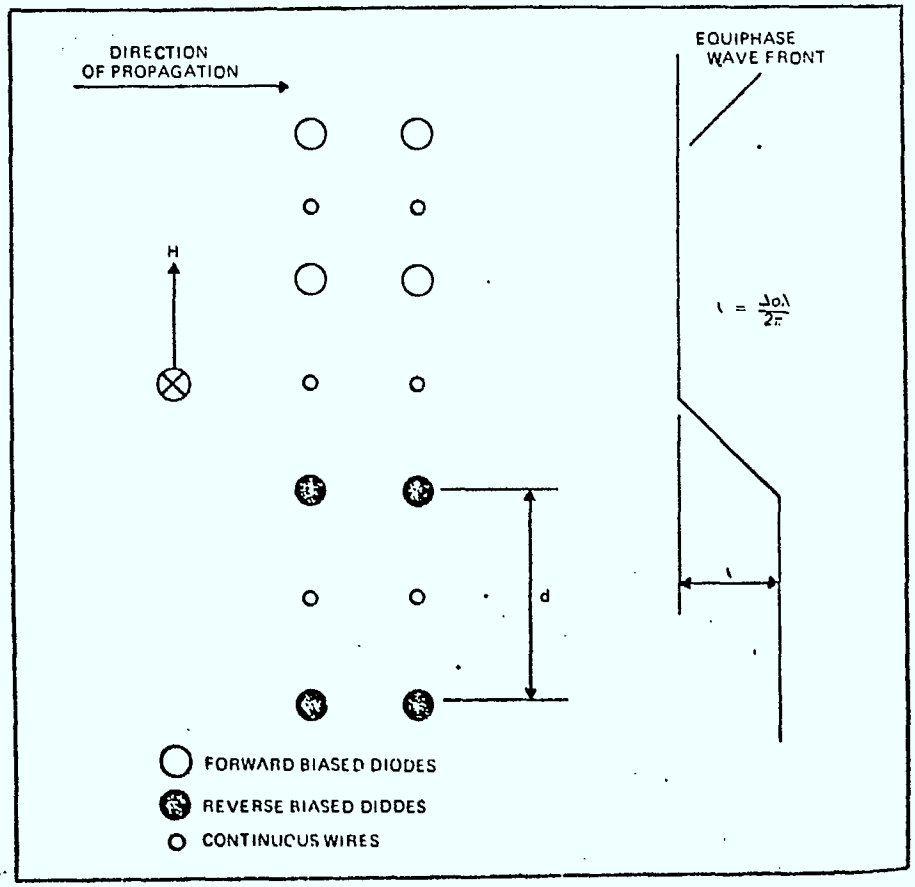

Phase shift as a function of diode biasing.

Fig. 9

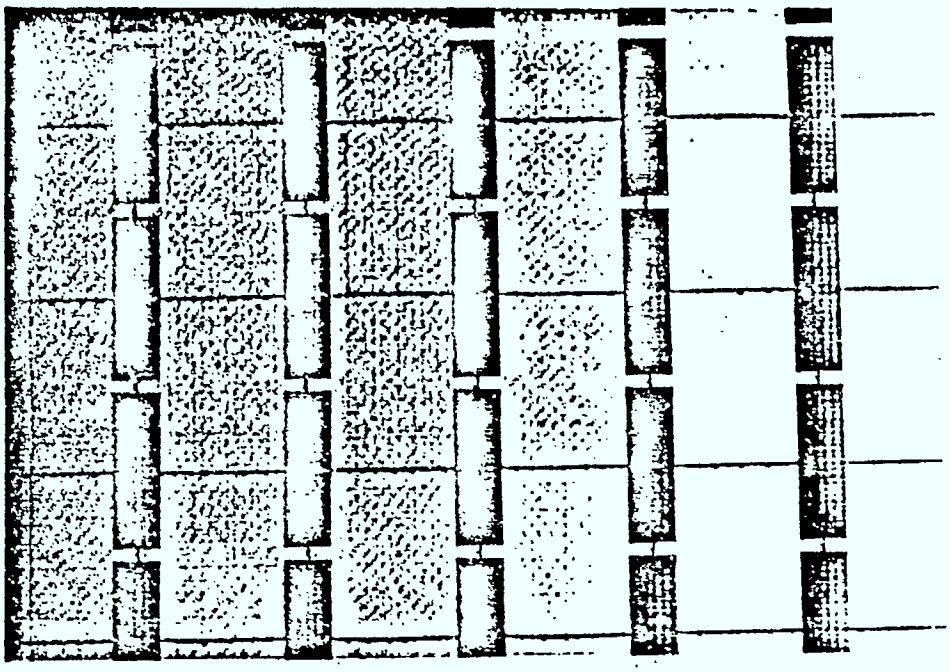

A diode-switched slot array.

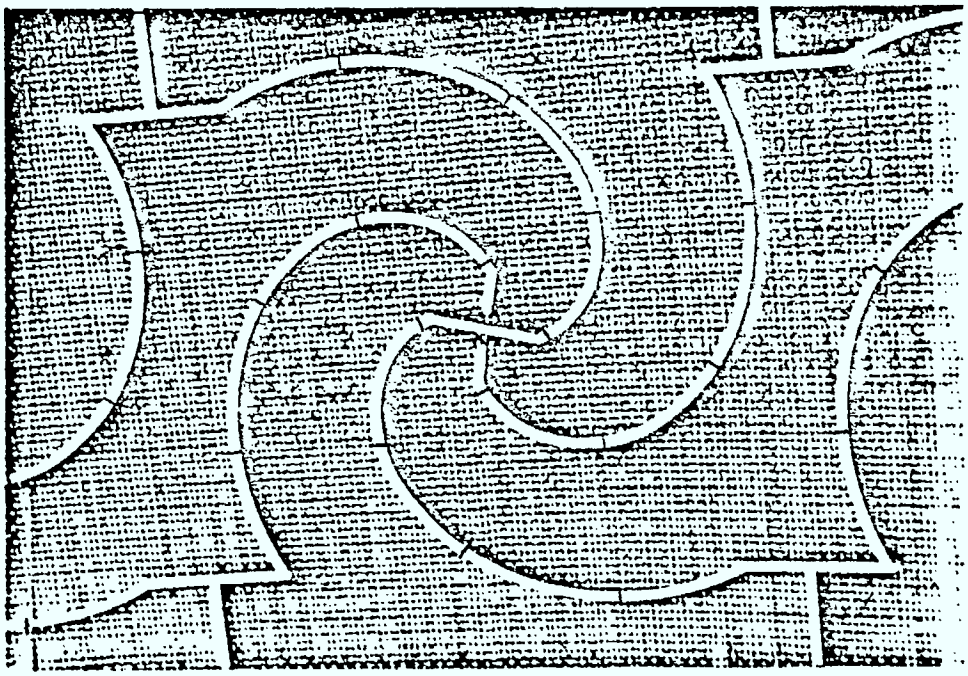

A diode-switched spiral array.

Fig. 10 Wang et al (1982)

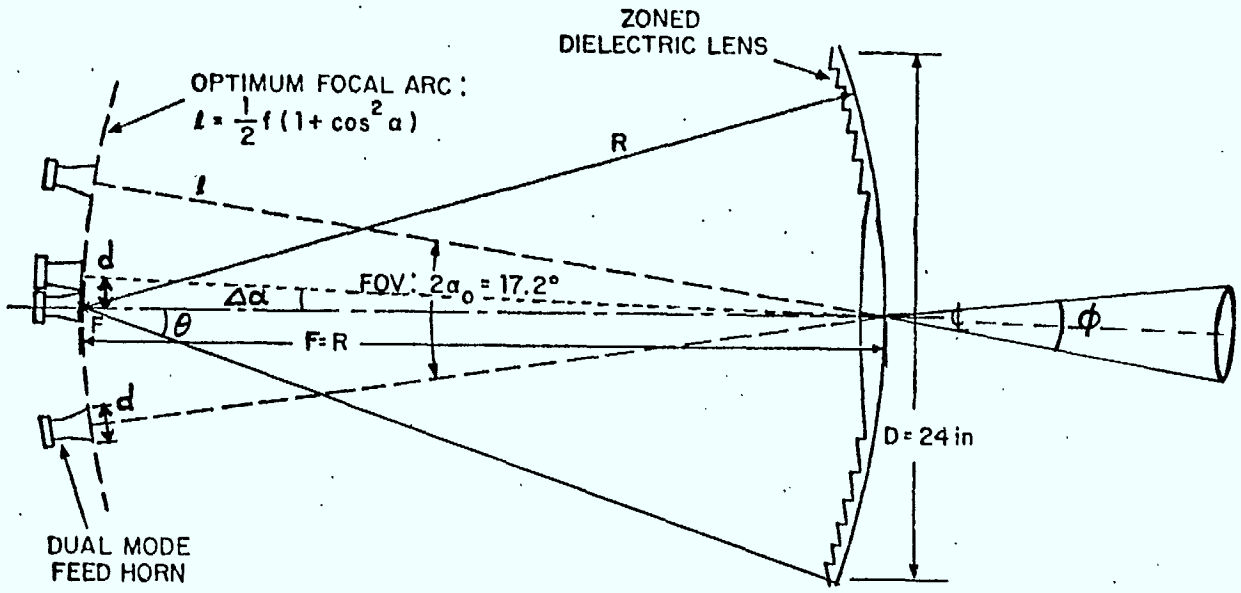

EHF aplanatic zoned dielectric lens.

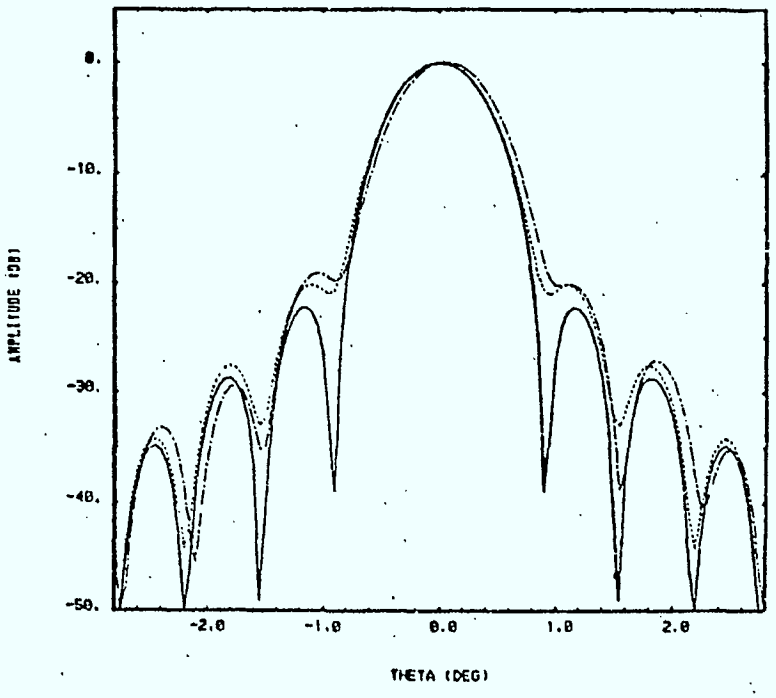

Calculated radiation patterns of zoned dielectric lens: (a) on-axis (solid line: θ=0°); (b) off-axis in plane of scan (dashed line: θ=8.6°; ϕ=90°); (c) off-axis orthogonal to plane of scan (dotted line: θ=8.6°; ϕ=0°)

Fig. 11 Rotman (1982)

Chapter 3

REFLECTOR ANTENNAS.

S. Dmitrevsky

1.

Introduction.

This section will review the major features of reflector antenna at microwave frequencies [1], [2].

The basic purpose of this type of antenna is to generate a distribution of amplitude, phase and polarization on a section of a surface, usually a plane, called the aperture, such that the far field pattern produced exhibits desirable properties such as beamwidth, sidelobe level, location of nulls and polarization.

The prime source of the electromagnetic field in free space is usually an area the dimensions of which are of the order of few wavelengths and the field radiated therefrom possesses approximately spherical equiphase surfaces. A common aperture distribution is one in which the phase is constant. With approximate spherical equiphase surfaces of the primary source an easy way to obtain this distribution is to reflect the wave emanating from the primary source by the surface of a paraboloid of revolution the focus of which is in the vicinity of the primary source. This basic concept has evolved into many forms dictated by system requirements and the need to optimize various aspects of the performance.

Methods of analysis of this category of antenna systems are simplified when the antenna dimensions are very large compared to the wavelengths: it is possible to obtain good approximation of the performance by employing methods of geometrical optics, to be complemented when necessary by inclusion of diffraction effects.

The major problem with reflector antennas is the fact that the feed located near the focus may lie in the region of reflected beam resulting in partial aperture blockage. This usually has an undesirable effect on the antenna performance. Another effect potentially degrading the performance is the distortion of polarization. These circumstances led to the development of several variants of the basic reflector antenna system described above, some of which will be described below.

Apecture blocking can be eliminated by using offset feed in which the feed located at the focus of the paraboloid illuminates a section of the reflector not centered on the axis. An example of this type of antenna is the parabolic horn antenna. This configuration eliminates the problem of aperture blocking. The penalty incurred is the fact that the asymmetric excitation of the reflector enhances the effects of geometric optical aberrations, the foremost of them being the coma, especially if the feed is extended, a feed array rather than a single source, as is the case in applications requiring scanning of the beam. An example of an antenna of this type is shown in Fig. 1.

Another limitation imposed on the system as a whole is that of the size. The dimensions of the paraboloid reflector are usually set by the requirements such as beamwidth or gain. The geometric optical performance improves with increasing ratio of focal length to the antenna dimension. This, however, may result in inconveniently large system, and may also require large dimensions of the primary source aperture to ensure that its diffraction pattern does not result in an objectionable level of spillover. The drawback may be removed by employing auxiliary reflectors, consisting usually of paraboloids, ellipsoids or hyperboloids of revolution, mutually confocal, the configuration having been so as chosen to obtain the desirable system features with respect to size and aperture blocking [3]. Fig. 2 shows an antenna system of this type. Another example in this category is the Cassegrain antenna.

It may be expected that the increased number of reflections in a multireflector configuration would contribute to the distortion of the original polarization generated in the feed. This effect can be reduced by employing two geometrical optical properties of systems of mutually confocal conoids of revolution. These are:

(i) The pattern and polarization of a beam originating in a focus of a conoid of revolution and propagating in the direction of the axis is preserved in the beam that diverges after reflection from the second focus.

(ii) A beam originating in a focus of a conoid of revolution and undergoing multiple reflections by a system of mutually confocal conoids undergoes the same distortion as a beam radiating and emerging from the focus of single equivalent conoid of revolution.

These two results may be employed to optimize the performance of multiple reflector antenna systems. An example of the optimization procedure is shown in Fig. 3.

2.

Steerable Beam Reflector Antennas.

The requirement that the antenna beam be scanned, and that a null be generated in a particular directions imposes additional demands on the antenna system and its feed. Scanning can be effected by mechanical means in that either the whole antenna system or the feed alone are displaced as required, or by electronic means. Beam shaping can be achieved by electronic means alone. Electronic means only will be considered in this report. These, however, can be studied in some depth only if some specific requirements are identified. For the system under consideration these are:

(i) Narrow band geostationary communications system.

(ii) Downlink frequency 20 *GHz.*

(iii) Uplink frequency 44 *GHz.*

(iv) Scan angle for both channels 4 °x 10 °.

(v) The uplink antenna to have a capability of synthesizing a null in arbitrary direction within this scan range.

There are two ways of effecting electronic scan in reflector type antennas. They are:

(i) The multiple beam and,

(ii) the phased array methods.

Employing optical terminology their operations can be described as follows:

(i) In a multiple beam system the antenna images the scanned area on its own focal plane [4].

(ii) In a phased array antenna the feed array is imaged on the aperture, the aperture distribution being the Fourier transform of the desired beam shape [5], [6].

It is evident that in both instances the primary feed covers finite area and is not even approximately a point source.

The choice between the two alternatives may be based on the considerations presented below.

The prime feed consists of a finite number of radiators of the horn or microstrip configuration. In a phased array system the signal in each of them has its amplitude and phase adjusted to a desired value. This is more easily done in a receiver application where these adjustments can be made at IF rather than at the signal frequency.

In a multiple beam system a sector of the target area is illuminated by an element of the feed array and scanning is accomplished by switching elements of the feed, a method suitable in transmitter applications.

For reasons mentioned above the review of the properties of antenna systems given below is based on the assumption that the downlink antenna will be of the multiple beam type while the uplink one will operate in the phased array mode.

3.

Dimensions of Main Reflectors.

This subsection will discuss the dimensions of main reflectors in relationship to the scan range, gain, beamwidth and the number of independently controlled feed elements. The following designations will be adopted:

(α, β): angular dimensions of the scan,

θ: the beamwidth,

N: the number of independently controlled elements or clusters in the feed array and,

D: the diameter of main reflector.

It is pointed out that the results obtained are approximate to within 20 percent in that they were developed on the basis of certain simplifying assumptions such as circular reflector shape and uniform aperture illumination. These assumptions were necessary unless one was to consider specific configurations as the basis for analysis.

The relations to be derived are slightly different for the multiple beam and phased array modes and will be discussed separately.

(i) Multiple beam systems:

Assuming hexagonal lattice coverage of the scan area, the beamwidth θ and the scanned solid angle $\alpha\ \beta$ are related by the equation

$$\alpha\ \beta = N\theta^2\ 27^{1/2}/8$$
$$\theta = 1.25(\alpha\ \beta/N)^{1/2} \tag{1}$$

The approximate expressions for the diameter D and the gain G follow (with α, β expressed in radians):

$$D = \lambda/\theta = 0.8\lambda(N/\alpha\ \beta)^{1/2} \tag{2a}$$

$$G = 4\pi/\theta^2 = 8N/\alpha\ \beta \tag{2b}$$

The values of θ, D and G are plotted against N in Fig. 4 for $\alpha = 10\ °$ and $\beta = 4\ °$ (approximately 1/6 and 1/14 radians respectively), and $\lambda = 1.5$ cm in the 20 *GHz* downlink. The choice of N as the independent variable was dictated by the expectation that it may be one of the limiting factors in the realization of the system.

(ii) Phased array systems:

The distribution of the field amplitude and phase in the aperture plane of the main reflector is a magnified image of the amplitude and phase distribution in the prime feed plane. In as much as the feed consists of N identical elements with signals differing only in their phases and amplitudes, the aperture plane is covered by N radiating areas with identical pattern which combine in the far field in accordance with their phase and amplitude relationships. The overall pattern is therefore the product of the pattern of individual feed element image in the aperture plane, and the array pattern determined by the relative amplitudes and phases of array elements. The discussion below is based on the following assumptions:

(a) individual array element has aperture distribution similar to that of TE_{11} waveguide mode (this assumption simplifies the calculations in that the pattern does not devieate excessively from being axially symmetric),

(b) amplitudes of all array elements are the same and,

(c) the phase of individual elements varies lineraly over the array.

Under the above assumptions the beamwidths θ' and Θ'' for a rectangular main reflector are given by

$$\theta' = \alpha/N_1 \quad , \quad \Theta'' = \alpha/N_2 \tag{3}$$

Combining the above relations to obtain the dependence of the total number of array elements $N_1 \; N_2 = N$ on the solid angle of the scan, $\alpha \; \beta$ one obtains

$$\theta' \; \Theta'' = \alpha\beta/N_1 \; N_2 = \alpha\beta/N \tag{4}$$

Introducing the effective circular beamwidth θ by the equation

$$\pi\theta^2/12^{1/2} = \theta' \; \Theta'' \tag{5}$$

one obtains the following equation

$$\theta = (12^{1/2}\pi)^{1/2}(\alpha\beta/N)^{1/2} = 1.05(\alpha\beta/N)^{1/2} \tag{6}$$

The diameter D and the gain G are then (with α and β expressed in radians)

$$D = \lambda/\theta = (\lambda/1.05) \; (N/\alpha\beta)^{1/2} \tag{7a}$$

$$G = 4\pi/\theta^2 = 11.3N/\alpha\beta \tag{7b}$$

The values of θ, D and G are plotted against N in Fig. 5 for $\alpha = 10$ °, $\beta = 4$ ° and $\lambda = 6.8$ mm in the 44 *GHz* uplink.

It is apparent from Fig. 5 and Eqn. 7b that the number of elements in an array, the scan angle and the antenna gain are dependent on each other. The complexity of the electronic circuitry in an adaptive system may limit the number of controlled elements reducing thereby the gain for a given scan range.

As has been mentioned before, the gain of a phased array antenna is the product of the gain associated with individual array element and the array factor. The beamwidth of the individual element must cover the whole scan range, determining thereby its gain. The beamwidth of the combined system is reduced by the application of the array factor which is inversely proportional to the number of elements. If this number is small the desired antenna gain can be obtained only by reducing the scan range. It is, however, possible to realize a large scan range with small number of individually controlled array clusters containing several array elements. The beamwidth associated with each cluster can be made sufficiently narrow to produce the desired system gain. To retain a large scan range the phasing of elements within individual clusters can be switched among several discrete states, identical for all clusters, to direct individual beams to the desired sectors of the scan range. The system would avoid the complexity of a large adaptive system in that only the outputs of the small number of clusters would be available for adaptive processing because the scan range switching is a discrete operation not requiring complicated circuitry.

As an example consider a system requiring about fifty elements to achieve the desired gain and scan capability, but in which the adaptive processing can handle seven inputs only. Both sets of requirements can be met if the array is split into seven clusters containing seven elements each. If the seven elements within each cluster are assigned seven appropriate, discrete phase distributions, identical for all clusters, the antenna system will exhibit the gain corresponding to a forty-nine element array, the desirable scan range and an adaptive processing system will seven inputs only.

4.

Feed Systems - Introduction

A feed system consists of a primary feed excited by or exciting the signal generating or processing portion of the communications link, and the interface between it and the main aperture. The primary feed element may be a horn, microstrip radiator, or any other source of electromagnetic radiation. At frequencies of interest in this study the wavelengths are appreciably smaller than the elements of the feed, excepting the primary sources, and method of geometrical optics may be applied to study the system behaviour, modified when appropriate by the limitations imposed by diffraction.

The prime purpose of the intermediate feed elements is two-fold:

(i) remove the feed from the main beam and,

(ii) reduce the size of the prime feed.

In the systems considered the main reflector aperture is always a section of a paraboloid of revolution. The feeds fall into two categories depending on whether one deals with the multiple beam or a phased array antenna.

5.

Feeds in Multiple Beam Systems.

In a multiple beam configuration a portion of the scanned area is imaged on a particular element in the feed array which must be located in the focal plane of the principal reflector, in the vicinity of the focus.

To avoid aperture blocking it is a common practice to employ offset feed geometry as shown in Fig. 1. The area A of the feed array is determined by the scan angles α and β and is given approximately by the equation

$$A = \alpha \beta f^2 \tag{8}$$

where f is the focal length of the paraboloid. The equation is only an approximation because for offset configuration the distance between the centre of the reflector and the focus is larger than f. If there are N elements in the array, the geometric mean of the dimensions of each element, d is given by

$$d = (A/N)^{1/2} = f(\alpha\beta/N)^{1/2} \tag{9a}$$

On substituting for N from Eqn. 2a this equation becomes

$$d = 0.8\, f\lambda/D \tag{9b}$$

The transition between the Fresnel and Fraunhofer regions for the feed element aperture, d^2/λ is approximately $0.5f^2/2D^2$ which, even for the smallest useful ratios D/f is much smaller than f. The main reflector thus lies in the Fraunhofer region of the feed aperture. The beamwidth λ of an uniformely illuminated aperture is

$$\lambda/d = 1.25D/f \tag{10a}$$

The dimension of the feed beam on the reflector aperture, $f\phi$ is thus equal to

$$\phi f = 1.25D \tag{10b}$$

This relation indicates the existence of some spillover. The phenomenon is due to the fact that in order to assure complete coverage of the scanned area some beam overlap is necessary, whereas no overlap of feed elements in the feed array are possible.

It was mentioned in the Introduction that small values of D/f ratio are desirable if aberrations are to be reduced. The disadvantages accruing are:

(i) increase in the dimensions of the antenna system and,

(ii) increase in the dimensions of the feed element aperture.

If d is to be equal to λ the combination of Eqn. 2 and Eqn. 10b results in the relation

$$D=0.8f \tag{11}$$

Should one employ a system with lower ratio of D/f, the dimensions of the feed element aperture, and the feed array itself may become inconveniently large. It is possible, however, to avoid this disadvantage and still retain low D/f ratio by employing a hyperboloid auxiliary reflector generating a virtual focus far from the main reflector as shown in Fig. 2.

6.

Feeds in Phased Array Systems.

The basic antenna arrangement in the phased array configuration consists of two paraboloids, the main reflector and the smaller, confocal, coaxial secondary reflector the function of which is to produce a magnified image of the feed array in the aperture of the main reflector. An example of such system is shown in Fig. 6. The magnification, equal to the ratio f^1/f^2 of the focal lengths of the main and the secondary reflectors ranges usually from 3 to 7. Because the focal length of the secondary reflector is appreciably smaller than that of the main one, the image of the aperture of the latter lies in the vicinity of the focal plane of the former.

It will be useful to estimate the size of the secondary reflector. If f is the focal length of the main reflector and n the magnification ratio, the focal length of the secondary reflector in f/n. The image of the main reflector aperture lies in a plane approxiamtely perpendicular to the axis of the paraboloids at the distance $(n+1)\ f/n^2$ from the vertex of the secondary reflector. The dimension of the feed array is D/n (D is the diameter of the main reflector). Due to the scan the dimensions of the secondary reflector will be larger as it has to intercept the rays coming from all directions of the scan range. The dimensions are:

$$\begin{aligned} d_\alpha &= (D/n)\ [1+\alpha(n+1)/q] \\ d_\beta &= (D/n)\ [1+\beta(n+1)/q] \end{aligned} \tag{12}$$

where q = D/f.

For the values of α =10 ° and β = 4 °, n = 5 and q = 0.67 the dimensions of the secondary reflector are

$$d_\alpha = D/2, \quad d_\beta = D/3$$

It follows from Eqn. 12 that the dimensions of the secondary reflector are reduced for increasing values of n, the magnification. This can be accomplished by increasing the focal length of the main reflector, or reducing the focal length of the secondary one. The disadvantage of the former method is that the overall dimensions of the system are increased while the second method is limited by the need to reduce the aberrations caused by the secondary reflector.

7.

Combined Uplink - Downlink Antenna System.

The switching mode of operation in the multiple beam system is more suitable for downlink operation while the phased array system is appropriate for the uplink service. It is also possible to employ a diplex system employing a common main reflector, a diplexer and dual feed system [6]-[8]. A possible configuration of the system might consist of:

(a) the main reflector,

(b) a hyperboloid subreflector removing the feeds from the path of the main beam,

(c) an interferometer diplexer operating in the transmission mode for the 44 *GHz* uplink and in the reflection mode for the 20 *GHz* downlink beams,

(d) a secondary reflector imaging the main aperture on the phased array feed of the 44 *GHz* uplink signal,

(e) another secondary reflector or a small lens imaging the scanned area on the feed array of the 20 *GHz* downlink signal and,

(f) the two feed arrays.

A dual feed system employing interferometer diplexer is shown in Fig. 7. It differs from the system discussed in this subsection in that both channels are of the phased array type.

A critical element in the system is the diplexer. It can be either of a metallic mesh type or a dielectric slab. The former suffers from the disadvantage that it is polarization sensitive and its operation depends critically on the directions of the main beams. Both of these disadvantages are eliminated with the employment of a dielectric slab of high permittivity. In this case the direction of propagation within the slab is only weakly dependent on the angles of incidence. Calculations show that a rutile ceramic slab (relative permittivity 100) about 7 mm thick would possess desirable characteristics.

References

1. P.J. Wood. "Reflector antenna analysis and design." The IEE, London, New York, 1980.
2. A.W. Love (ed.). "Reflector Antennas." IEEE Press, New York, 1978.
3. C. Dragone. "Offset multi reflector antennas with perfect pattern symmetry and polarization discrimination." *Bell System Technical Journal*, Vol. 57, No. 7, pp. 2663-2684 (September), 1978.
4. A.S. Acampora, C. Dragone, D.O. Reudnik. *IEEE Transactions on Communications*, Vol. COM-27, No. 10, pp. 1406-1415 (October), 1979.
5. C. Dragone, H.J. Gans. "Imaging reflector arrangements to form a scanning beam using a small array." *Bell System Technical Journal*, Vol. 58, No. 2, pp. 501-515 (February), 1979.
6. C. Dragone, M.J. Gans. "Satellite phased arrays: use of imaging reflectors with spatial filtering in the focal plane to reduce grating lobes." *Bell System Technical Journal*, Vol. 19, No. 3 pp. 449-461 (March), 1980.
7. P.F. Goldsmith. "A quasioptical feed system for radioastronomical operations at millimeter wavelengths." *Bell System Technical Journal*, Vol. 56, No. 8, pp. 1483-1501 (October), 1977.
8. J.J. Fratamico, Jr., M.J. Gans, G.J. Owens. "A wide scan quasi-optical frequency diplexer." *IEEE Trans. on Microwave Theory and Tech.*, Vol. MTT-30, No. 1, pp. 20-27 (January), 1982.

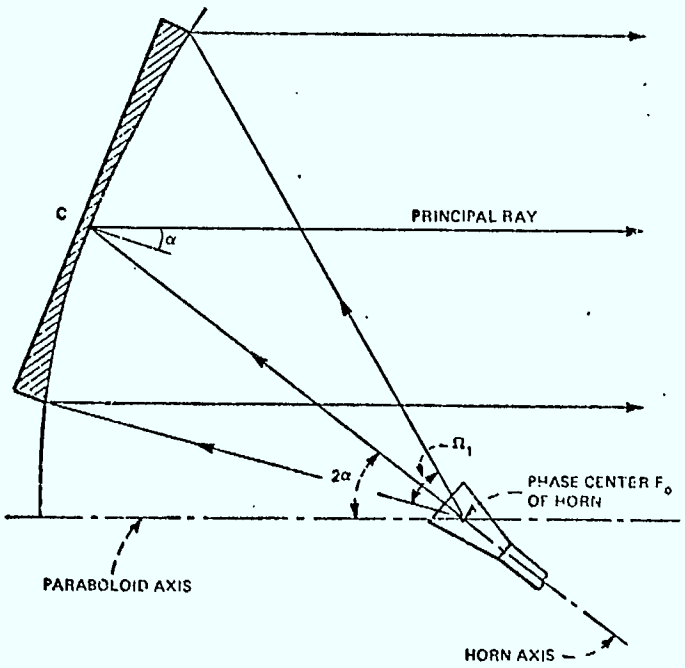

The spherical wave radiated from F_0 by a corrugated feed is transformed by an offset paraboloid into a plane wave.

Fig. 1.
Offset paraboloid reflector,
(C. Dragone, BSTJ, Vol. 57, No. 7,
p. 2664).

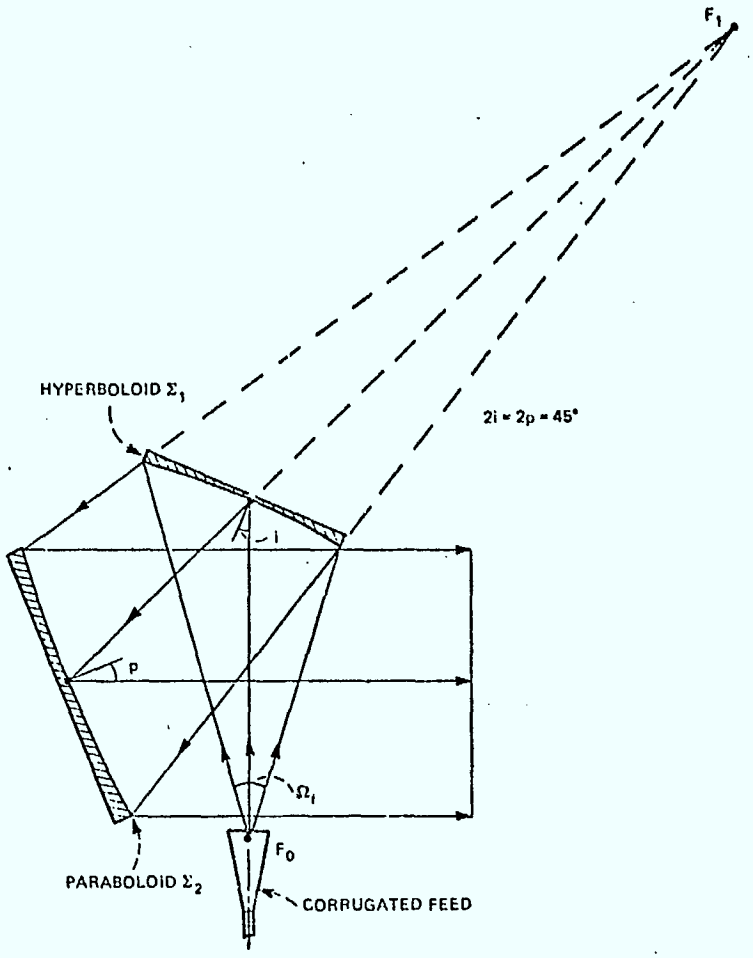

-A vertical feed and two reflectors with $i + p = 45$ degrees producing a horizontal beam without symmetry distortion.

Fig. 2.
Multireflector antenna
(C. Dragone, BSTJ, Vol. 57, No. 7,
p. 2678).

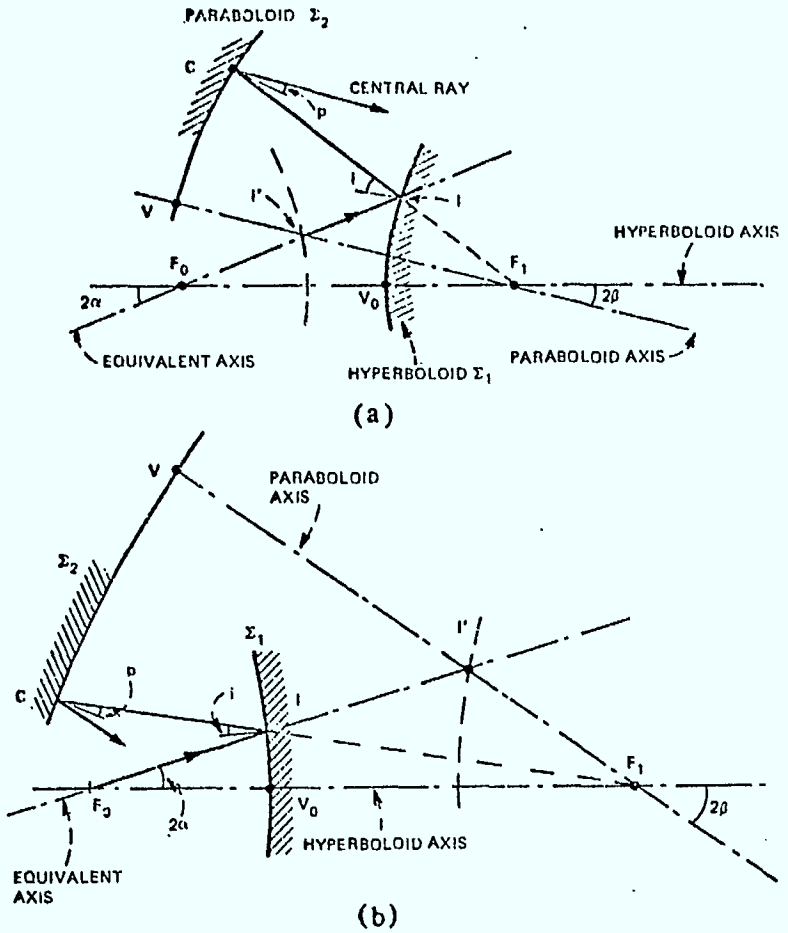

How to determine the central path and the equivalent axis of a paraboloid combined in (a) with a convex hyperboloid and in (b) with a concave hyperboloid.

Fig. 3.
Optimization procedure for multireflector antennas (C. Dragone, BSTJ, Vol. 57, No. 7, p. 2671).

Fig. 4.
Diameter D, beam width θ,
gain G vs. array size N
at 20GHz.

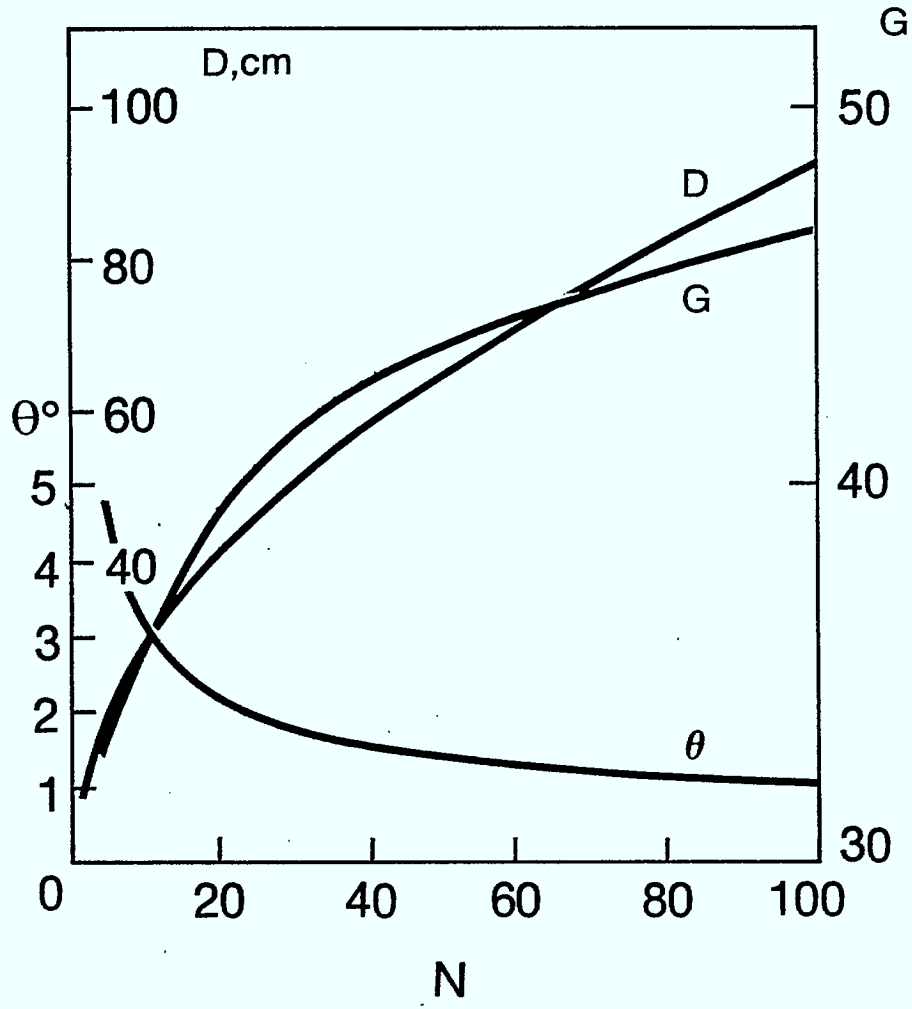

Fig. 5.
Diameter D, beam width θ,
gain G vs. array size N
at 44GHz.

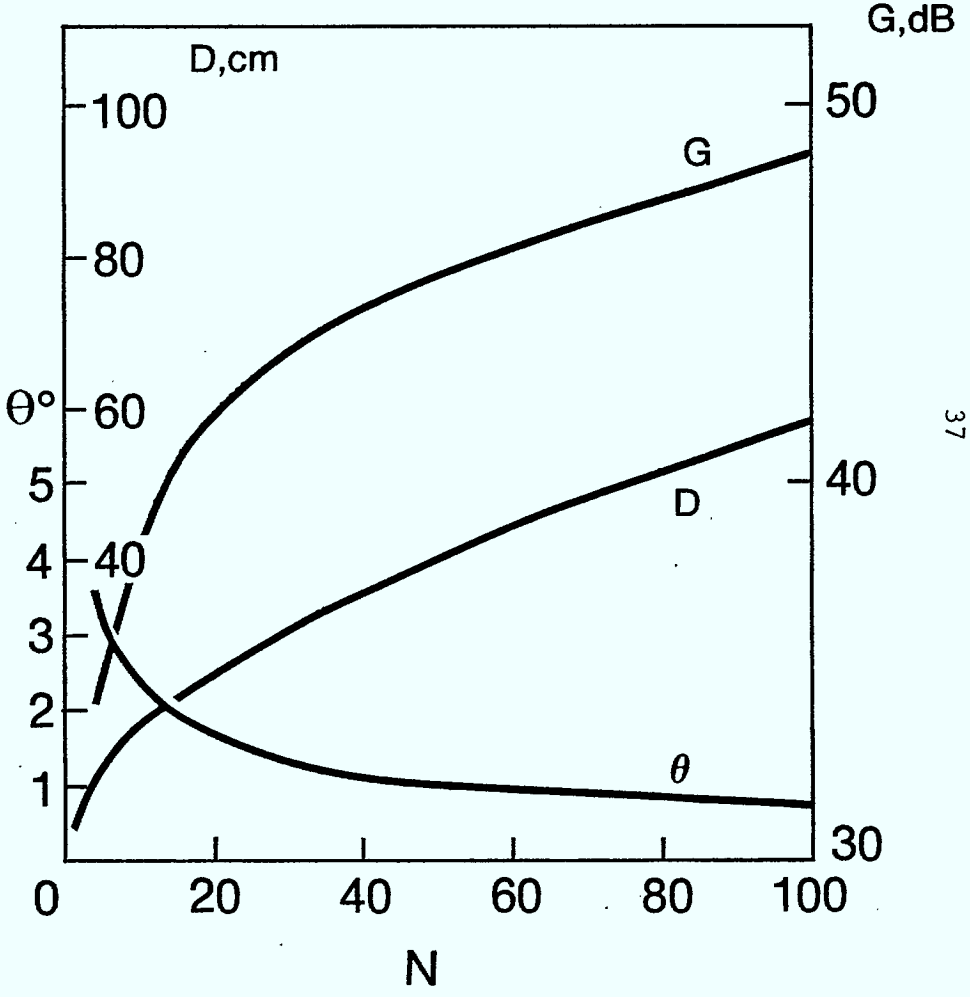

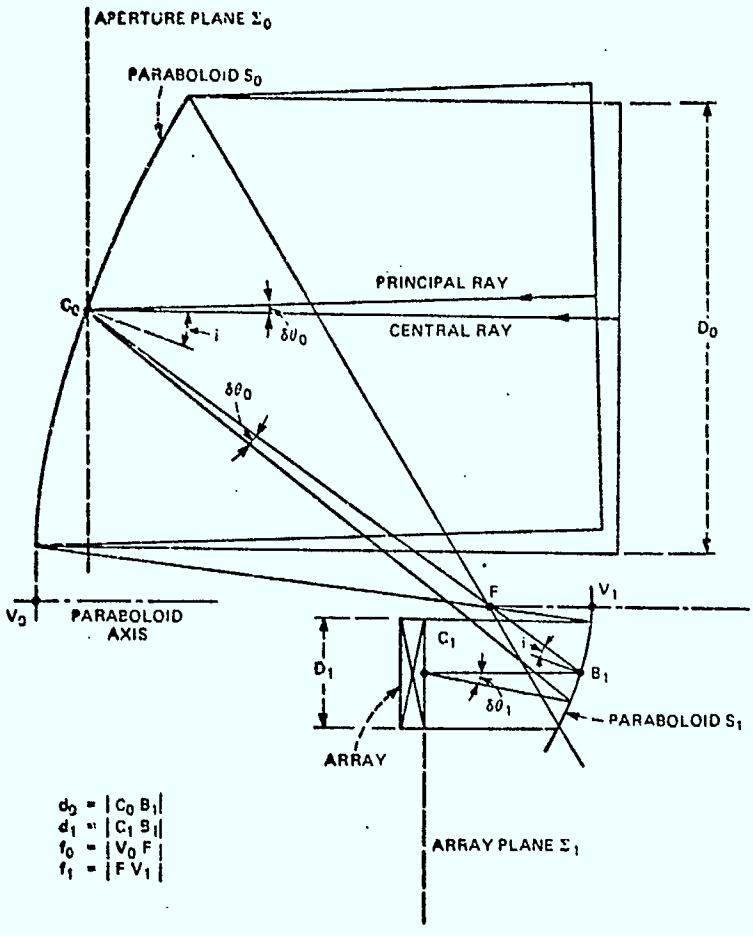

A Gregorian arrangement of two confocal paraboloids magnifying a small array. The main reflector S_0 and the array are conjugate elements.

Fig. 6.
Phased array reflector antenna
(C. Dragone, M.J. Gans, BSTJ
Vol. 58, No. 2, p. 503).

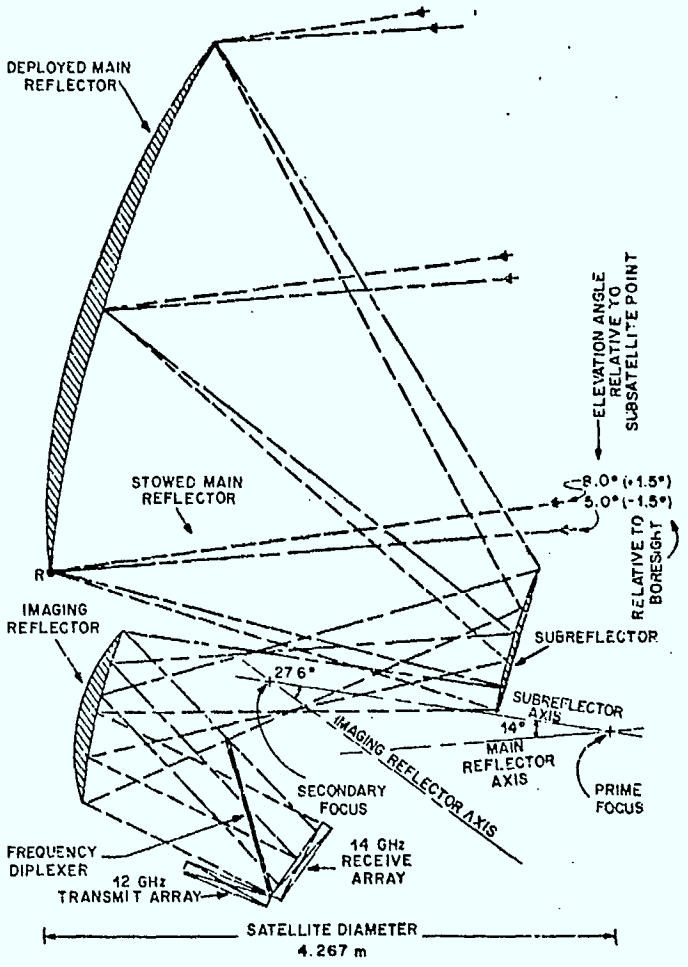

Imaging satellite antenna with 12/14-GHz frequency diplexing and overall magnification of 7.

Fig. 7.
Diplexer configuration of a multireflector antenna (J.J. Fratamico, Jr., M.J. Gans, G.J. Owens, IEEE Transactions on Microwave Theory and Tech., Vol. MTT-30, No. 1, p. 20).

Chapter 4

MICROSTRIP ARRAYS.

Y.L. Chow

1.

Introduction.

A microstrip antenna, like a printed circuit board, is compact, light weight, easily transportable and can be made to conform to the structure of the carrying vehicle such as a ship or an aircraft. Because it can be made without pertruding parts, it is very rugged mechanically. Because it is printed, it is simple and low cost when compared to other types of antennas such as horns or reflectors.

Due to these advantages, the microstrip antenna is a logical choice for the earth-terminal antenna for SATCOM. A microstrip antenna generally has a narrow bandwidth, say 2 to 5 percent. Fortunately, this is the bandwidth required for the earth-terminal antenna.

We shall separate this discussion in microstrip antennas in two parts. The first part is the literature survey and general discussions. The second part is the discussion of a recommended microstrip antenna in the form of an antenna array for high gain.

Part A: The Literature Survey and General Discussions.

In this part of the report, we shall study:

(i) the number of microstrip antennas needed for the directive gain requirement;

(ii) the effect and implementation of the beam scanning;

(iii) the shape and feed of the antenna elements to satisfy the requirements of versatility in polarization and reduction in coupling between elements;

(iv) the corporate feed for a rectangular array;

(v) the material of the microstrip substrate for low loss and compliability to form a conformed array on the carrying vehicle.

2.

The Number of Elements in the Antenna Array.

Bach [1] gave a formula of the following form for the directive gain D of a microstrip antenna array of N elements:

$$D = G_{el} + 10 \log_{10} N \quad (db) \tag{1}$$

where G_{el} is the element gain in *dB*. Because of the loading of the electric substrate, a microstrip antenna element is normally small in terms of wavelength and gives low antenna gain. However, because the microstrip antenna radiates only in one direction due to the ground plane the gain is doubled. As a result, we can say $G_{el} = 4\ dB$ for a microstrip antenna of any simple shape, such as a dipole, a square or circular patch.

If we require an uplink gain of $D = 48\ dB$, this would make the number of elements required in (1) to be $N = 2.51 \times 10^4$. This number is far too large and is impractical for an array.

If we take the back-off position of $D = 36\ dB$, then with $G_{el} = 4\ dB$, the number of elements required in (1) is $N = 1580$. To suit the corporate feeding network required for phase scanning of the array, we raise N to 2048, i.e. 2^{11} or reduce N to 1024, i.e. 2^{10}. These are reasonable numbers of elements since Murphy [2] has built a SEASAT satellite array of 1024 elements (see Fig.1).

The directive gain assumes no losses in the feeding network. With the network losses, the absolute gain can be substantially lower than the directive gain. An example of this is given by James, et al. [3].

Because of the losses in the feeding network increase with the array size James, et al. [3] show that there is an upper limit to the absolute gain of the array. The absolute gain actually decreases beyond this limit of array size.

The array configuration can be a rectangular or a hexagonal (or triangular) grid. A hexagonal grid configuration may be more desirable because of the distance of grating lobes to the main beam is farther for a given element density in the array. On the other hand it may be difficult to use the corporate feed for the hexagonal grid. Therefore, if the corporate feed problem cannot be solved we may have to use the rectangular grid.

3.

The Effect and Implementation of Scanning.

When the array beam is electronically scanned from its broadside direction, the beam broadens. The broadening is proportional to the secant of the polar angle θ from the broadside. At $\theta = 60$ ° it is observed that $sec\theta=2$ and an array directive gain only suffers a loss of 3 *dB*. The directive gain deteriorates rapidly beyond this point. It is recommended, therefore, mechanical scanning be used for θ beyond 60 °.

The electronic beam scanning requires a corporate feeding network to the radiating antennas. If 2048 elements are used, 2048 pin diode phase shifters are required. The details of the increments in the phase shifting, especially for the hexagonal array arrangement or for a curve surface are to be designed.

4.

Corporate Feed for a Rectangular Array.

The corporate feed for a hexagonal array presents a difficult problem and is to be worked out. The corporate feed for a rectangular array on the other hand is straight forward. An example is given below.

A phase shifter can be attached to each element for scanning purpose. The number of phase shifters will then be equal to the number of elements. If each of the elements has two inputs (for circular polarization, cf. Section 5) then two corporate feed networks are required. Thus, the number of phase shifters will be equal to twice the number of elements.

In the corporate feed, various power splitters as in Fig. 2 (a), (b), (c) and (d) can be used. Types (a) and (b) have insulation between the two branches and therefore the radiating elements have no coupling through the feeding network. However, such splitters are larger than types (c) and (d).

The power splitter can be made asymmetrical for nonuniform illumination across the array. The phase error introduced can be compensated by a technique shown in (e) and (f). The detail of the technique is given in [13].

5.

The Shape and Feed of an Antenna Element.

A versatile patch antenna which gives both linear and circular polarizations may be a square patch fed by a 90 ° hybrid [4], as shown in Fig. 3. By suitably adjusting the phases and amplitudes of feeds 1 and 2 various polarization can be obtained.

A circular patch may be used without much difference in the radiation pattern of the element. Because of the 90 ° hybrid feed, it may be difficult to space the antennas to form an

array, especially the hexagonal grid array. Therefore, one may have to consider a "two RF boards structure", that is: the radiating antenna on top of the ground plane and the hybrid feed below the ground plane. The interconnections are made by feed-through pins.

The square patch elements are more suitable for the square grid array and the circular patch element are suitable for both the rectangular and hexagonal grid array.

Based on the experiments by Jedlicka, et al. [5] and the theoretical results by Chow and Fang [6], it seems that the coupling between the square patch elements is about 4 *dB* higher than that between the circular elements. This makes the circular patch elements a better choice as the array elements.

The above coupling results are for elements on flat surfaces. It is believed that the coupling results are similar for elements on a curved surface in a conformal array. Other types of circularly polarized patch elements that are different from that in Fig. 3 are available. Some examples are given below in Figs. 4 and 5. Their effect on coupling is not known but can be calculated from the theory of Chow and Fang [6].

6.

The Material of the Substrate.

The substrate materials for a microstrip antenna and array are available in a Ball Aerospace Report [7] or a book by Bahl and Bhartia [8]. Some of them are listed below.

(i) Fibreglass reinforced with polyolefin ($\epsilon_r = 24$)

(ii) styrene copolymer ($\epsilon_r = 2.53$)

(iii) sapphire ($\epsilon_r = 9$)

(iv) aluminium ($\epsilon_r = 9.8$)

(v) types of PTFE (Polytetra fluoruethylene) ($\epsilon_r = 2.1$ to 2.5).

They all appear to give about the same loss tangent (of the order of 1×10^{-4}). It appears that higher dielectric constant material give smaller patches and therefore less coupling. However, the material is more fragile and non-conformal. Because of the confomity difficulty it appears that a lower ϵ_r material such as teflon-fiberglass may be suitable.

7.

Conclusions.

In summary, the above shows that one may be able to get 36 *dB* directive gain from a 1580 element hexagonal array. The element may be circular and gives linear and circular polizations. The feed is connected through a 90 ° hybrid and is fed from below the ground plane to the antenna above. The substrate of the microstrip may be teflon-fiberglass with mechanical flexibility required in a conformal array. The conventional feeding network is the corporate feed. The phase shifters are of the pin diode type.

In the next part of this discussion we shall study the design of a particular microstrip array.

Part B: A Tentative Design of a Microstrip Antenna Array.

Part A discussed in general terms the design requirements of the microstrip phased array and their possible solutions. In Part B we shall be specific by discussing the design of a particular array. In this part, specific choices of design are chosen either because the choice of design is better than the alternative, or because the choice is taken simply to eliminate unnecessary decision between two or more equally well designs.

For the specific array design we study the following:

(i) The 3-faced array pyramid for horizon to horizon scanning coverage.

(ii) The circular disk antenna element for the circular polarization.

(iii) The phase shifters.

(iv) The array layout on each face of the array pyramid.

(v) The feeder systems for the array.

In Section 12 the loss of the feeder system is discussed and from the discussion, the microstrip feeder system (instead of the image line one) is chosen.

An novel feeder system, which has the lower loss than the image line system, but has an easier fabrication than the microstrip system, is discussed at the end of this report.

The conclusion of this part discusses the array designs as a whole and gives some explanations, with reference to Part A why some choices in the designs are made.

It may be noted that in this part we shall call the corporate feed a corporate feeder, and the horn reflector feed the horn reflector feeder. These new terms are used so that the antennas inside the horn reflector later in Fig. 18 can be called feeder antennas so that they are not confused with the feed waveguide of the horn reflector or the antennas of the microstrip antenna array.

8.

The Three-Faced Array Pyramid.

Before discussion the array pyramid we shall establish two points:

(i) For scanning without grating lobes but with the maximum gain, the element separation should be kept at 0.5 λ_0 (free space wavelength) in the array. This rules out the possibility of piggy-backing of the high frequency array elements on the low frequency ones. Therefore we need in fact two separate arrays, one for the uplink frequency (44 *GHz*) and one for the downlink frequency (21 *GHz*).

(ii) A circular polarization is needed for the array since a mobile earth terminal cannot maintain a constant linear polarization of its antennas with respect to that of the antenna of the satellite.

With these two points established we shall now discuss the three-faced array pyramid.

A planar array cannot be scanned to the horizon because of the fattening of the beam shape and the loss of circular polarization. Therefore, it can only be scanned to a maximum of, say ± 60 ° from its normal direction. To enable the scanning to the horizon Therefore, three antenna arrays are needed, each one is to be mounted on a face of the pyramid of Fig. 6.

We may assume that the normal for each pyramid face is 45 ° from the zenith direction. Then each face of the pyramid will have a shape as shown in Fig. 7.

The uplink array has only half the linear dimension of the downlink array, therefore both arrays can be fitted comfortably on a pyramid face as shown.

Except for the reduction in size, the uplink array and its antenna elements are identical to those of the downlink array, therefore we need not distinguish these two frequencies in the discussion of the design of the antenna array.

9.

The Radiative Element of the Array.

The radiative element of the array chosen for this design is the circular disk with a centre short circuit and two-feed points at 90 ° in azimuth angle from each other as shown in Fig. 8.

Such locations of the feed points excite two orthogonal TM_{11} modes in the circular disk. The root of the TM_{11} mode is $ka = 1.84$ whre a is the radius of the disk. With $\epsilon_r = 2.1$ for PTFE substrate, we get

$$a = \frac{1.84}{\omega\sqrt{\epsilon_r \mu_0 \epsilon_0}} = \frac{6.06 \times 10^9}{f} \tag{2}$$

Therefore at frequency $f = 20$ *GHz*, $a = 3$ *mm*, and $f = 40$ *GHz*, $a = 1.5$ *mm*.

The PTFE substrate thickness can be 10 mil or 0.25 mm. This is acceptable as this thickness amounts to 10 °electrically in free space even at 40 *GHz*.

The feed point location along a radius is not decided yet. However, from Long, et al. [9] or from Bahl and Bhartia [10] one observes that it should be 1/3 radius out from the centre to give a radiation impedance of 50 *ohms*.

10.

The Phase Shifters.

The directive gain of the array is given by

$$D = G_{el} + 10 \log \quad N \quad dB \tag{3}$$

With $G_{el} = 5$ *dB*, $N = 1024$ elements, we get $D = 35$ *dB* or the beamwidth of 3.5 °. For a ±60 °scan we need approximately 32 beam positions this means a 5 bit phase shifter.

Following the phase shifter design of Amitay and Grace [11], the 5-bit phase shifter will have the form shown in Fig. 9, 10 and 11. Fig. 11 is the driver for 4-bit phase shifter. A 5-bit phase shifter is similar.

The detailed discussion on the phase shifter appears in Chapter 8 by Tiltek Limited in this report, therefore it will not be repeated here.

11.

The Array Layout

A microstrip antenna array on the pyramid face is formed on a copper plate coated on the top side by 0.25 mm of PTFE dielectric. On the top side the 1024 circular patch antennas are arranged in a 32 x 32 square grid as shown in Fig. 12. For circular polarization, each antenna has two outputs this makes 64 outputs per row of antennas and there are 32 rows in the array. Each row of outputs from the bottom of the grid plane of the arrays is connected to a perpendicular phase shifter and driver card as shown in Fig. 13. Each card has 64 inputs, and every two inputs are connected to a hybrid for the required circular polarization. One arm of the hybrid is corrected to a 5-bit phase shifter as shown in Fig. 14. Each phase shifter has an output, and a driver board to activate the pin diodes.

12.

The Feeder Systems

a) The Corporate Feeder.

The corporate feeder is assembled in a series of T-junction cards as shown in Figs. 15 and 16 that is, each 32 to 1 corporate feeder is to be etched on a card of aluminium coated copper plate. As observed Fig. 15 a total of 33 such cards will be sufficient for the corporate feeder system.

The Wilkinson isolated splitter [13] is used for each T-junction The Wilkinson isolated splitter is shown in Fig. 2.

(b) The Insertion Loss in a Corporate Feeder System

As pointed by James, et al. [14] that the conduction loss in microstrip feed line forms a significant limit to the achievable gain in a microstrip array. As the array size grows, the directive gain will increase proportionally. However, as the array size grows the feed line lengths become long and the feed line loss will eventually increase faster then the directional gain and the net power gain of the array will therefore decrease.

Collier [15] has quantified the maximum of the net power gain if an array with corporate feeder. Following his approach we arrive at the following for an N element square array with elements spaced at $0.5\ \lambda_0$ (free space wavelength) from each other. First the directive gain is that of Bach [1].

$$D = G_{el} + 10 \log_{10} N \quad dB \tag{4}$$

where G_{el} is the element gain, say 5 *dB* for microstrip paths.

The $0.5\lambda_0$ spacing of the elements implies that if the array area is L^2, then $4\ L^2 / \lambda_0^2 = N$, where N is the number of array elements. As observed in Fig. 17 that in a corporate feeder the length of feed line from the input point to any element is at least L or, more likely, $L\ 3/2$. Then the net power gain of the array, modified from (4), is

$$G = G_{el} + 10 \log_{10} N - \sqrt{N}\ \frac{3}{4} F \tag{5}$$

where F is the feed line loss in *dB* per wavelength.

For a microstrip line based on the measurements by Hori and Itanami [16] the factor F seems to be a constant (with the minimum at about 0.04 to 0.06 dB per unit wavelength for PTFE substrate), independent of frequency. This means that the net power gain in (3) is a function only of the number of elements in the array. The higher loss in *dB* per metre in a higher frequency does not affect the net power gain, as in this frequency the dimensions of the array, and therefore the feed line lengths are shorter.

Fig. 17 plots the net power gain of the array versus the element number for different losses. It appears that for 1024 elements. The microstrip line corporate feeder will have an insertion loss of between 2 to 5 *dB* respectively for line lossess between 0.08 *dB* / λ_0 to 0.2 *dB* / λ_0. This kind of losses appear to be tolerable.

The image line has a loss less than 0.02 *dB* / λ_0 according to Hori and Itanami [16]. Fig. 17 then shows that the corporate feed insertion loss can be no more than 0.5 *dB*. Such reduced loss is accompanied by the expense of fabricating the image line and by the possibility of leakage from the dimensionally larger image line.

The two paragraphs above and Fig. 17 therefore show that if the feed line length can be kept to 3 $L/2$ and the line loss can be kept to 0.05 *dB* / λ_0, then the microstrip line corporate feeder can be used, even at 44 *GHz*.

To end it is to be pointed out the insertion loss of pin diode phase shifter (5-bit) may be on the average 2 *dB*. This loss was not included in the above calculations, but should be included to get the absolute gain.

(c) An Alternate (Horn Reflector) Feeder System

The previous section states that the insertion loss in the corporate feeder with image line can have 0.5 *dB* loss. But because of its difficultly in construction, especially in the T-junctions and quarter wave transformers, and because of the possibility of leakage, the microstrip line is favoured. The corporate feeder of the latter line has a loss of about 1 to 3 *dB*.

To achieve the lower insertion loss of 1 *dB*, one has to be very careful in the etching process of the microstrip line, especially at the high frequency of 44 *GHz* for the uplink. An alternative system of feeding seems to be able to reduce the difficulty in construction and reduce the insertion loss at the same time. This system is the horn-reflector system.

A horn reflector [17] is a well known antenna as shown in Fig. 18. It is converted to a feeder system through covering its aperture with an array of N feeder antennas, the antennas may be linearly polarized microstrip patches.

The advantages of this system are as follows:

(1) It is a system easy to construct,

(2) It has low loss. According to Crawford, et al [17] the loss of the antenna is only 0.09 *dB*. We can expect a similar small number for the corresponding feeder system.

(3) It's dimension normal to the aperture of the microstrip antenna array is not large, but about the same as the aperture. In fact, this may be only twice as long as the dimension of the corporate feeder mounted at the back of the microstrip antenna array as shown in Fig. 15.

(4) The horn reflector feeder system lends mechanical support to the flat microstrip antenna array.

The feeder antennas that radiate into the horn reflector have linear polarization, therefore they can be simple circular disks identical to that in Fig. 8, but with only one, instead of two, feeding point. Because of the similarity between the two antennas the details of the latter are not repeated here.

13.

The Conclusions

The specific design of the array uses the three faced pyramid to enable the array to scan from horizon to horizon. A planar phased array with some mechanical steering may do the same, however, for mechanical clearance the mechanical steering device must raise the planar array above the body of the carrying vehicle and therefore distroys the aerodynamic smoothness in an airborne carrier. Therefore the mechanical steering is not considered.

As mentioned in Part A that the circular elements have less coupling than the rectangular ones. Therefore they are easy to arrange in a square grid in Fig. 12 for the corporate feeder of Fig. 15.

The phase shifter is taken from Tiltek's Chapter 8 in this report. this phase shifter needs two pin diodes per bit.

The array layout is a square grid. It is chosen instead of the hexagonal grid because square grid is easier to feed by the corporate feeder. However, if the horn reflector feeder is used then the hexagonal grid may be used.

For ease of manufacturing and ease of packaging at the high frequencies of 21 and 44 *GHz* all phase shifters and corporate feeders are printed on cards. This also makes it easier to delete the corporate feeders cards and mount the array with its phase shifter cards directly on the horn reflector feeder of Fig. 18.

An unexpected discovery in the report is that of the element separations are kept at 0.5 wavelength for arrays of all frequencies. then the insertion loss is nearly constant. This means the microstrip corporate feeder can be used instead of the image line feeder. This way reduce the complexity in the construction of the microstrip antenna array.

The horn reflector feeder is a novel idea, it is easy to construct, it has low loss and it can feed a hexagonal array layout. Therefore it is a feeder that may warrant some serious considerations.

Finally, we may say that the above discussion points to the conviction that a 1024 element microstrip antenna can be built. The insertion loss can be only 3 or 4 *dB* even for a microstrip corporate feeder at 44 *GHz*.

References

1. H. Bach. "Directivity diagrams for uniform linear arrays." *Microwave J.*, 15, pp. 41-44, 1972.
2. L.R. Murphy. "SEASAT and SIR-A microstrip antennas." Proc., Workshop, Antenna Technology, New Mexico State University, USA., pp. 1-18 to 18-20, 1979.
3. J.R. James, P.S. Hull, C. Wood. "Microstrip antennas theory and design." P. Peregrinus Ltd. and IEE London, pp. 188-189, 1981.
4. K.R. Carver and J.W. Mink. "Microstrip antenna technology." *IEEE Trans. on Antennas Propagat.*, Vol. AP-29, pp. 2-24, 1981.
5. R.P. Jedlicka, M.T. Poe and K.R. Carver. "Measured mutual coupling between microstrip antennas." *IEEE Trans. on Antennas Propagat.*, Vol. AP-29, pp. 147-149, 1981.
6. Y.L. Chow and D.G. Fang. "Mutual couplings between two microstrip antenna patches." Submitted to: *IEEE Trans. on Antennas Propagat.*, 1981.
7. R. Stodeton and M.M. Balint. "15 GHz microstrip array development." Ball Aerospace Systems Division, Technical Report: TR-80-403, 1980.
8. I.J. Bahl and P. Bhartia. "Microstrip Antennas." Artech House, Dedham, MA, pp. 317-327, 1980.
9. S.A. Long, et al, "Impedance of a circular-disc printed circuit antenna." *Electronics Letters*, 14:684-686, 1978.
10. J.J. Bahl and P. Bhartia, "Microstrip Antennas." Artech House, Dedham, MA, pp. 91-95, 1980.
11. A. Amitay and B. Grace, "Switching performance of a 12 GHz pin phase shifter/driver module for satellite communication phased array." *IEEE Trans. on Commun.*, 29:46-50, 1981.
12. J.L. Yen, "Interim Report: Study of EHF controlled-beam antenna for SATCOM." Dept. Electrical Engineering, University of Toronto, for the Dept. Communications, Ottawa, Ont., 1982.
13. J.R. James, P.S. Holland, C. Wood, "Microstrip antenna theory and designs." Peter Peregrinus Ltd., Stevenage, U.K. pp. 176-177, 1981.
14. J.R. James, P.S. Hall and C. Wood., "Ibid cit." pp. 186-190.
15. M. Collier, "Microstrip antenna array for 12 GHz TV." *Microwave J.*, 20:67-71, 1977.
16. T.Hori and T. Itamani, "Circular polarized linear antenna using a dielectric image line." *IEEE Trans. on Microwave Theory and Technical*, MTT-29, pp. 967-970, 1981.
17. A.B. Crawford, D.C. Hogg and L.E. Hunt, "A horn-reflector antenna for space communication." *Bell System Technical J.*, Vol. 40, pp. 1095-1116, 1961.

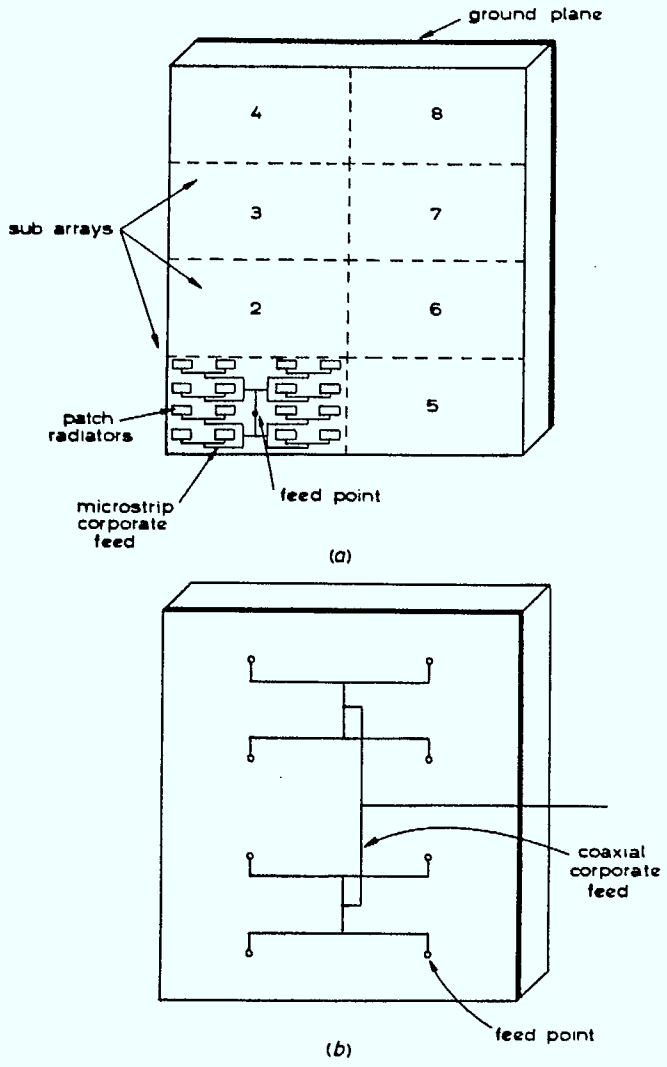

Fig. 1 One panel of 1024-element microstrip array for SEASAT satellite antenna.

(a) Front view, showing 8 subarrays of microstrip patches with integral micrstrip corporate feeds.

(b) Rear view of one panel showing co-axial feed conneting 8 microstrip subarrays.

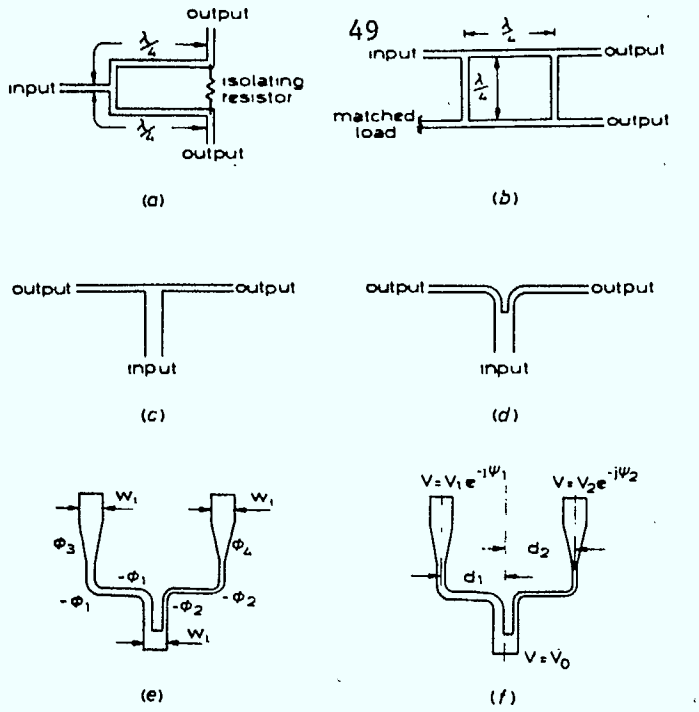

Fig. 2 Types of power splitter and phase errors that occur in in-line splitters.

(a) Wilkinson isolated splitter.

(b) Two-arm branch line isolated splitter.

(c) T-junction splitter.

(d) In-line splitter.

(e) Phase errors in an asymmetric power splitter. 0 = (actual electrical length - physical mean path length) 01,02 = phase errors at bends; 03,04 = phase at tapers ω_i = line width at input and outputs.

(f) Compensation method for phase errors in (e):

If $\Psi_1 > \Psi_2$ then $d_1 > d_2$ for $\exp(-j\ \omega\ t)$ time variation.

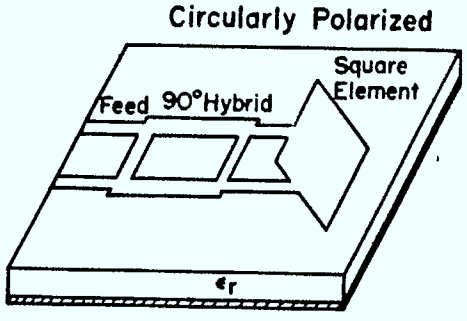

Fig. 3 Square patch antenna.

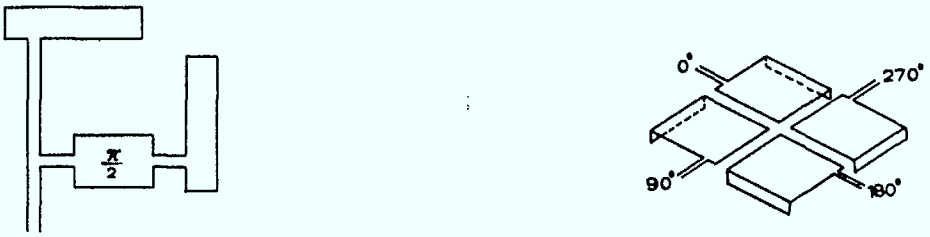

Fig. 4 Some possible configurations of microstrip patches for circular polarized applications.
(a) Offset rectangular open-circuit patches.
(b) Crossed-slot using four short-circuit patches.

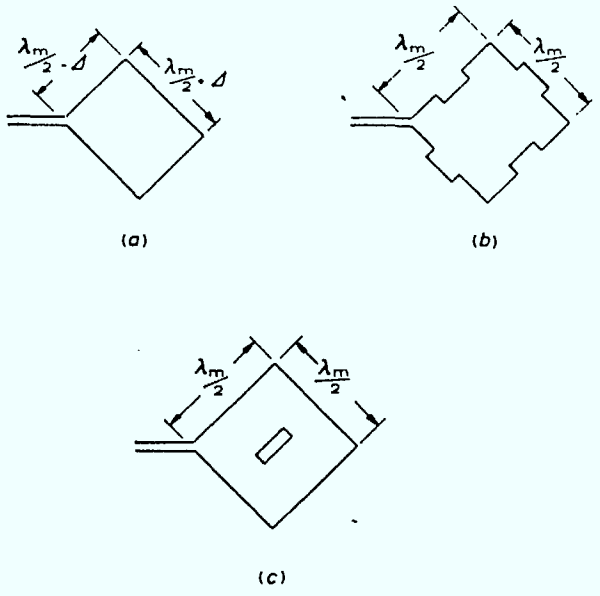

Fig. 5 Circular polarization of patches obtained by detuning of orthogonal modes.
(a) Almost square patch.
(b) Modes capacitively detuned with tabs and gaps at edges.
(c) Modes inductively detuned with central slot.

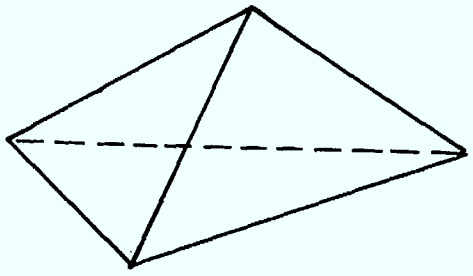

Fig. 6 The pyramid with three equal faces for mounting the arrays.

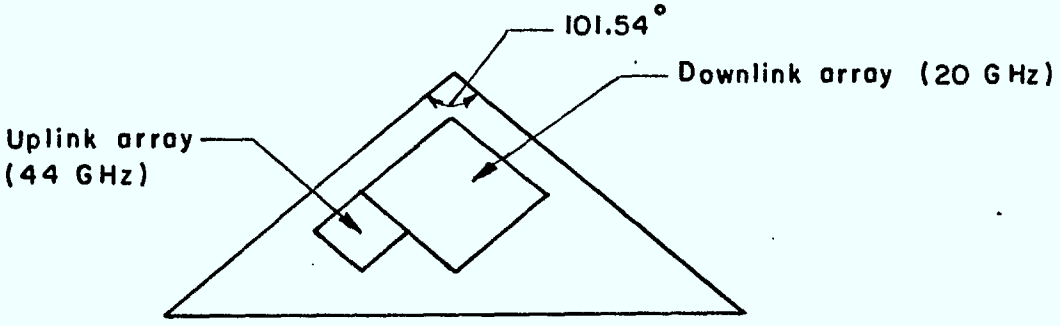

Fig. 7 The layout of the arrays for up- and downlinks on each face of the pyramid.

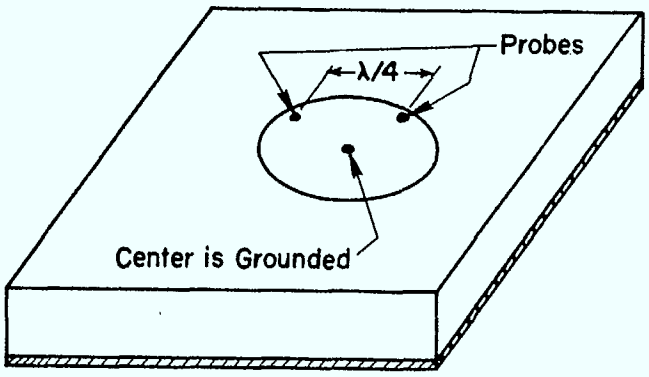

Fig. 8 Circularly polarized disk antenna.

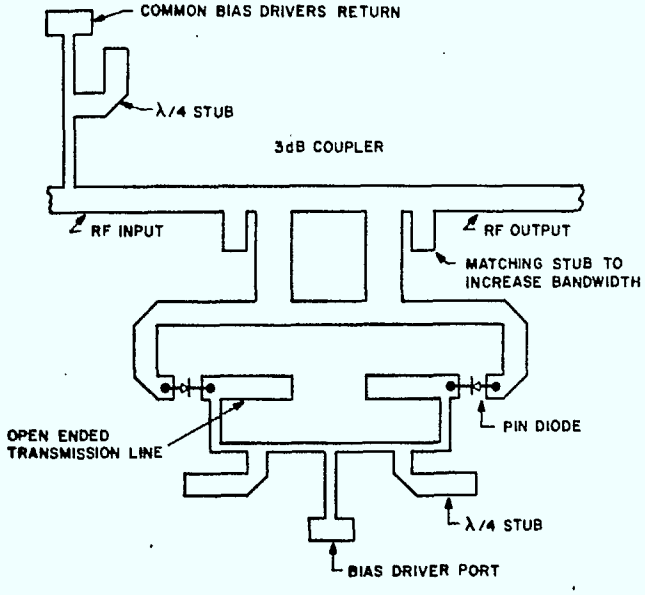

Fig. 9 Schematic description of an individual phase shifter cell depicting p-i-n diodes, 3 *dB* coupler, and biasing circuit.

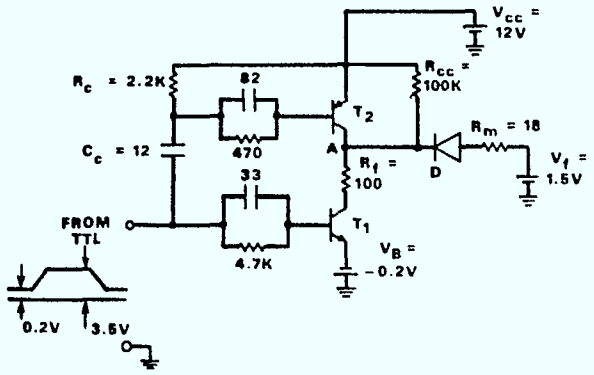

Fig. 10 Schematic diagram of an individual bit driver T_1 - HP35824A; T_2 - 2N4261.

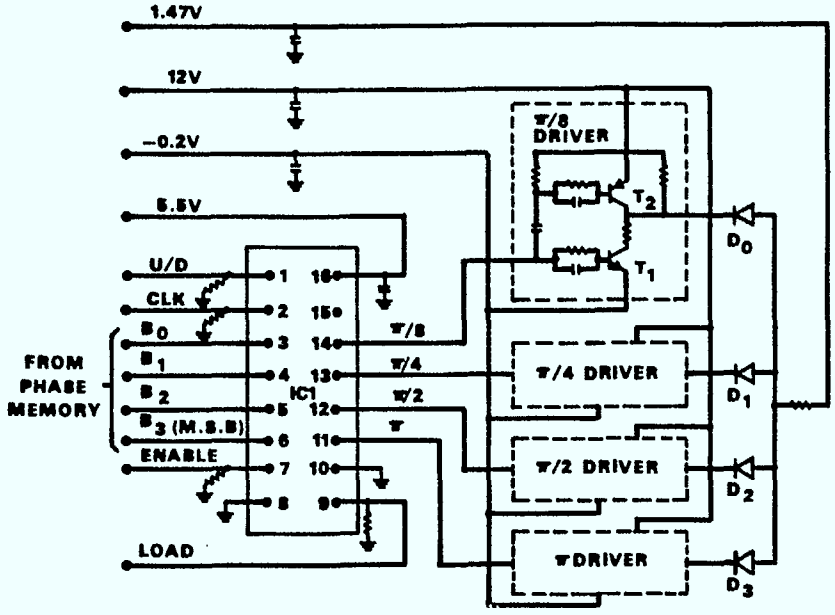

Fig. 11 Schematic diagram of the driver circuit board. T_1 - HP35824A; T_2 - 2N4261; IC1 - SN74LS669W.

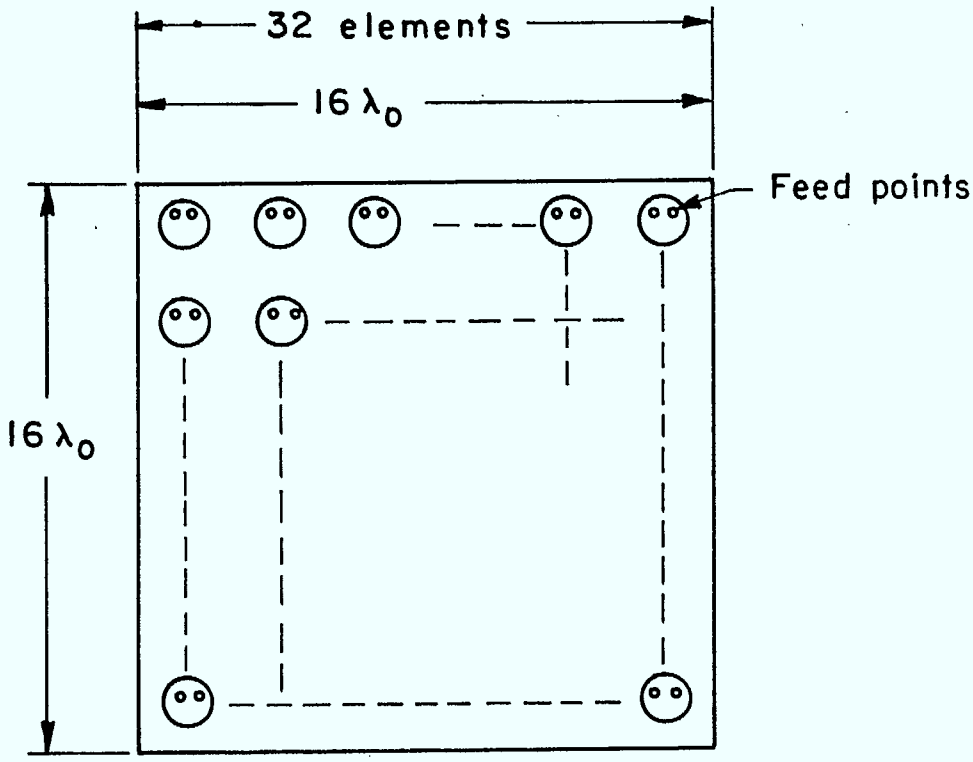

Fig. 12 TOP VIEW OF THE ANTENNA CARD

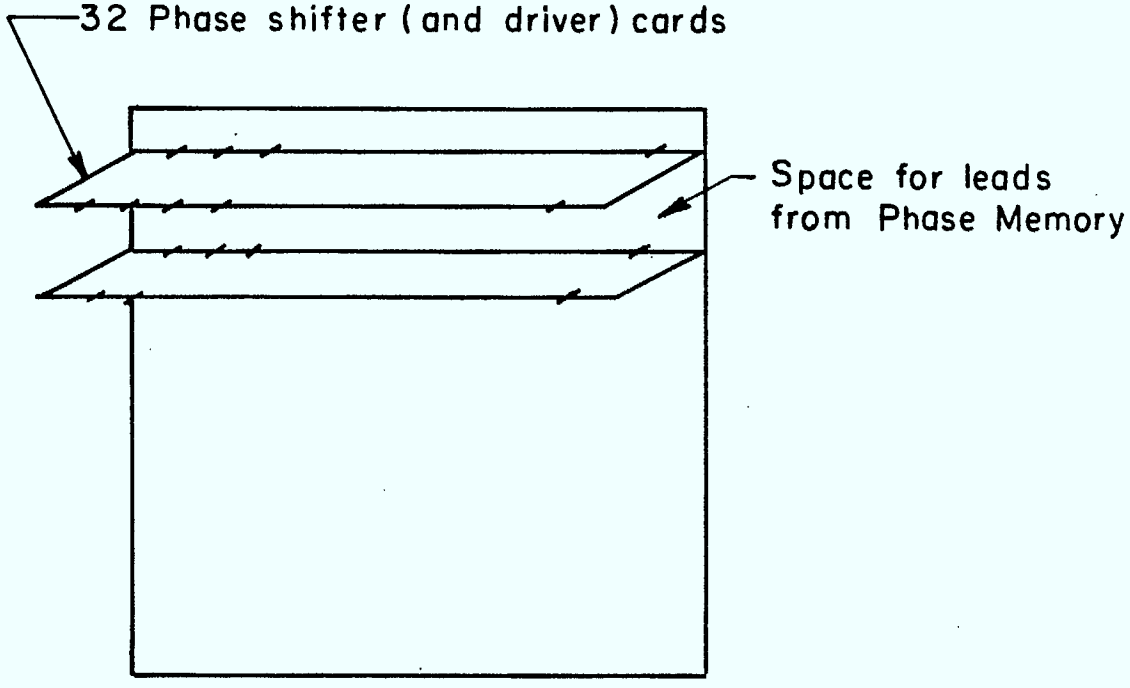

Fig. 13 THIS FIGURE SHOWS :
THE CONNECTION OF THE PHASE SHIFTER CARDS
TO THE BOTTOM SURFACE OF THE ANTENNA CARD

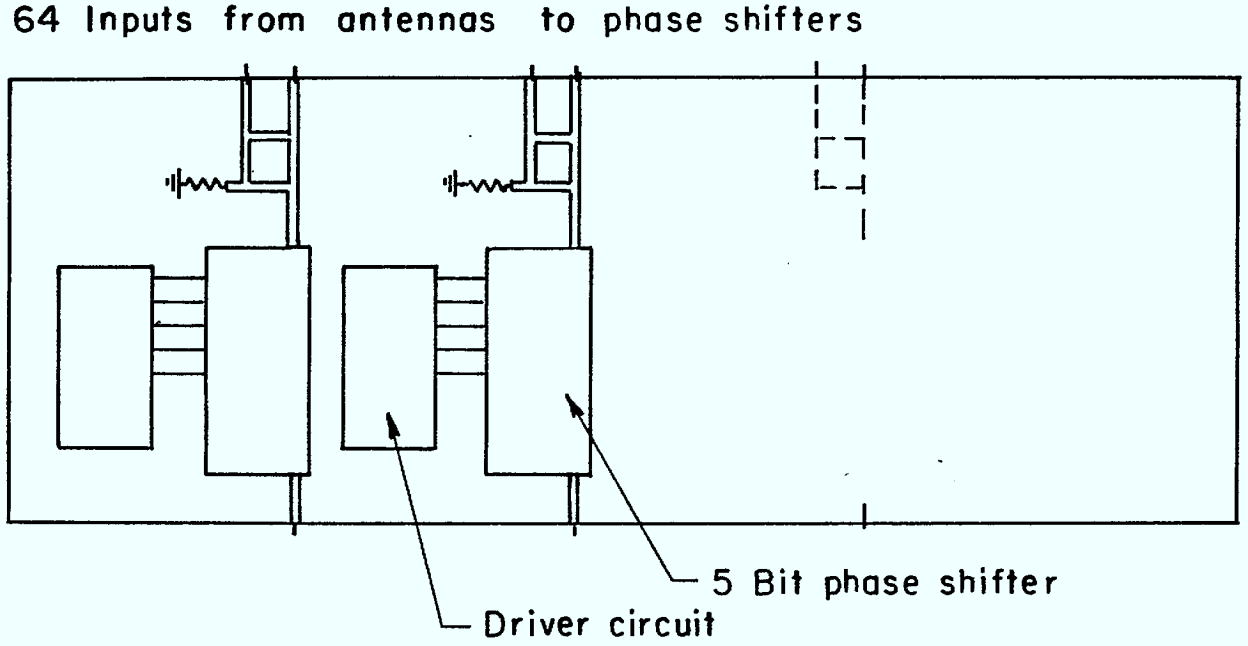

Fig. 14 A PHASE SHIFTER-DRIVER CARD

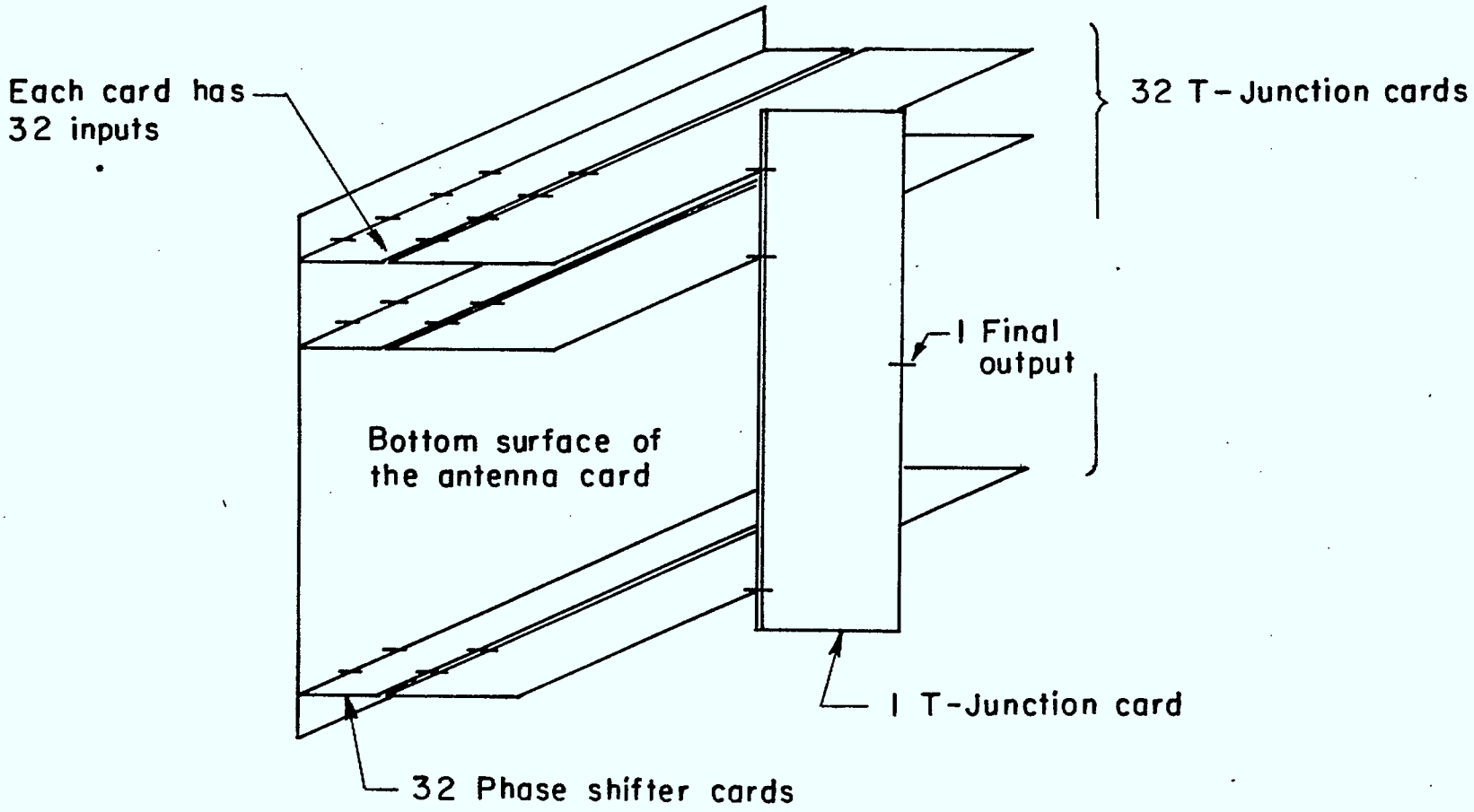

Fig. 15
THE MOUNTING OF T-JUNCTION CARDS AT THE BACK OF THE MICROSTRIP ANTENNA

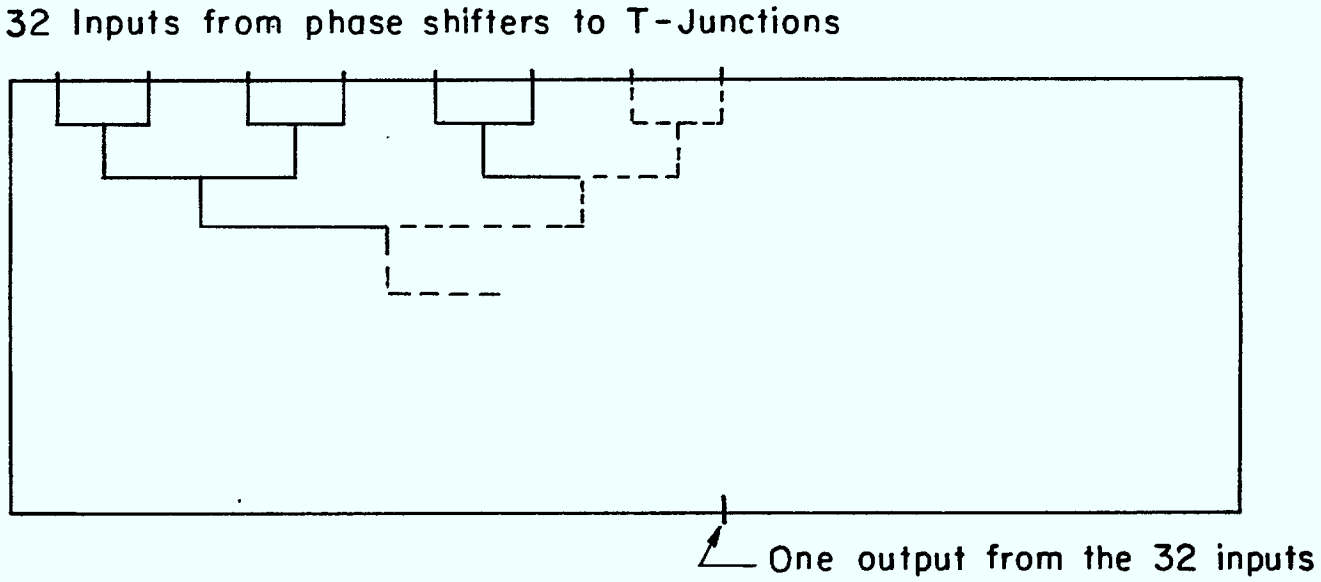

A T-JUNCTION CARD

Fig. 16
THE LAYOUT OF T-JUNCTIONS ON EACH CARD

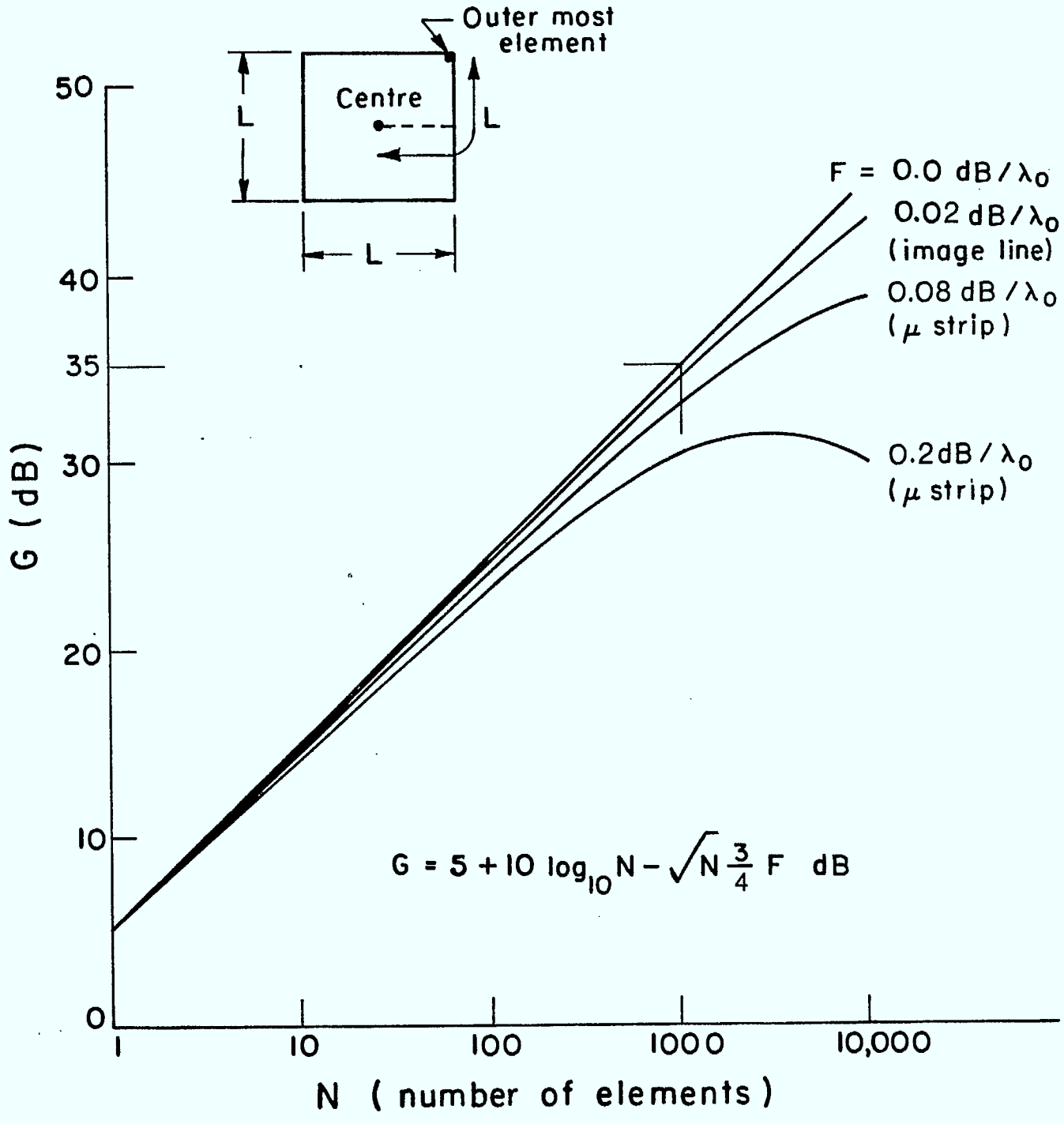

Fig. 17 The net power gain of the microstrip array with corporate feeder versus the array element number for different line losses F.

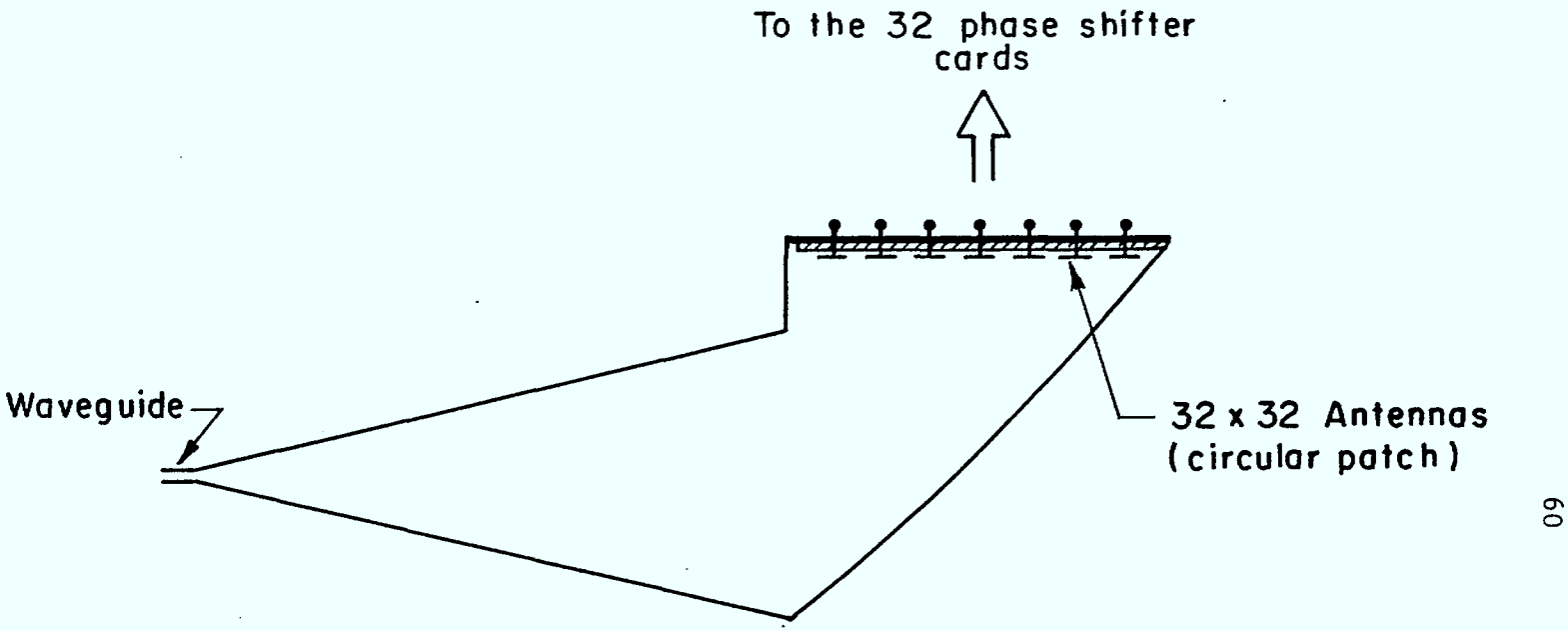

Fig. 18 HORN REFLECTOR FEEDER SYSTEM

Chapter 5

REFLECTOR ARRAYS

Tiltek Limited

1.

General

In a large class of antennas there is a primary antenna or feed, and a secondary antenna which may be either a reflector or a lens.

The feed can take the form of one or more low gain horns, dipole-reflectors, or other type of low gain structure intended mainly to illuminate an aperture of the secondary radiator.

The secondary surface is used to transform the incoming radiation from the feed into a narrow beam emanating in the desired direction.

In the case where the secondary radiator is a reflector, it is common to have a shaped surface such that the reflected beam may be derived from the incident rays by means of the principles of geometric optics, at least to a first order. Such is the case with parabolic and paraboloidal sections. The surface impedance of such reflectors is usually zero since they are considered to be perfectly conducting. The effects of such reflectors my be determined purely by their geometry. There is a more general class of reflectors, however, in which both the surface geometry and the surface impedance may be used to redirect the incoming rays. This class will be referred to here as reflector arrays since the change in surface impedance may be implemented by properly choosing the terminal reactances of individual array elements.

An example of such a reflector array, termed a "reflectarray antenna" was given by Berry, Malich and Kennedy [1]. Their experimental antenna surface was approximated by open-ended surfaces of waveguides which were short circuited at appropriate distances behind the reflector aperture which was flat (Fig. 1). With this array, aperture efficiencies of 60 percent or more were obtained. It was also found that circular polarization could be achieved reasonably well with this type of array.

The reason why the "reflectorarray", and in particular the waveguide "reflectorarray", was chosen lay in the opportunity which was presented for electronic steering. All that needed to be done was to change the electrical length of the waveguide sections in an appropriate manner. In the example cited, this was accomplished through the use of shorting diodes in each guide. Thus, rapid scanning could be carried out without the necessity of employing elaborate corporate feed structures. It was discovered that the short-circuit points could be calculated reasonably well with a geometric optics approximation. It was found that diode losses could be kept to less than 1 *dB* if 3 diodes per waveguide were used and beamwidths of 4 ° to 5 ° were required. Despite the seeming benefits of this type of antenna, not much more appeared for some time. This could be due to several reasons, including the need for further diode development, the fabrication costs of large numbers of waveguide sections, and the concentration on other reflector and lens types.

The surface impedance concept was however used in both passive [2] and active retrodirective antennas [3], [4].

Comparisons between different theoretical approaches to some of the problems involved were made by Appel-Hansen [5] who considered a Van Atta Reflector consisting of Half-Wave Dipoles. He was able to determine the effect of scattering and coupling on the radiation pattern.

Recently Wang, Blount, Ryan and Puskar have studied "Diode-Switched Reflectors and Lenses" [6]. In these structures, antennas sections were switched in or out, by means of pin diodes which were connected in series between them. One of the authors has mentioned (Wang) that a lack of low-cost pin diodes would probably hinder the use at present of this type

of antenna.

A possible competition for the reflector array is the so-called "Radant" antenna mentioned elsewhere. This is a switched lens type of antenna in which diodes are used to switch the lens properties. Compared to a switchable reflector, a switched lens has several drawbacks which will be enumerated later.

2.

Possible Use of Electronically Controlled Reflector Arrays at EHF.

One of the main criticisms which may be laid against the use of electronically controlled reflector arrays at EHF is the high cost of the phase or amplitude controlling elements. Yet this is really no different from the cost of controlling elements in any kind of phased array, and in fact the requirements may not be as stringent in the reflecting case.

A great advantage of the diode controlled refecting array over the switched lens lies in the biasing circuitry of the former which can be accessed from the back of a conducting plane.

A further advantage of the reflector is the possibility of fabricating (printing) all of the reflecting elements, plus the coupling lines and reactances, on a flat plate, thus largely obviating the need for an elaborate three dimensional structure.

Another benefit lies in the possibility of designing a reflector array as a conformal surface when this is required. Additionally, the inclusion of an elementary sub-program in the overall control program could perform the task of electronic beam stabilization, should this be required.

3.

Areas of Investigation.

In considering a circularly polarized reflector array the following areas of investigation should be included:

- Type of array element. It is felt that these should be flat structures such as crossed-dipoles, patches, slots, etc.;
- grounding of elements. Attention must be paid to the grounding in order to minimize fabrication cost and simplify the biasing circuits;
- feed circuits and location, including types of 90 ° phase shifters for polarizers, etc.;
- phase shifting mechanisms;
- cell size necessary to approximate a continuous impedance surface. Relationship between number of cells, cell size, gain, etc.;
- connecting lines between elements and the allowable space between elements on which to mount (or print) associated components;
- possibility of using dual frequency elements; number, size and position of feed elements;
- probable cost per element.

4.

Method of Approach.

In an investigation such as that envisaged here, a theoretical model, probably based on the impedance surface concept, would be devised. Both computer studies and model experiments would be carried-out to establish the validity of the basic concepts.

The reflector array in principle seems capable of producing, at one extreme, the same kind of agile performance as the phase array, while at the other extreme it may also be capable of

performing the function of a more usual multi-beam reflector antenna. It has an extra advantage in the fact that its geometry lends itself to fabrication methods compatible with future microwave integrated circuit techniques.

References.

1. D.G. Berry, R.G. Malech and W.A. Kennedy, "The Reflectarray Antenna." *IEEE Trans. on Antennas and Propag.*, November 1963, pp. 645-651.
2. E.M. Rutz-Phillipp, "Sperical Retrodirective Array." *IEEE Trans. on Antennas and Propag.*, March 1964, pp. 187-194.
3. C.Y. Pon, "Retrodirective Array Using the Heterodyne Technique." *IEEE Trans. on Antennas and Propag.*, March 1964, pp. 176-180.
4. S.N. Andre and D.J. Leonard, "An Active Retrodirective Array for Satellite Communications." *IEEE Trans. on Antennas and Propag.*, March 1964, pp. 181-215.
5. J. Appel-Hansen, "A Van Atta Reflector Consisting of Half-Wave Dipoles." *IEEE Trans. on Antennas and Propag.*, November 1966, pp. 694-700.
6. J.J.H. Wang, D.R. Blount, C.E. Ryan, Jr., R.J. Paskar, "Diode Switched Reflectors and Lenses." *APS Symposium on Antennas and Propag.*, May 1952.

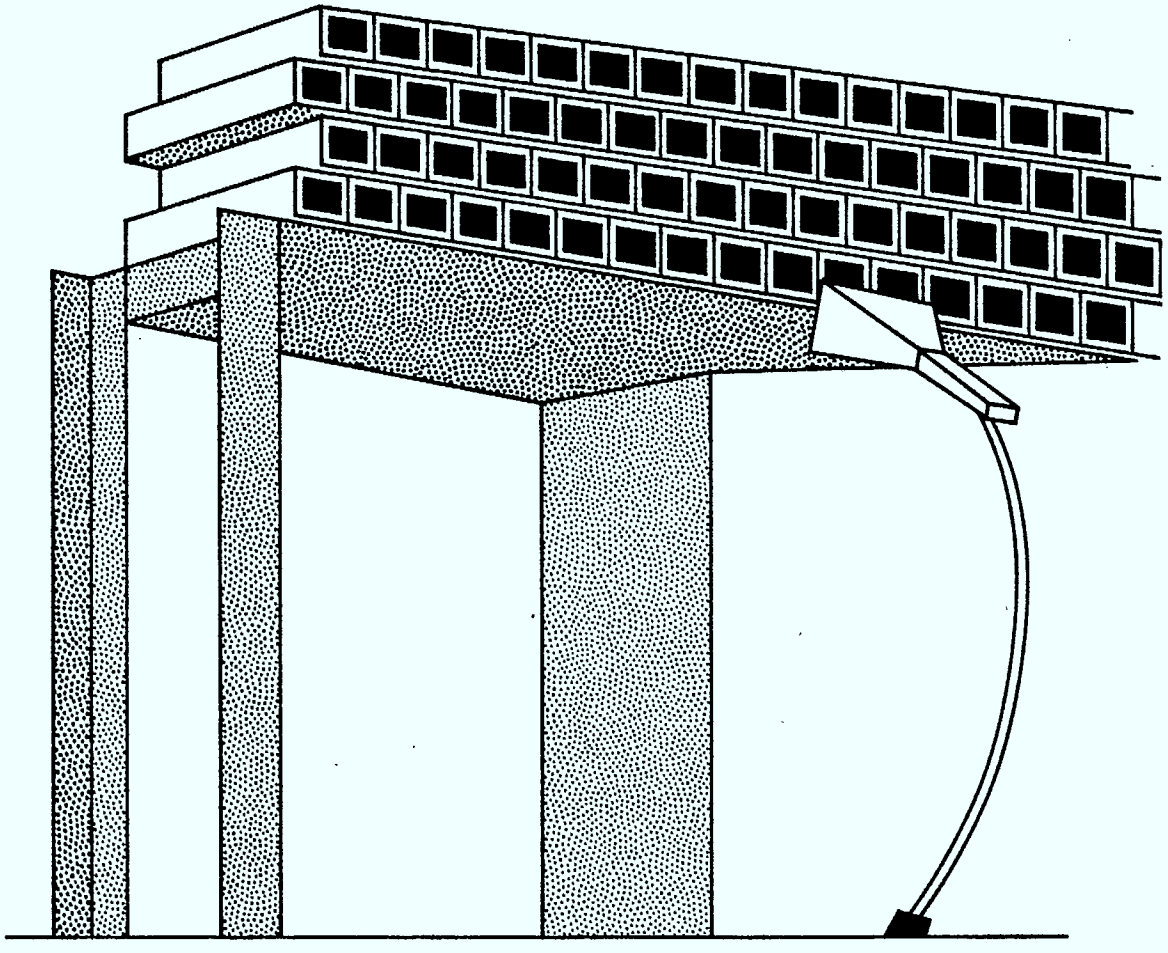

Figure 1 Waveguide array reflectarry with staggered rows

Chapter 6

CONTROLLED-BEAM ANTENNAS.

J.L. Yen

1.

Introduction.

The most unique character of satellite communications (SATCOM) systems is that many users in widely separated locations can share the same satellite. The sharing can be based on time, frequency, the way in which the signal is coded and the position of the user. This very character which makes SATCOM so useful also makes it very vunerable to disruption by interference. For secure communications it is therefore necessary to encode the signals with unique time, frequency and code characteristics so as to make the channel impervious to interference. When these methods fail further discrimination based on the spatial separation between user and interference using antennas capable of sophisticated beam control has to be introduced. Because both user and interference often move and change their transmissions, methods capable to adapt to changing scenarios need be used. In this Section we survey controlled-beam or adaptive antennas with special emphasis on EHF SATCOM. In addition, we list some unsolved problems and some promising approaches to practical systems. The hardware required for implementation are discussed in Section 7 of this report.

Adaptive antennas for extraction of desired signals from undesired interferences were first introduced in radar and sonar. Lately, considerations for communications purposes are gaining attention. The adaptive concept, being general and robust, have found many other fields of application such as noise cancelling, echo suppression, equalization and in adaptive control systems. It is also related to many nonlinear spectral estimation techniques such as auto regressive and maximum entropy methods. A large body of knowledge on adaptive system is in existence. As examples we quote the recent special issues [1], [2] of IEEE publications devoted to these topics. Interests on adaptive antennas are gaining even at a faster rate. Prior to 1979 the number of papers on the topic are limited. This is followed by over 20 papers in 1980 and 30 in 1981 published in open journals. In addition, two books [3], [4] appeared in 1981. Certain laboratories have also emerged as leaders in the field. For a review of adaptive systems in general we refer to the tutorial paper by Widrow [5], and for adaptive satellite antennas, we refer to the excellent surveys by Cummings, Jain, and Ricardi [6] and by Mayhan [7]. In view of the vast amount of material available, the following contains a concise review of the fundamental concepts emphazising some new aspects important for SATCOM which have not been studied before.

2.

Controlled-Beam Antennas.

A controlled-beam antenna is a system that in the presence of many signals incident from different directions, it is capable of separating the desired ones according to control instructions and deliver them to the system output. It performs two functions, beam steering under external control and removal of undesired interference by identifying them as they are received. It is a steerable beam adaptive antenna. Fig. 1 shows the structure of a controlled-beam antenna. It consists of a number of fixed elements each with an independent output port. The signals from the element ports are linearly combined in a separator to remove the undesired interferences. To locate the directions of desired and undesired signals the element ports are also connected to a correlator which estimates the coherence matrix of the scenario. The controller then analyses the scenario and, together with external control commands and the system outputs, controls the separator to select the desired signals.

The outputs of the antenna should be undistorted replicas of the desired incident signals. For antenna configurations in which an incident signal arrives at each element with no relative delay, separation of different signals can be accomplished by weighting of each element before combining. If a signal arrives at each element with different delays, delay compensation using a transversal filter is required [8]. When the fractional bandwidth is small delay compensation is replaced by phase shifting. The signal separator can therefore be implemented in the fashions of Fig. 2. The degree of separation that can be achieved, i.e. the nulling resolution, depends on the antenna configuration, the element field patterns and the signal bandwidth.

When a single signal is incident on the antenna the response of each element port has a unique phase and amplitude, depending on the antenna configuration and the source direction. When many signals from different directions are incident on the antenna, the cross correlations of signals generated at the element ports, i.e. the coherence matrix, characterize the powers and directions of the incident scenario. The correlator estimates the coherence matrix from which the control processor takes action. When the incident signals are mutually independent, the coherence matrix and hence the ability to analyse different scenarios depends on the element cross power pattern, the baseline (or element position difference) configuration and the signal bandwidth. These dependences have not been fully noted before and will be discussed later in more detail.

The signal separation is commonly optimized according to certain criterion of performance and the separator weights are derived from the well known Wiener filter theory. Let the criterion be that the mean square error between the antenna output and the desired signal is a minimum. Let X; be the jth element port output, d the desired signal, W the weight vector, R the coherence matrix

$$R = E[x_j\, x_k^*]$$

and S the steering vector

$$S = E[x_j\, d^*]$$

The optimum weights are given by the Wiener solution

$$W^0 = R^{-1}S$$

If all incident signals are stationary, using W_0 determined from the received signal statistics will achieve the optimum output in the steady state. The controller derives the optimum separator weights W_0 from the coherence matrix and external control constraints. The constraints can be in the form of the coded nature of the desired signal [9], the desired signal direction [10], [11] or the power level [12]. In fact, it is possible to separate all the signals when its number is less than the number of elements in the antenna using the eigenvector beams [13], [14]. The implementation of the processor can make use of different algorithms. With some very simple and widely used iterative algorithms such as the LMS [5], the coherence matrix R need not be estimated explicitly, hence the correlator and the controller merge into a single unit.

In some systems the desired signals come from fixed locations having fixed frequencies while in others the signals come from different directions at different times at varying frequencies. In most situations interferences are of unknown locations with varying frequencies and can turn on and off unexpectedly. The antenna therefore sees many different scenarios and must adapt to each scenario to discriminate against undesired interferences. To achieve this the antenna configuration must be chosen so it can satisfy the steady state performance required. In addition, fast adaptation to varying desired and undesired signals is also necessary. The convergence time of various adaptive algorithms and their trade-off with processing complexity, an aspect which is now well understood, will be discussed later.

3.

Antenna Configuration and Signal Separation.

In earlier works on adaptive antennas small elements with little directivity are used to form an array. The output of elements are combined with appropriate weights just as in an ordinary antenna array, but with the added requirement of not only having maximum response in a desired direction, it must also have nulls at the directions of the interferences. Hence, the term adaptive array is used. More recently, considerations for SATCOM applications lead to the use of narrow beam antennas as elements. In addition to considering element locations the element directive pattern also has to be included. In a series of papers [15] - [19], Mayhan and his colleagues analyzed many aspects of antenna configurations and their nulling properties. However, most of these studies were based on numerical simulations. Due to the importance in the selection of appropriate configuration to achieve given objectives, we discuss the basic relation between antenna configuration and signal separation from a heuristic point of view for better understanding.

First it is necessary to distinguish between a phased array and a multi-beam antenna. A phased array consists of many similar elements with their phase centers distributed over a certain array configuration. A signal arrives the at elements with a particular delay distribution depending on the element positions, and the direction of incidence. With each element having a beam covering the required field of view, the signal of each element port will have almost the same amplitude but with different delay or, in case of narrow band signals, different phase. A multi-beam antenna on the other hand makes use of a large aperture with different feeds generating almost similar beams in a certain beam configuration. The beams must overlap somewhat so that the cluster covers the desired field of view (FOV). A signal arriving from a particular direction will generate a large signal from the port whose beam points toward the source. As discussed in Sections 2 and 3, the optics of a phased array is to image the aperture onto the feeds while a multi-beam antenna images infinity onto the feeds. Thus, the array configuration and output phases of element ports provide information on incidence directions in a phased array while the beam field pattern configuration and output amplitudes of beam ports yield information on direction for a multi-beam antenna.

Consider the hexagonal multi-beam antenna discussed by Mayhan [15], [16], a seven beam cluster covering the field of view, as shown in Fig. 3a. The circles are equal level contours which describes the amount of overlap. Due to symmetry, the equal level contours between two adjacent beams are seen to be the hexagon correpsonding to the inverse lattice as shown in Fig. 3b. The seven beams are combined with equal amplitude and phase to cover the entire FOV in the quiescent mode. If an interference located within the centre beam as shown in Fig. 4a is to be cancelled while covering the entire FOV as completely as possible, it is seen that the central beam should have a negative sign with reduced amplitude while the outer beams remain the same so that the desired null is produced. The numerical result of [15] is shown in Fig. 4b for comparison. However, due to hexagonal symmetry a ring null would be produced which is undesirable. To reduce this effect, introduce a small phase difference between the beams to destroy the hexagonal symmetry, but not large enough to produce ripples in quiescent beam. In the presence of interference the central beam need to change both amplitude and phase to produce the desired null. Since there is no hexagonal symmetry the null will no longer be a ring as shown in Fig. 5a. The corresponding numerical results in [18] are shown in Fig. 5b. Finally, instead of requiring near complete coverage of FOV, it is required to maximize the gain at desired position while nulling the interferences. For the scenario of Fig. 6a we need to change the sign in one beam to produce the null and in two beams in the opposite side to enhance the desired direction by adding the side lobes. As a result two null contours are introduced which compares well with the numerical result of [15] shown in the same Figure. As the frequency is changed the beam shape of a multi-beam antenna will change. If the beams are generated using nondispersive means the beam directions will not vary with frequency. The hexagonal equal level contour between adjacent beams depends only on beam directions and hence will remain unchanged. If an interference source is

located on the equal level hexagon, the beam weightings required to cancel the interference will not depend on frequency. Thus we expect the signal separation ability of a multi-beam antenna to be relatively independent of frequency.

Next we consider phased arrays. A phased array generally makes use of identical elements each with a beam covering the FOV. The phase centres of the elements are located in certain regular or irregular fashion forming the array. The elements collectively cover an aperture area either densely or thinly. A beam is formed by appropriate weighting of the elements. The phase distribution in relation to the array configuration determines the direction of the beam while the amplitude distribution controls the beam shape. Since the steering of a phased array requires insertion of delay, which can be approximated by phase shift only for small fractional bandwidths, adaptive antennas using phased arrays are in general more frequency dependent, and hence requiring transversal filters for large bandwidths. An adaptive array can be considered as a superposition of two patterns, a quiescent beam and a maximum directivity beam scanned to the direction of the interference source by appropriate phasing and weighted to form a null at the interference direction. Most of previous work on adaptive antennas dealt with uniformly spaced linear arrays with the odd papers discussing circular arrays [13]. Recently Mayhan and his colleagues [17], [19] discussed thinned arrays for adaptive antennas. These arrays appear to perform well on their nulling resolution.

The beam forming properties of arrays are well understood since the early studies of Schelkunoff [20]. Extensive literature on many aspects of arrays including phased arrays [21], [22] are in existence. The radiation pattern of an array distributed over a regular lattice is characterized by periodic patterns with respect to the inverse lattice of the array. Only the portion of the pattern in the visible spectrum is important. The main beam of the array is inversely proportional to its total dimension. With the same number of elements, the main beam can be made smaller by using large element spacings. However, this reduces the spacings of the inverse lattice such that a copy of the main beam can move into the visible spectrum resulting in undesirable grating lobes. By using nonuniform spacings the grating lobes can be smeared into plateaus [23]. An example of improvement in average coverage of adaptive arrays realized by nonuniform spacing due to Mayhan [17] is shown in Fig. 7.

Among the measures describing the effectiveness of adaptive antennas against interference, the minimum loss in gain in the user direction as a function of the angular user-interference separation characterizing nulling resolution is of importance. Since interference cancellation depends on a maximum directivity beam pointing towards the interference direction, the maximum dimension of the antenna D/λ is the principal factor controlling nulling resolution. Fig. 8 from Mayhan [7] shows a typical result with angular spacing replaced by miles on earth's surface at 20 ° elevation angle from a geostationary satellite. It can be used as a general guide to decide on D/λ for specified nulling performance. Another important measure, again from Mayhan, is the average percent coverage of FOV with a given link margin as a function of $D/\lambda \sin\theta m$, where θm is the half angle of FOV. In this case the antenna is required to cover as much of the FOV as possible since the desired user position is unknown. Fig. 9 shows the degradation of coverage versus increase in number of interference sources.

4.

Antenna Configuration and Scenario Analysis.

The last section discusses the ability of an antenna configuration in separating from different directions. The way a controlled-beam antenna adapts to a scenario of incident signals depends on the coherence matrix of the signals incident on the antenna, which in turn depends on the cross power patterns between element pairs. Although this is related to the signal separation characteristics of the antenna configuration, the latter relation being dependent on the element field patterns is quite different. In an N-element antenna there are only N weights for signal separation while the coherence matrix has N (N + 1) /2 independent elements for scenario analysis. Early work on adpative linear arrays of uniform spacing deals with signals

delayed by equal amounts; hence, it is closely related to the temporal behaviour of signals on a delay line [24]. The coherence matrix is of Toeplitz form due to the redundancy of baselines. The large amount of literature on temporal signal analysis can therefore be directly applied. As soon as two dimensional antenna configurations are introduced the added spatial dimension no longer have equivalence in the temporal behaviour of signals. Thus, the ability of an antenna configuration to analyse scenarios through the coherence matrix need be fully understood before a configuration can be selected intellegently. This aspect of the problem has not received attention in existing work on adaptive antennas. In the following we discuss some of the fundamental considerations and the questions that need be answered.

For a single source located in one of the element beams of a multi- beam antenna the coherence matrix has a single large diagonal element for that beam and has smaller magnitudes for correlation between that beam and its close neighbors. The coherence matrix is Hermitian but non Toeplitz despite that for a configuration of regular form the cross power pattern between elements exhibit certain symmetry. The detailed behaviour of the coherence matrix depends on beam overlap and the side lobe distribution of each beam. For the seven element hexagonal beam antenna of Fig. 3 the regions in the FOV where various cross power patterns are significant are shown in Figure 10. The responses of the cross power patterns constitute the coherence matrix of the signal scenario.

For a phased array the response of all elements have the same magnitude but with different phases. The coherence matrix therefore has element phases depending on the baseline or position different between elements in relation to the incidence directions. For an N element array there are N (N-1)/2 baselines. If the array is linear and uniformly spaced there are only N-1 independent baselines, all the others being redundant. The coherence matrix is then Toeplitz and much of our knowledge on such matrices applies. It is well known in radio interferometry that the coherence matrix are samples of the Fourier transform of the source distribution. From these samples the source positions and intensities can be deduced. It is the basis of image reconstruction of incoherent source distribution by synthesis radio telescopes [25]. The relation between baseline configuration and image reconstruction is well understood, particular for nonuniform element distributions. For example a five element Arsac linear array with spacings 1,1,4,3 will sample baselines 1-9 with only one redundancy. This array is therefore superior to a uninform five element array in source resolution. Various two dimensional arrays for nearly uniform sampling of the baseline space have been well studied [26]. The role of baseline distribution in adaptive arrays has not yet been studied. For example in [19] a seven element triangular array is compared with a seven element rotated double triangle array by simulation. It is found that the variations of weight versus frequency for the two arrays are strikingly different, the former being much more simple. It is possible that baseline redundancy is the cause of the adverse frequency dependence of the double triangle array. As shown in Fig. 11 the rotated triangular array has only 15 independent baselines out of the total of 21, while the triangle as 18 independent ones. In [17] the uniform circular array was found to have superior performance over a triangular one. We again conjecture that this is because of the superior baseline configurations of the uniform circular array. In fact, an odd element circular array has completely nonredundant baselines covering a circle as shown in Fig. 12. It is therefore important to investigate the effects of baseline configuration on scenario analysis, adaptive algorithm, and in turn, source separation and nulling bandwidth.

5.

Adaptive Algorithms.

Many algorithms have been used in deriving element weights by the controller for desired signal separation. The most direct algorithm is to estimate the coherence matrix and perform a matrix inversion. This is known as sample marix inversion algorithm or SMI [27]. For an N element uniform linear array it is found that approximately 2N snapshots is sufficient to derive the optimum weights. In terms of data required the SMI is probably the most efficient. However, since matrix inversion requires N^3 multiplications it implies excessive computational

burden. Furthermore, it is difficult to implement without using a microprocessor.

A much simpler algorithm is a gradient method known as the least mean square or LMS algorithm [5]. In this method the coherence matrix need not be estimated, instead an iterative procedure is used to update the weights based on the current input and the error from desired output. This procedure is very simple to implement (see Fig. 13) in either analog or digital form, hence is widely used. However, the convergence depends on the spread of signal powers and thermal noise in the system. The larger the spread the slower is the convergence. The simplicity in implementation is negated by more snapshots of input signals required to approach the steady state. It is therefore inferior in adapting to fast changing scenarios. A third method is to diagonalize one row and one column of the coherence matrix at a time [28] to decorrelate the channels as shown in Fig. 14. The parallel-pipe-line operations permit faster implementation of the algorithm. Finally, SMI does not measure the state of the weights as part of the algorithm for error correction. A feedback path based on Kalman filter can be introduced [29]. For a detailed comparison of the different algorithms we refer to the excellent paper by Hudson [30].

Among the extensive works on adaptive algorithms we note two major areas of neglect. The first is that the space-time behaviour of signals have not been properly taken into account in the transversal filter treatment of broad band signals. If a system requies a K tap delay line for each of the N elements the total number element-delay ports is KN [8]. The usual way is to treat the KN dimension coherence matrix in the same way as if they are completely independent. However, if the signals are divided into K narrow band channels there is a common threat between the scenarios from the different channels. Thus, it should be possible to analyse the overall scenario by treating K coherence matrices of dimension N instead of a single matrix of dimension KN. The second area of neglect is the role of antenna configuration, in particular baseline configuration, on the convergence of the algorithms. Since, as we stated before, the antenna configuration has important bearing on scenario analysis, it should also effect the convergence of direct and iterative procedures in the controller. Such relations are completely unknown at this time.

6.

Prior Constraints.

The problem of prior constraints remain a principle one from a systems point of view. Some particular aspects directly influencing system design are as follows. If the users are on moving platforms it would not be possible to use desired directions as constraints, only a desired field of view can be adapted. If a direct sequence is used for signalling, a copy of the desired signal is known, however, code acquisition time may unduly degrade the system performance. Basing signal separation on large interference levels may induce the deployment of a large number of medium power jammers to confuse the system. System planning must therefore be preceded by detailed study of the possible scenarios.

7.

Implementation of Adaptive Systems.

Simplicity and robustness must be principle concerns in implementation. Between RF, IF or baseband signal separation, the choice lies in availability of control elements, their resolution and accuracy. The correlator would be difficult to realize at RF, hence IF or baseband must be used. Although analog implementation is simple as discussed in Section 7 it may suffer from lack of accuracy and dynamic range. It appears that digital implementation should be chosen whenever possible.

One-bit quantization offers simplification in processing and for dynamic range compression [31]. Recent studies of hard limiting however indicates failure in signal separation when the coherence matrix has two or more eigenvalues of differing magnitudes [32]. It is therefore

important to consider system performance versus data precision so as to optimize the trade-off with controller simplicity. Finally, the approach to constrained direction adaptive antennas using hardware differencing amplifiers recently proposed by Griffiths and Jim [33] appears to be useful in simplifying implementation.

8. Conclusions.

From the above discussions it is evident that in the design of controlled-beam SATCOM antennas the following must be considered.

(i) Trade-offs between unreasonableness of threats and cost to deploy a system capable of surviving actual or potential threats [34].

(ii) Selection of prior constraints based on a steerable beam concept.

(iii) Choice between multi-beam antenna and phased array.

(iv) Selection of antenna configuration with particular attention to baseline redundancy in scenario analysis.

(v) Selection of quantization levels in correlator implementation.

(vi) Selection of algorithm to optimize convergence time and computing burden. The ability of digital implementation using fast multipliers and other advanced IC's will be considered.

Some of these considerations are illustrated in the conceptual design of a reflector-antenna system with hybrid steering in Chapter 9.

References

1. IEEE Trans. Acust., Speech, Signal Proc., Vol. ASSP-29, Special issue on adaptive signal processing, June 1981.
2. IEEE Proc., Vol. 64, Special issue on adaptive systems, August 1976.
3. J.E. Hudson, "Adaptive Array Principles." New York, Peter Peregrihus Ltd., 1981.
4. R.A. Munzingo and T.W. Miller, "Introduction to Adaptive Arrays." New York: Wiley-Interscience, 1980.
5. B. Widrow, In: Aspects of Network and System Theory. Kalman and DeClaris (eds). New York: Holt, Rinehart and Winston, 1971.
6. W.C. Cummings, P.C. Jain and L.J. Ricardi, "Fundamental performance characteristics that influence EHF MILSATCOM systems." *IEEE Trans. on Commun.*, Vol. COM-27, pp. 1423-1434, October 1979.
7. J.T. Mayhan, "Adaptive Nulling with Satellite Antennas." In: Proc., 1980 Int. Conf. Commun., pp. 59.1.1-59.1.8 (June), 1980.
8. L.J. Griffiths, "A simple adaptive algorithm for real-time processing in antenna arrays." *IEEE Proc.*, Vol. 47, pp. 1696-1704, October 1969.
9. R.T. Compton, Jr., "An adaptive array in a spread spectrum communication system." *IEEE Proc.*, Vol. 66, pp. 289-298, March 1978.
10. O.L. Frost III, "An algorithm for linearly constrained adaptive array processing." *IEEE Proc.*, Vol. 60, pp. 926-935, August 1972.
11. S.P. Applebaum, "Adaptive arrays." *IEEE Trans. on Antennas Propagat.*, Vol. AP-24, pp. 585-598, September 1976.
12. R.T. Compton, Jr., "The power-inversion adaptive array: concept and performance." *IEEE, Trans. on Aerosp. Electron. Syst.*, Vol. AES-15, pp. 803-814, November 1979.
13. W.F.Gabriel, "Adaptive arrays -- an introduction." *IEEE Proc.*, Vol. 64, pp. 234-272, February 1976.
14. C.M. Hackett, Jr., "Adaptive arrays can be used to separate communication signals." *IEEE Trans. on Aerosp. Electron. Syst.*, Vol. AES-17, pp. 234-247, March 1981.
15. J.T. Mayhan, "Nulling limitations for a multiple-beam antenna." *IEEE Trans. on Antennas Propagat.*, Vol. AP-24, pp. 769-779, November 1976.
16. J.T. Mayhan, "Adaptive nulling with multiple-beam antennas." *IEEE Trans. on Antennas Propagat.*, Vol. AP-26, pp. 267-273, March 1978.
17. J.T. Mayhan, "Thinned array configurations for use with satellite based adaptive antennas." *IEEE Trans. on Antennas Propagat.*, Vol. AP-28, pp. 846-856, November 1980.
18. B.M. Potts, J.T. Mayhan and A.J. Simmons, "Some factors affecting resolution in an adaptive antenna." In: Proc., Int. Conf. Commun., June 1981, pp. 10.4.1-10.4.9.
19. J.T. Mayhan, A.J. Simmons, and W.C. Cummings, "Wide-band adaptive antenna nulling using tapped delay lines." *IEEE Trans. on Antennas Propagat.*, Vol. AP-29, pp. 923-935, November 1981.
20. S.A. Schelkunoff, "Electromagnetic Waves." New York: Van Nostrand, 1943.
21. A.A. Oliner, G.H. Knittel (ed.), "Phased Array Antennas." Artech House, Dedham, MA, 1972.
22. L. Stark, "Microwave theory of phased-array antennas -- a review." *IEEE Proc.*, Vol. 62, pp. 1661-1701, December 1974.
23. Y.L. Chow, "On grating plateaux of nonuniformly spaced arrays." *IEEE Trans. Antennas Propagat.*, Vol. AP-13, pp. 208-215, March 1965.

24. W.F. Gabriel, "Spectral analysis and adaptive array superresolution techniques." *IEEE Proc.*, Vol. 68, pp. 654-666, June 1980.

25. E.B. Fomalont, "Earth-rotation aperture synthesis." *IEEE Proc.*, Vol. 61, pp. 1211-1218, September 1973.

26. Y.L. Chow, "On designing a supersynthesis antenna array." *IEEE Trans. on Antennas Propagat.*, Vol. AP-20, pp. 30-35, June 1972.

27. I.S. Reed, J.D. Mullett and L.E. Brennan, "Rapid convergence rate in adaptive arrays." *IEEE Trans. on Aerosp. Electron. Syst.*, Vol. AES-10, pp. 853-863, November 1974.

28. W.D. White, "Adaptive cascade networks for deep nulling." *IEEE Trans. on Antennas Propagat.*, Vol. AP-26, pp. 396-402, May 1978.

29. J.E. Hudson, " Sidelobe cancellation using recursive Newton-Raphson and Kalman algorithm." Adaptive Antenna Workshop, Mulrem 1979.

30. J.E. Hudson, "Methods of accelerated convergence in adaptive antenna." Dept. of Elec. Eng., University of Technology, Loughborough, 1980.

31. L.E. Brennan and I.S. Reed, "Effect of envelope limiting in adaptive array control loops." *IEEE Trans. Aerosp. Electron. Syst.*, Vol. AES-7, pp. 698-700, July 1971.

32. F.W. Floyd, Jr. and J.T. Mayhan, "Some effects of hard limiting in adaptive antenna systems." *IEEE Trans. Aerosp. Electron. Systm.*, Vol AES-16, pp. 839-850, November 1980.

33. L.J. Griffiths and C.W. Jim, "An alternative approach to linearly constrained adaptive beamforming." *IEEE Trans. Antennas Propagat.*, Vol. AP-30, pp. 27-34, January 1982.

34. W.T. Brandon, "Design trade-offs in antijam military satellite communications." In: Proc., 1981 Nat. Tel. Conf., pp. D 9.2.1-D 9.2.5 (December), 1981.

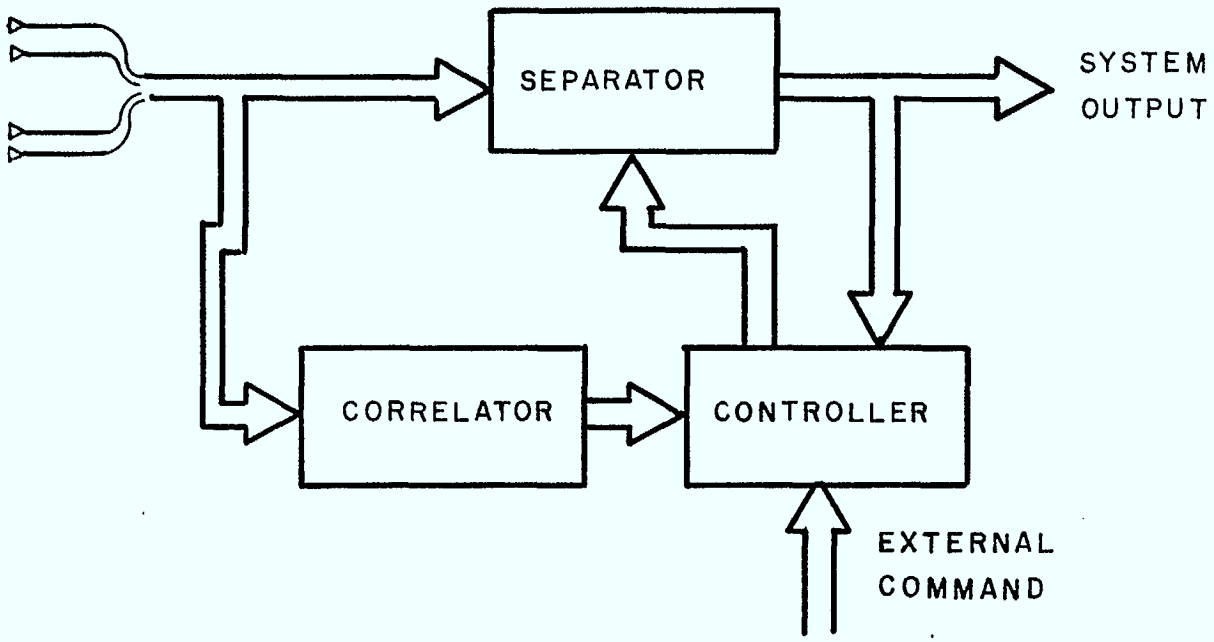

Fig.1

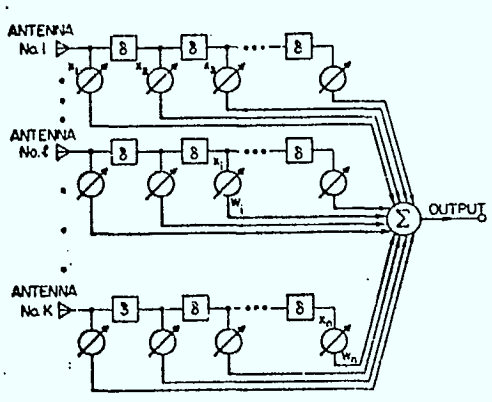

Adaptive array configuration for receiving broadband signals.

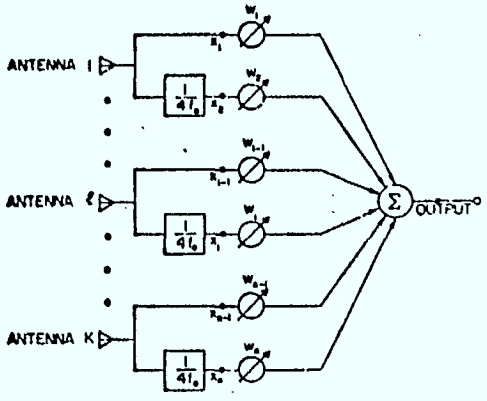

Adaptive array configuration for receiving narrowband signals.

Fig.2 From (8)

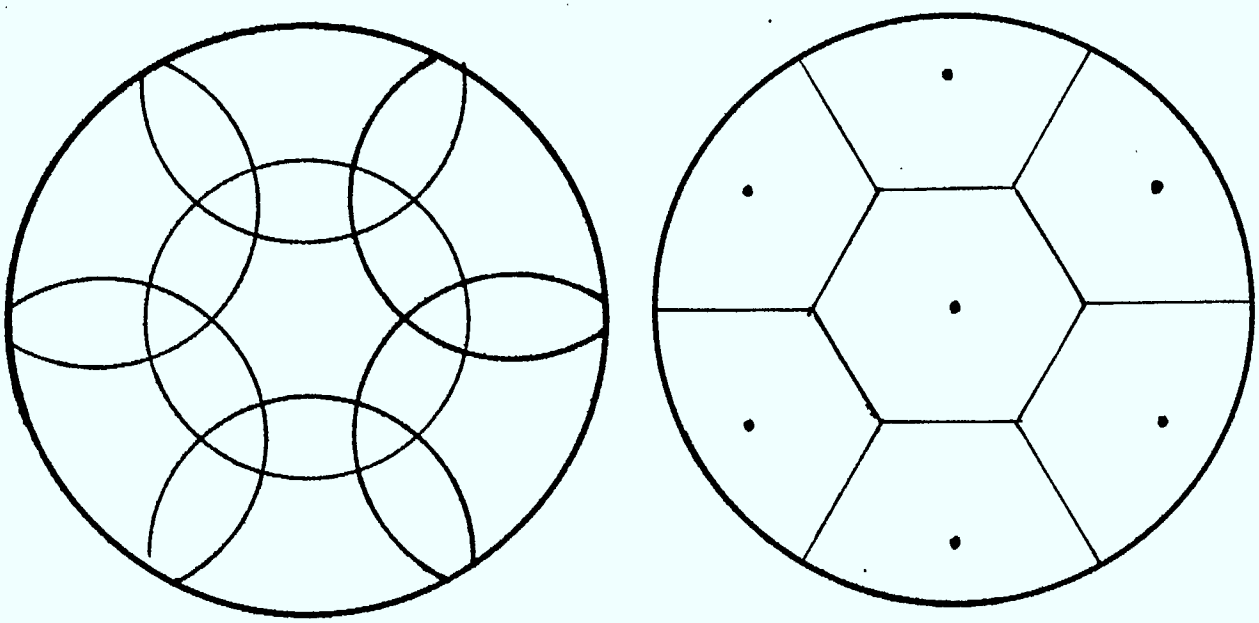

a b

Fig.3

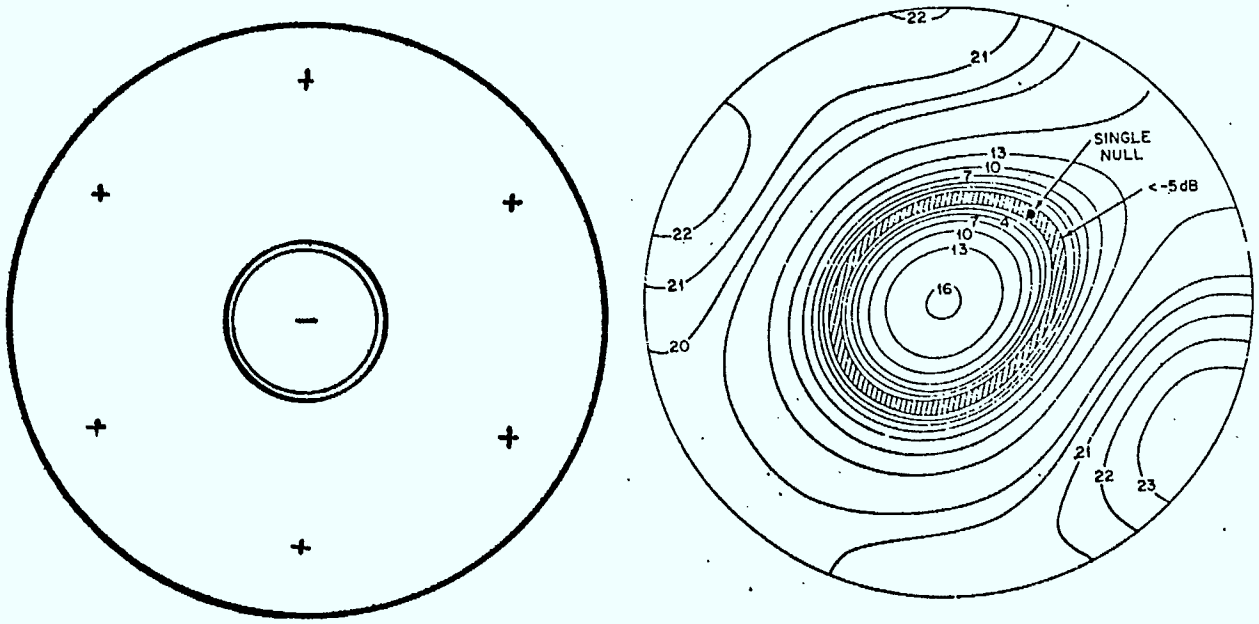

a b From (7)

Fig.4

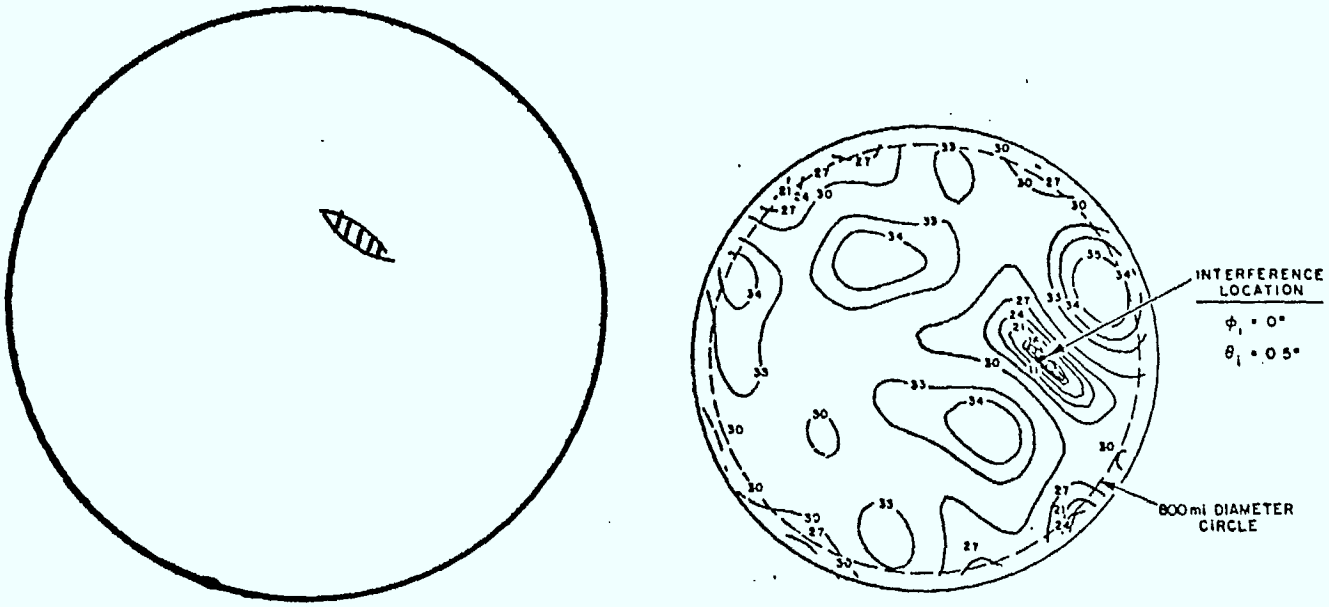

a b From (18)

Fig.5

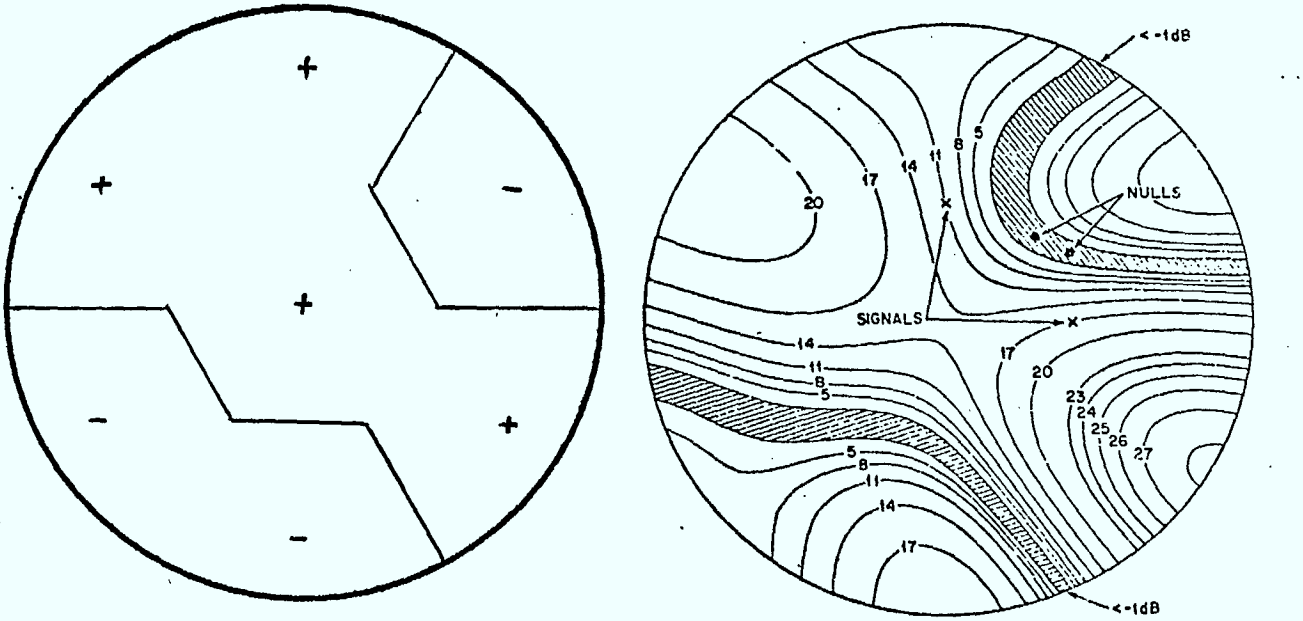

a b From (15)

Fig.6

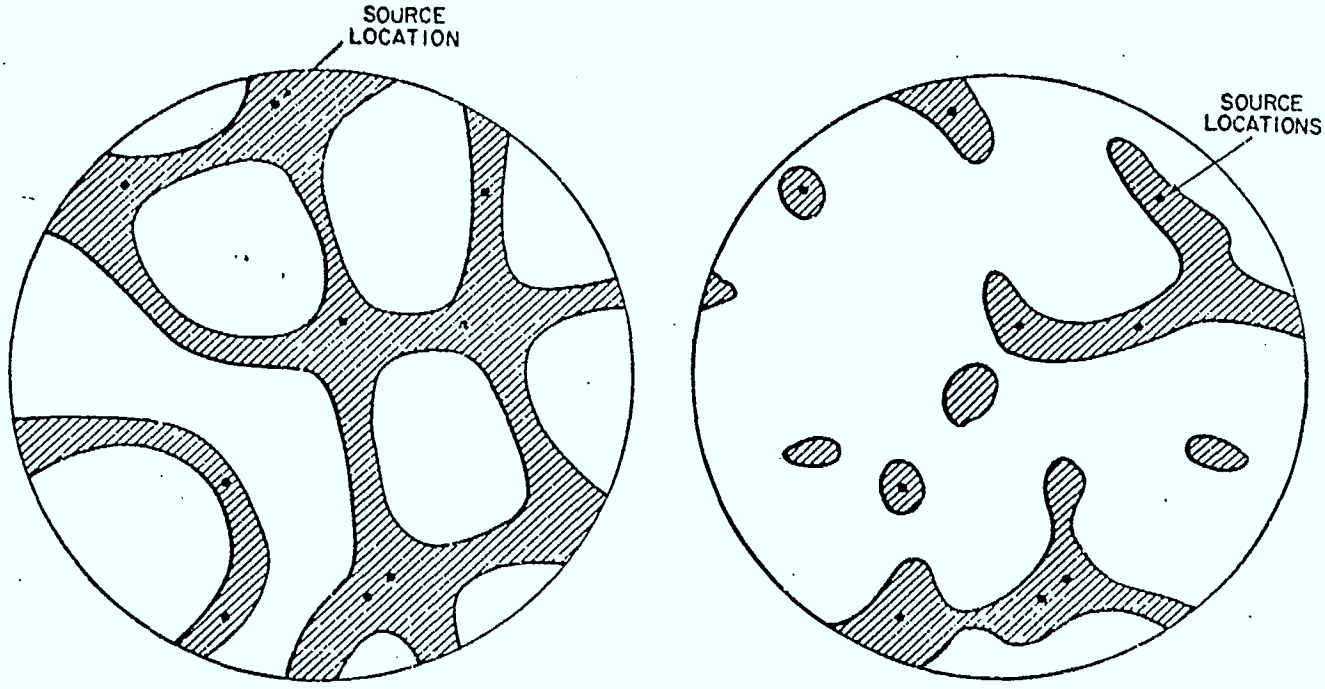

Fig.7 From (17)

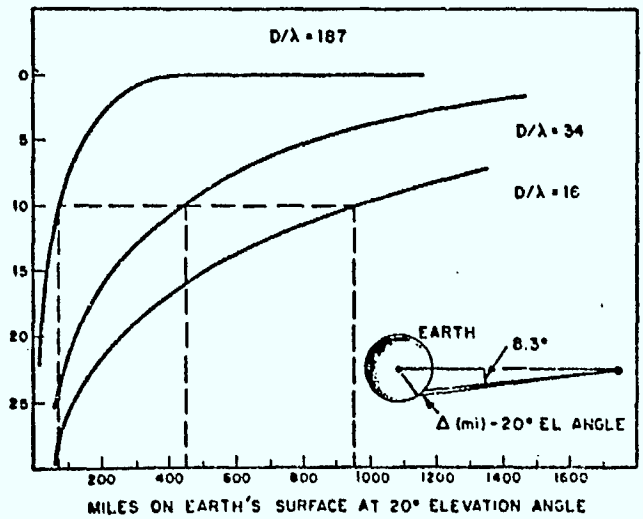

Fig.8 From (7)

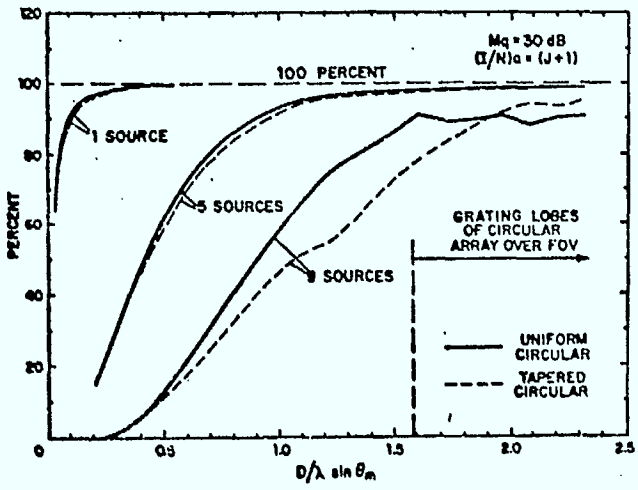

Fig.9 From (7)

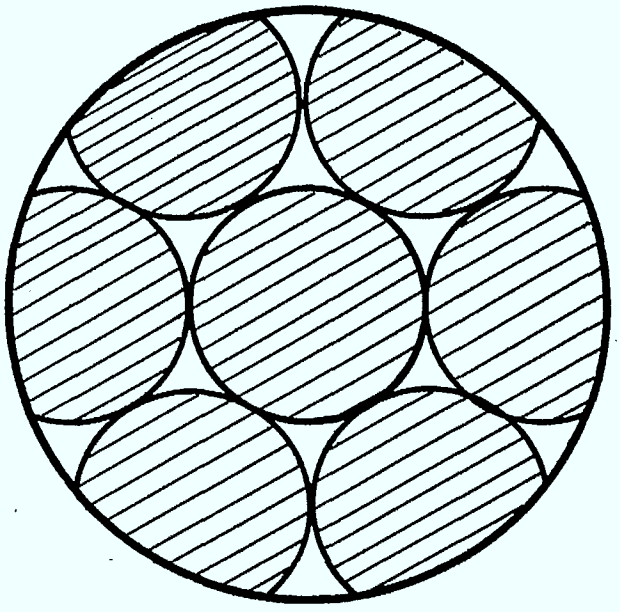

BEAM
POWER PATTERN

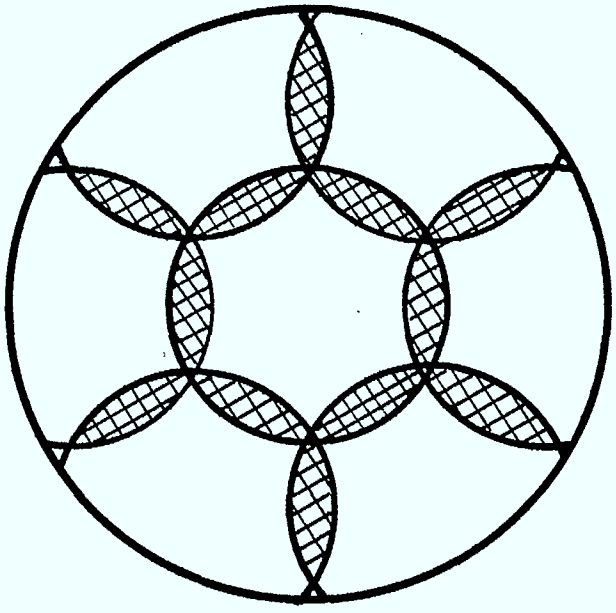

ADJACENT BEAM
CROSS POWER PATTERN

Fig.10

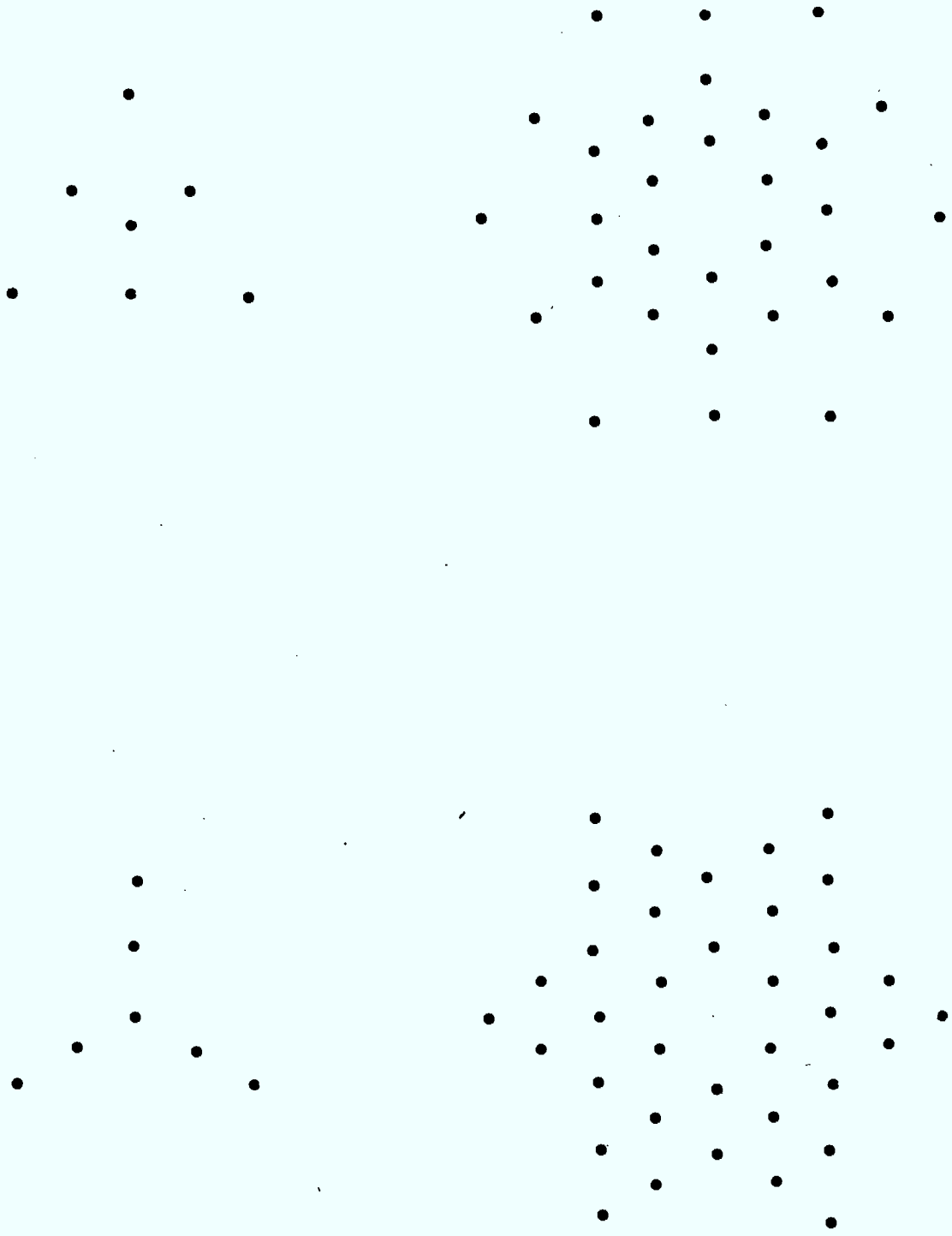

Fig.11

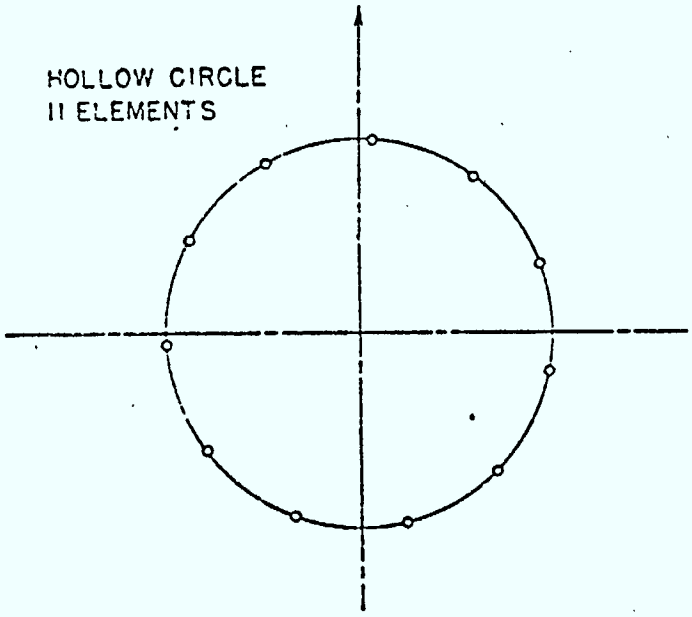

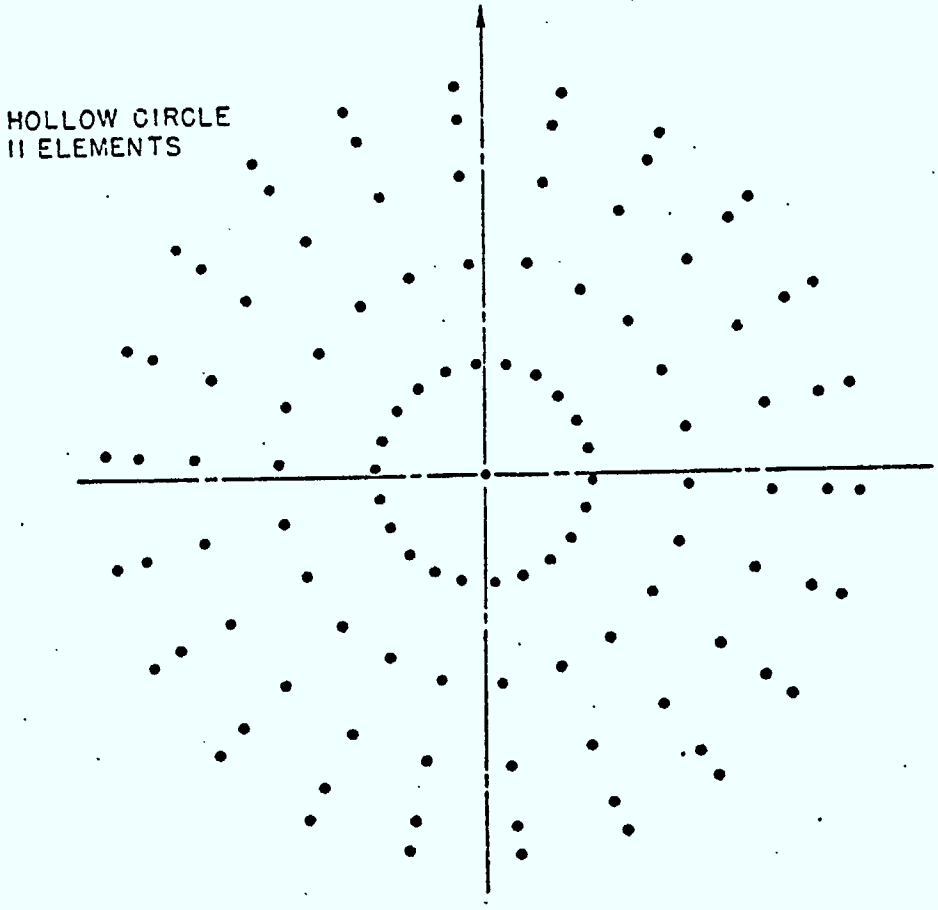

Fig.12

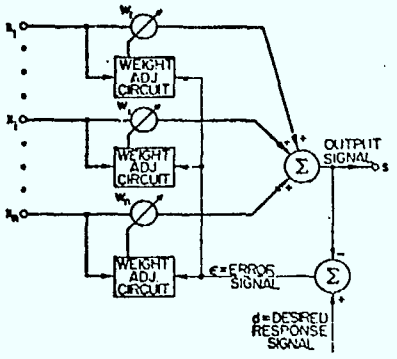

Analog/digital implementation of LMS weight-adjustment algorithm.

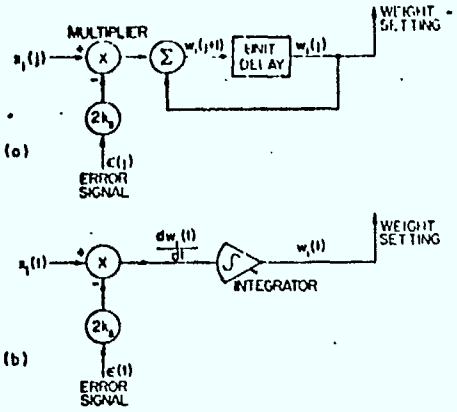

Block diagram representation of LMS algorithm. (a) Digital realization. (b) Analog realization.

Fig.13 From (8)

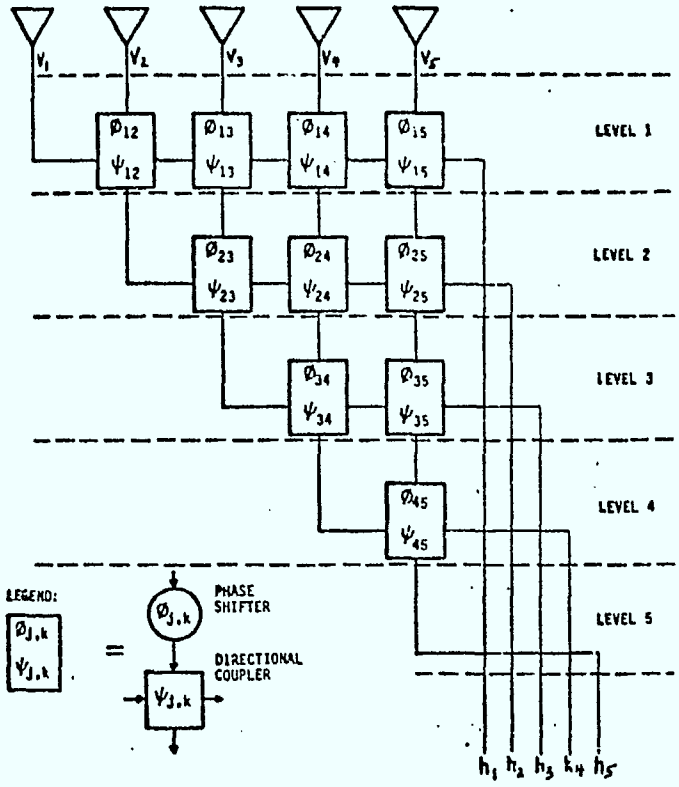

Fig.14 From (28)

Chapter 7

IMPLEMENTATION OF AN IF ADAPTIVE CONTROLLER.

K. Iizuka

1.

Introduction.

Soon after the search for the literature on adaptive array started it was found that the majority of the papers were either highly abstractive or highly mathematical. Experimental papers on the subject were extremely rare. As a result it was decided to construct an adaptive array with two elements in our own laboratory. From the experience of the experiments physical rather than mathematical explanation of the adaptive mechanisms of the array was aimed for.

A two-element array is the most basic and perhaps the simplest configuration among the adaptive arrays, but it can be more than just a theoretical example because it can perform functions of a low cost steerable adaptive interference canceller.

As long as the number of the interference sources is limited to one, probably the most likely event, its performance is not excessively inferior to multi-element arrays.

2.

Summary of Experimental Papers.

In this section the experimental papers brought to the author's attention will be summarized.

In 1976, G. George Passmeiler, et al. [1] of Harris Corporation in Florida reported the experimental results with four element adaptive array at 6 *GHz*. The least mean square (LMS) adaptive algorithm was implemented using analogue components. The control circuit was installed at 300 *MHz* IF. With this rather high IF frequency the bandwidth of 60-100 *MHz* was obtained. The emphasis was placed on the light weight and compact construction of the module. The size of the control module for each channel is 5.7" x 2.7" x 0.4". The depth of the null obtained was 25-30 *dB* below the main beam.

In the same year R.T. Compton, Jr., of Ohio State University [2] reported the experimental results with quite similar arrangement. This array used the same LMS algorithm implemented by analogue circuits. The frequency of operation was at 300 *MHz* and the control was made at IF of 70 *MHz*. The nulling of 15-25 *dB* from the main beam was obtained. He made investigation with various orientations of the jammer.

In 1968, R.T. Compton, Jr., of Ohio State University rebuilt the previously reported four element adaptive array into a spread-spectrum communication system [3]. The desired signal was modulated by pseudonoise code (PN code).

A striking feature of this system is that the system can generate its reference signal in the receiver and abbreviates the necessity of the external reference signal. This, indeed, removed the inherent weakness of the LMS algorithm.

The reference signal for the adaptive array was generated by mixing the received signal with a coded local-oscillator signal. The coded local-oscillator was obtained by modulating a CW signal with the same pseudonoise code used to modulate the desired signal at the transmitter. This code is known at the receiving site in order to produce the coded local-oscillator.

The RF signal was at 70 *MHz* and the processing was performed at 25 *MHz* IF stages. The interference to signal ratio I/S (nulling ratio) of 15-25 *dB* is reported.

In 1979, L.L. Horowitz of MIT Lincoln Laboratory reported the results of their four element adaptive array with the sample matrix inversion algorithm (SMI algorithm). It was intended for an airborne omnidirectional communication.

The necessary features peculiar to the airborne communication are:

(1) Friendly signals come from unknown directions.

(2) Rapid adaptation is mandatory to compensate for motion of the aircraft.

It is therefore important that the computation time is short. The SMI algorithm was used because for a small number of elements the SMI algorithm requires much shorter time than the LMS algorithm does.

The systems so far reported all used analog signal control but this system used the digital system for the first time. The control was implemented at 60 *MHz* IF stage (Somehow, the frequency of the RF is not mentioned in the paper.). Improvement of S/N ratio with the control loop over that without the control loop is reported as 19.5 *dB*.

In 1981, there are two experimental papers reported. They are by J.D. Richman of the Mitre Corporation and by Takao, et al. of Kyoto University of Japan. Both systems use a hybrid analog/digital implementation of the LMS weight control algorithm. Richman's system has four element antennas whereas Takao's system, two elements.

The values of the control signal were calculated by a digital computer. The output from the computer controlled either PIN diode attenuator (Rickman's) or a variable gain amplifier (Takao's) to generate analog R-F frequency weights.

Rickman's system could null the jammer signal to 35 *dB* below a desired signal over 5 *MHz* bandwidth. The RF signal was at 70 *MHz*. The nulling capability of Takao's system was 20-30 *dB*, and RF signal was 50 *MHz*.

3.

Principle of Operation (LMS Algorithm).

The present system assumes that the reference signal can be generated either from the knowledge about the signal during the absence of the jammer or by the code modulation in case of a spread spectrum communication [3]. The Least Mean Square algorithm was implemented by analogue components. The general scheme employed is similar to the systems described in the literature [2], [8] & [9].

Fig. 1 shows a configuration of a two-element LMS algorithm adaptive array. There are two types of implementations; one is complex signal implementation such as shown in Fig. 1a and the other is real signal implementation such as shown in Fig. 1b.

The complex signal implementation expresses the amplitude and phase (or real and imaginary) of the signal by a complex number and the treatment is by complex numbers. The real signal implementation immediately separates the received signal into in-phase and quadrature channels and no distinction in treatment is made between the two channels with only real numbers used. Even though mathematical representation becomes slightly more cumbersome, mathematical concepts such as derivative become more straightforward than in the case of complex signal implementation.

The following analysis is based upon the real signal implementation.

Referring to Fig. 1b the principle of N-element LMS algorithm adaptive array will be explained. Signal from a receiver antenna is first separated into in-phase and quadrature channels by a 90 ° phase shifter. Signal level in each channel is controlled by a weighter W_k which in turn is controlled by the error signal $\epsilon(t)$. Signals out of all weighters are summed by an adder. The output from the adder is the array output $Y_{out}(t)$.

Besides the desired signal, the reference signal $R(t)$ which is to be generated from the spread spectrum system [3] is required. The values W_k of the weighters are varied until the mean square error $\epsilon(t)^2$ between the reference output $R(t)$ and the desired signal $Y_{out}(t)$ is minimized.

A vector representation of the error signal $\epsilon(t)$ for the real signal implementation is

$$\epsilon(t)=\mathbf{x}(t)^t\mathbf{W}-R(t) \tag{1}$$

where

$$\mathbf{W}=\begin{bmatrix} W_1 \\ W_2 \\ W_3 \\ \\ W_{2N} \end{bmatrix} \tag{2}$$

$$\mathbf{W}^t=\begin{bmatrix} W_1, & W_2, & W_3 & , \ldots , & W_{2N} \end{bmatrix} \tag{3}$$

$$\mathbf{X}=\begin{bmatrix} X_1(t) \\ X_2(t) \\ X_3(t) \\ \vdots \\ X_{2N}(t) \end{bmatrix} \tag{4}$$

$$\mathbf{X}^t=\begin{bmatrix} X_1(t), & X_2(t), & X_3(t), \ldots , X_{2N} \end{bmatrix} \tag{5}$$

The mean square error

$$\overline{\epsilon(t)^2}=\overline{\left[\mathbf{X}(t)^t\mathbf{W}-R(t)\right]^2} \tag{6}$$

is a quadratic function of the weights, so there is a unique optimum value for each weight W_k where $\overline{\epsilon(t)^2}$ will be minimized. To this end a partial derivative of $\epsilon(t)^2$ with respect to one of the vector elements W_k is calculated:

$$\overline{\frac{\delta\epsilon(t)^2}{\delta W_k}}=\overline{2X_k(t)\left[\mathbf{X}(t)^t\mathbf{W}-R(t)\right]}=\overline{2X_k(t)\epsilon(t)} \tag{7}$$

Note that differentiation inside the time average is permissible.

Repeating the same procedure with respect to all other elements of $\mathbf{W}$ the gradient vector $\mathbf{G}$ of $\epsilon(t)^2$ is obtained:

$$\mathbf{G}=\nabla_\mu\ \overline{\left[\epsilon(t)^2\right]}=\overline{2\mathbf{X}(t)\left[\mathbf{X}(t)^t\mathbf{W}-R(t)\right]} \tag{8}$$

or

$$\mathbf{G}=\overline{2\mathbf{X}(t)\epsilon(t)} \tag{9}$$

Once the value of the gradient is known, the condition of minimizing the mean square error is found by choosing the direction of the steepest descent in the direction of $-\mathbf{G}$. The value of $\mathbf{G}$ is the time average of the vector made up of the product of the element signal and the error signal. This can be easily implemented by an electronic circuit.

If W_k is continuously changed with respect to time, derivative with respect to W_k can be converted into the derivative with respect to time and

$$\frac{d\ W(t)}{dt} = -\mu G(t) \tag{10}$$

where μ is a physical constant associated with the conversion between the two variables. The final value of $W(t)$ is found from Eqn. 10 and is given by

$$W(t) = W(0) - 2\mu \int_0^t X(t)\epsilon(t)\,dt \tag{11}$$

The optimum value $W(t)$ is obtained by implementing Eqn. 11 with analogue electronic circuits.

4.

Experimental Arrangement.

Fig. 2a shows the overall system block diagram while Fig. 2b explains the function of the control loop. An X band frequency was chosen as the RF signal and the adaptive control was performed at the IF stage.

In case of a two element adaptive array as shown in Fig. 2a, the output signal is always determined by the relative phase between the two channels and it is sufficient to install the adaptive loop only on one of the two elements. Only the signal from antenna A_2 is controlled by the feedback loop. The 12 *GHz* input signal beats with a 12,060 *GHz* LO to generate 60 *MHz* IF signal. The feedback is imposed on the IF signal. Signal from the A_2 is divided into in-phase and quadrature components. The amplitude of both components are controlled by a weighter W_1 (only the circuit for the in phase component is included for clarity). The output from all channels is summed to produce the array output Y_{out}.

The function of the feedback is explained with reference to Fig. 2b. The weighter W_1 is essentially a voltage controlled attenuator and the value of the attenuation is determined by the feedback loop which adjusts the W_1 to minimize the mean-square value of the error signal $\epsilon(t)$ defined by Eqn. 1.

The R(t) is at first preset to be equal to y (t) in the absence of the jammer signal. With this presetting any non-zero error signal implies the presence of either jammer or thermal noise of the system. The function of the control loop is an automatic search for zero or minimum $\epsilon^2(t)$.

In a rough sense, as long as $\epsilon(t)$ is positive the DC output voltage reduces the value of W_1 until $\epsilon(t)$ becomes zero, on the other hand, if $\epsilon(t)$ is negative the DC output voltage boosts up the value of W_1 until $\epsilon(t)$ becomes zero.

The correlator C followed by an integrator in Fig. 2b implement the integration of Eqn. 11. The major advantage of the LMS adaptive loop is that no knowledge of the direction of the jammer is used for the control.

5.

Detailed Examination of Components.

A double balanced mixer (Mini-Circuit Corp. type ZAD-3SH) which is normally used as frquency converter was employed as correlator C and weighter *W*. It was important to find exact mixer characteristics when the mixer were used in the dual role.

First, the characteristics of the mixer when used as a correlator was studied. The 60 *MHz* signal, AM modulated by a triangular wave was fed to the L and R terminals of the mixer and the DC voltage induced at the IF terminal was observed. The output from the correlator

$$V_c = V_L\ V_R\ \cos\phi \tag{12}$$

was examined.

Fig. 3 shows the results. The top photograph is a display of the output for the condition that V_L and V_R are in phase. The output V_c from the IF terminal is DC and the polarity is negative. The V_c is later used as a control signal. Significant saturation effect is observed at the V_L voltage beyond 800 mV. A good null voltage is obtained with 0=90 °. When V_L and V_R are 180 ° out of phase, the polarity of V_c is reversed and becomes positive. There is some differences in the shapes of V_c for positive output and negative output cases.

Next, the dynamic range of the correlator was examined. The input to L was kept fixed and the input to R was varied by a variable attenuator. Fig. 4 shows the results. When the setting of the attenuator becomes more than 10 *dB*, the V_c voltage stops to increase linearly with V_c. In fact the display for 42 *dB* attenuator and the open circuit in R terminal showed no difference.

Next, the characteristics of the double balanced mixer as a voltage controlled attenuator was tested. The results are shown in Fig. 5. The 60 *MHz* signal was fed from L terminal and the output from R terminal was observed with various DC voltages applied to the IF terminal. The output steeply decreased if the DC voltage at the IF terminal dropped below 0.8 volt. The maximum DC voltage is +1.5 volts. The dynamic range is quite limited. This result leads to the conclusion that if the mixer were used as a correlator it should be accompanied by an amplifier with AGC control.

When the DC voltage applied to the IF terminal is positive, the phase at R becomes identical with that at L, however, when the voltage is changed to negative the phase at R is reversed and the phases at R and L become 180 °out of phase.

6.

Test of the Feedback Loop.

Before the feedback loop was installed into the antenna system, its performance was tested using two signal generators. Fig. 6 shows the feedback loop. Both jammer and desired signals were fed to the input of the loop. The signal level of the jammer and the desired signal were independently controlled. The amplitude of the reference signal was AM modulated by a triangular wave.

A criterion of the performance of the loop used was how closely the output Y_{out} at point 3 in the Fig. 6 followed the ramped amplitude of the reference signal.

Simultaneous displays of

input to the loop,
control voltage V_c
output voltage Y_{out},
reference voltage V_R,

were made for close observation. An example of the scope display is shown at the bottom of the figure.

Fig. 7a shows the display with no jamming signal. It is seen that the output Y_{out} follows the reference signal. Fig. 7b shows the case when jamming signal which is close to 60 *MHz* is present. Significant change in the shape of the control signal is observed, but the output Y_{out} follows the reference signal. Fig. 7c shows the input signal when the jammer is present.

The frequencies of the two input oscillators were pulled to each other as they were brought close due to the entrainment of the signal generator. Fig. 7d shows the display at this time. Fig. 7e demonstrates that as soon as the reference voltage was brought to zero the output voltage Y_{out} also becomes zero. Fig. 7f shows the signal when the jammer generator is off. The displays verified that the feedback loop was properly functioning.

Finally, the feedback loop was installed onto the antenna system (only the in-phase channel is ready at present). Fig. 8a shows the case when no jammer was present. The antenna of

the jammer was placed about 15 degrees away from the main beam. The antenna of the desired signal was in the broad-side direction. The expanded display of the input X_2 in the absence of jammer is shown in Fig. 8a. Small AM modulation due to the leakage from the ramped reference signal is observable in this expanded display. Fig. 8b shows the case when the jammer generator was on. The display demonstrates that the output Y_{out} was very little influenced by the jammer. The degree of the jamming is shown in Fig. 8b. Fig. 8c shows the case when the jammer signal was further increased. The erratic output is observed. The degree of the jamming is shown in Fig. 8c'. Dynamic range of the jamming control is rather small at present. Optimization of the components and installation of quadrature channel is in progress.

7. Conclusion.

Even though the scale of the preliminary experiments were quite limited, it led to the following conclusions:

(i) Dynamic range of the correlator of the double balanced mixer is limited to the output less than 800 mV.

(ii) The characteristics curves for $0 = 0\ °$ and $0 = 180\ °$ are not quite of the same shape.

(iii) In the range for which the difference between V_R and V_L is more than 10 dB, the correlation voltage is not proportional to the input voltage.

(iv) Dynamic range of the double balanced mixer lies between 0.8 to 1.5 V only requiring inclusion of an amplifier with AGC.

(v) Isolation amplifiers are needed where the direction of the signal flow is critical. For instance unless an isolation amplifier is present between the adder and W_1, the reference signal reaches W_1 and the performance of W_1 becomes erratic.

References

(1) G. George Passweiler, M.R. Williams, L.M. Payne and G.P. Martin. "A miniturized light weight wideband null steerer." *IEEE Trans. on Antennas Propagat.*, Vol. AP-24, pp. 749-754, 1976.

(2) R.T. Compton, Jr. "An experimental four-element adaptive array." *IEEE Trans. on Antennas Propagat.*, Vol. AP-24, pp. 697-706, 1976.

(3) R.T. Compton, Jr. "An adaptive array in a spread-spectrum communication system." *Proc. of IEEE*, Vol. 66, No. 3, pp. 289-298, 1978.

(4) L.L. Horowitz, H. Blatt, W.G. Brodsky and K.D. Senne. "Controlling adaptive antenna arrays with the sample matrix inversion algorithm." *IEEE Trans. on Aerosp. Electron.*, Vol. AES-15, No. 6, pp. 840-848, 1979.

(5) J.D. Rickman, Jr. "Results from a four-element adaptive antenna experiment." *IEEE Trans. on Aerosp. Electron.*, Vol. AES-17, pp. 35-47, 1981.

(6) K. Takao, O. Kawamura, K. Komiyama, K. Hashimoto and I. Kimura. "Experiment of a hybrid-type implementation of an adaptive array under directional constraints." *J. Institute of Electronics and Communication Engineers of Japan*, Part B, pp. 126-133, 1981.

(7) J.A. Cummins, G.Y. Delisle and M.G. Pelletier. "An adaptive array with 'ON-OFF' control." Institute of Electrical Engineering (London). Antennas and Propagat., Symposium, pp. 55-59 (April), 1981.

(8) B. Widrow, P.E. Mantey, L.J. Griffiths and B.B. Goode. "Adaptive antenna systems." *Proc. IEEE*, Vol. 55, No. 12, pp. 2143-2159, 1967.

(9) J.E. Hudson. "Adaptive array principles." Peter Peregrinus Ltd., London, 1981.

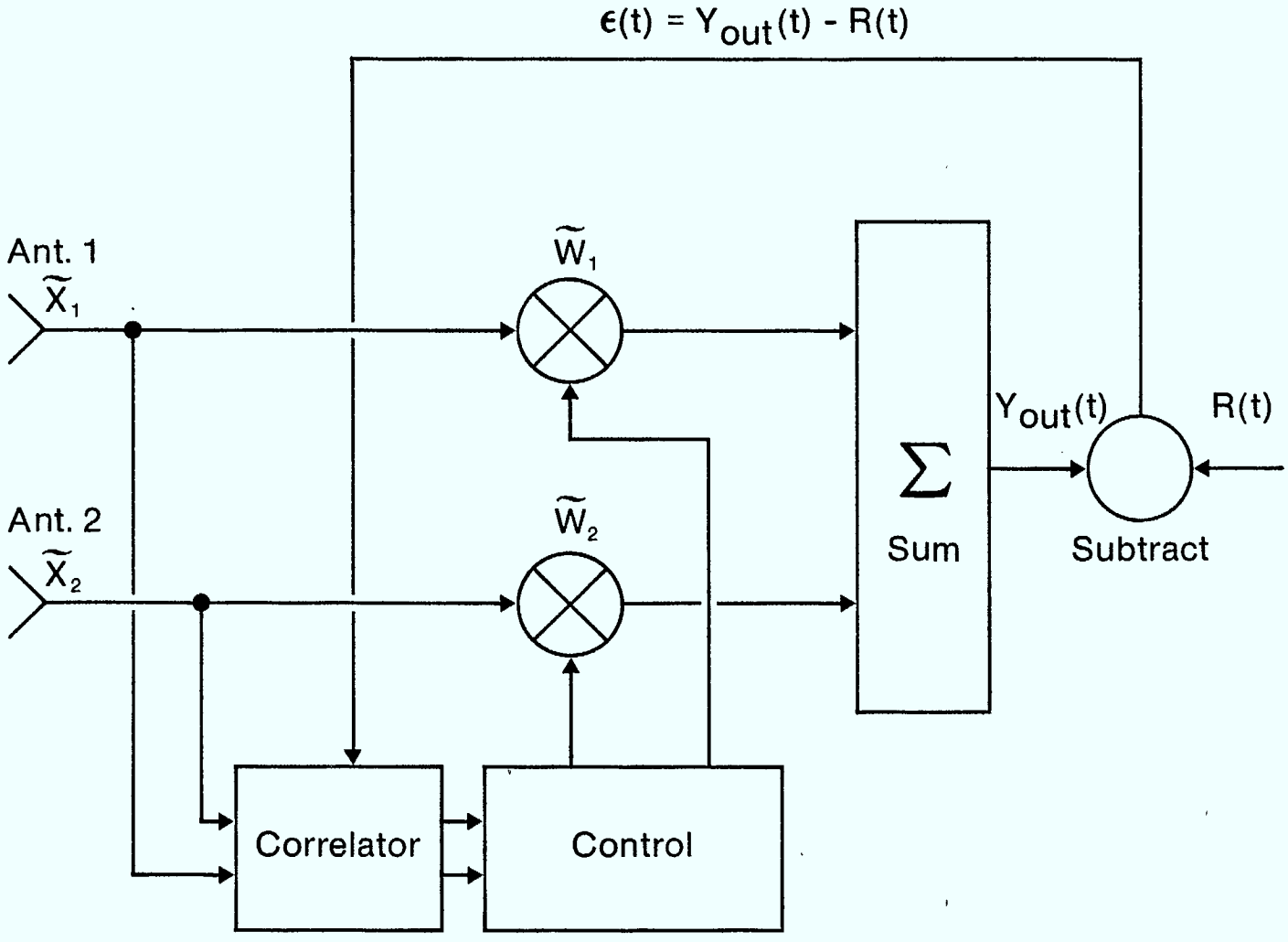

Two element adaptive array
(complex signal implementation)

Fig. 1a Implementation of the LMS alogrithm

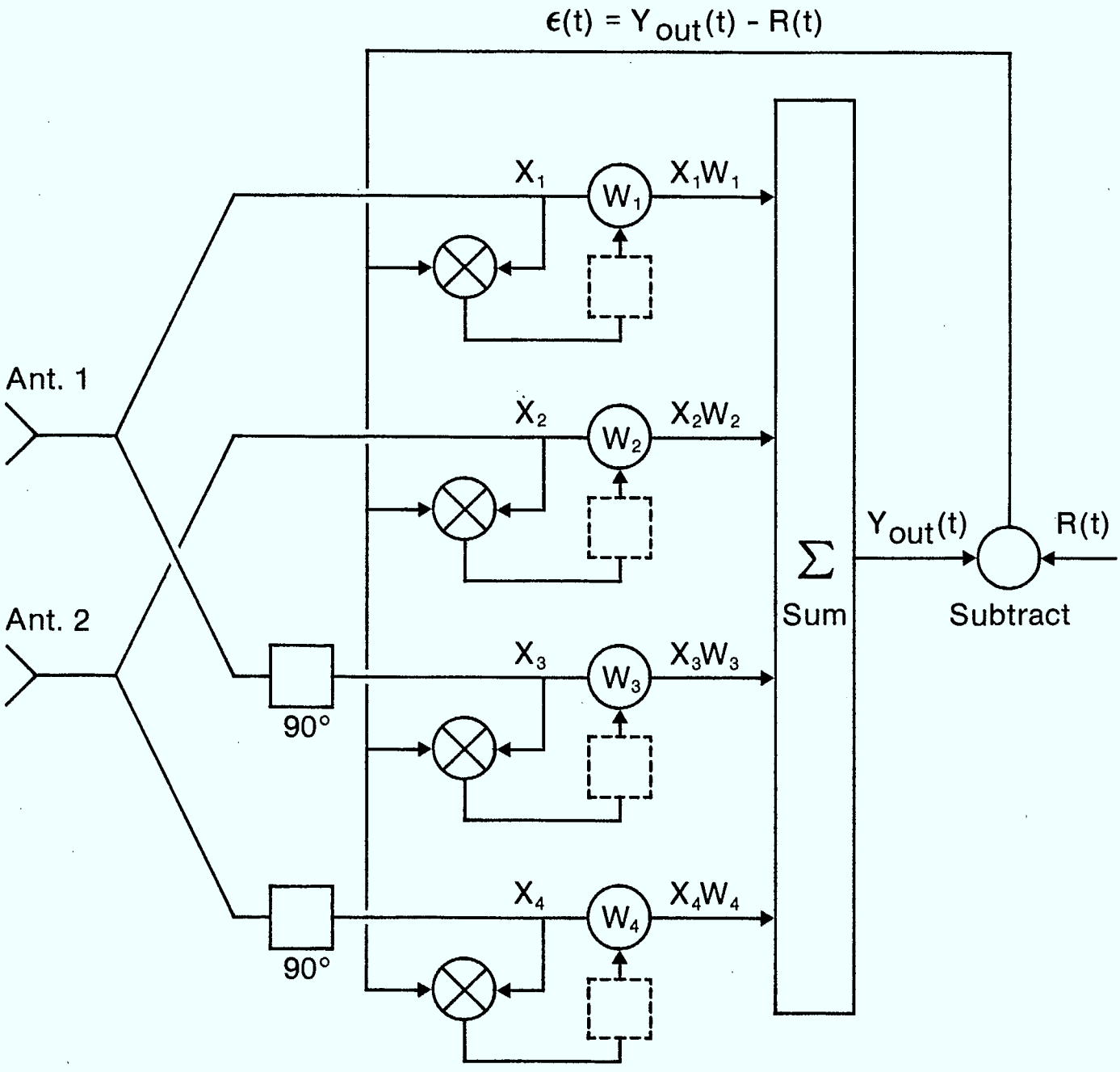

Two element adaptive array
(Real-signal implementation)

Fig. 1b Implementation of the LMS alogrithm

Fig. 2 a. Block diagram of two element adaptive array

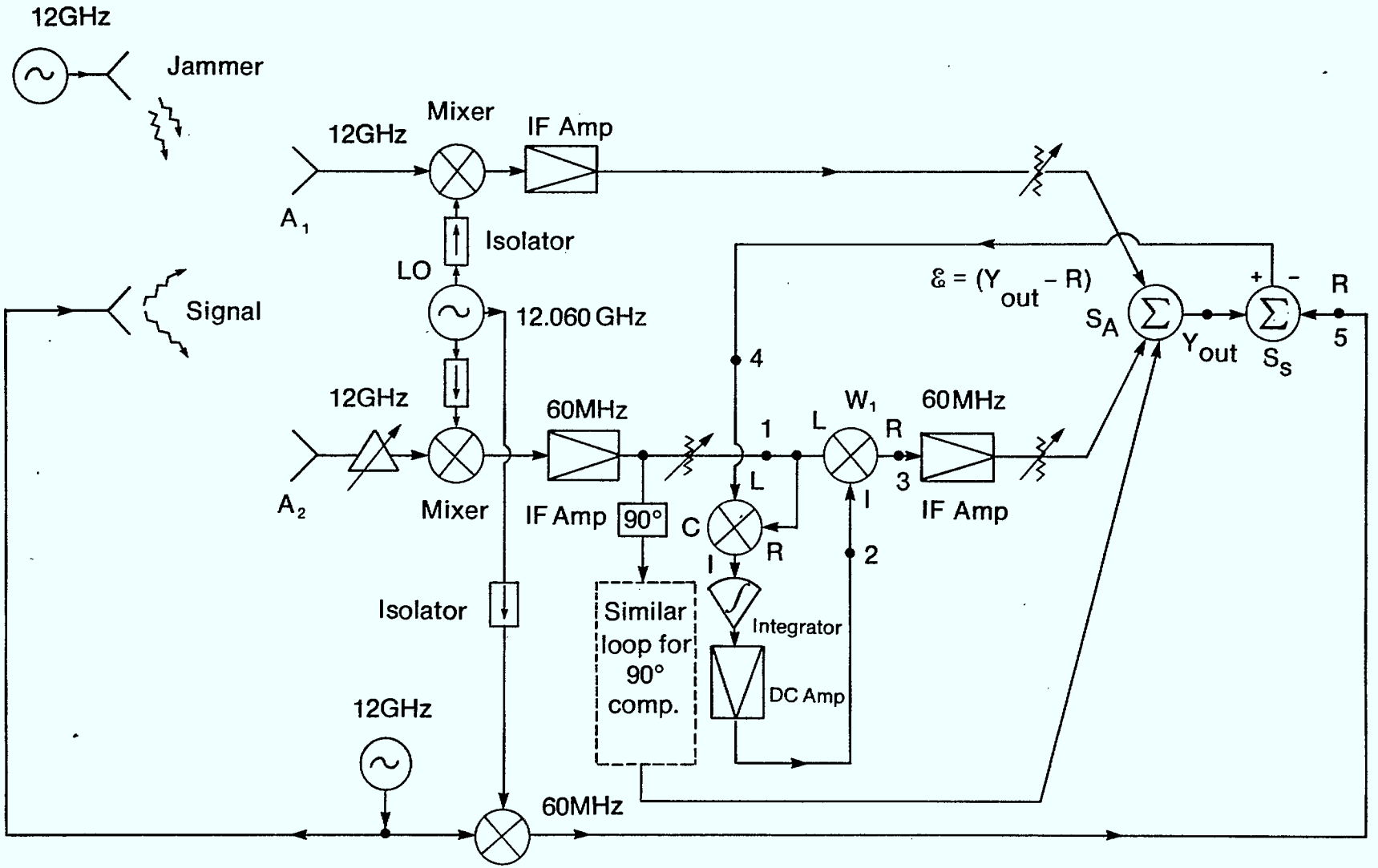

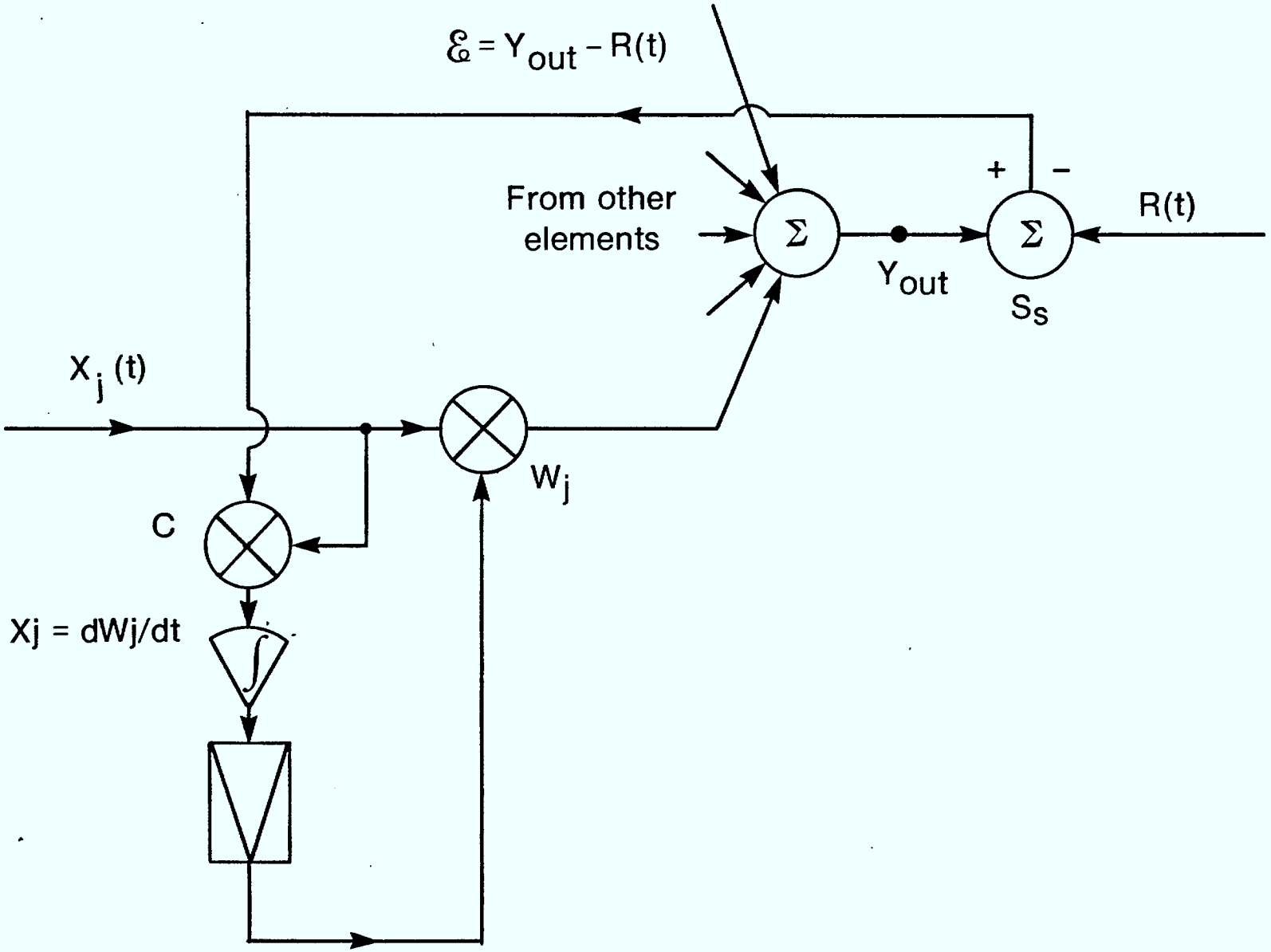

Fig. 2(b) Adaptive array feedback loop

Fig. 3
Characteristics of a double balanced mixer when used as a correlator

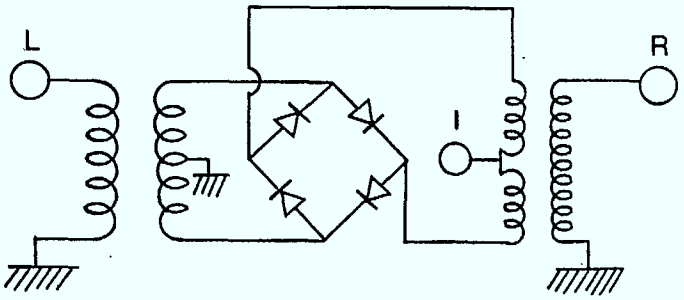

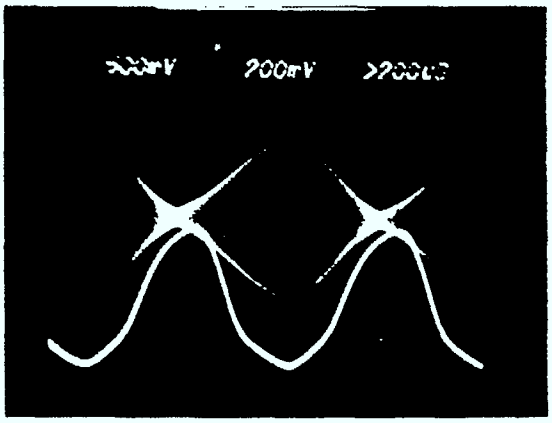

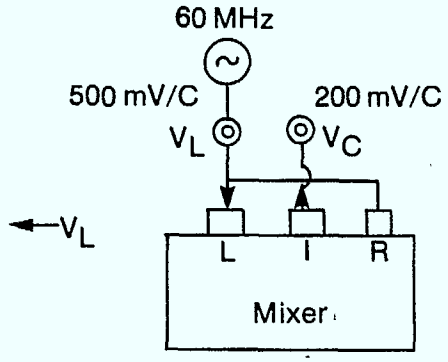

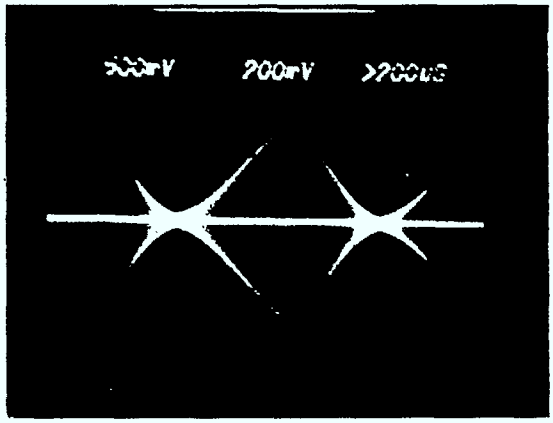

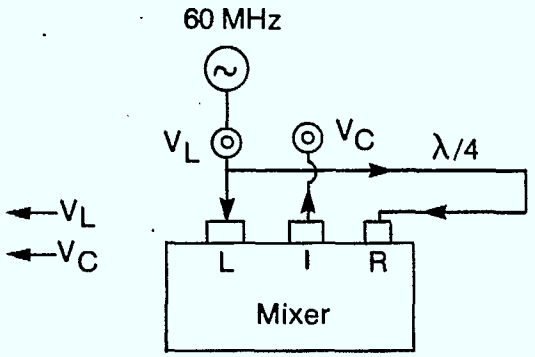

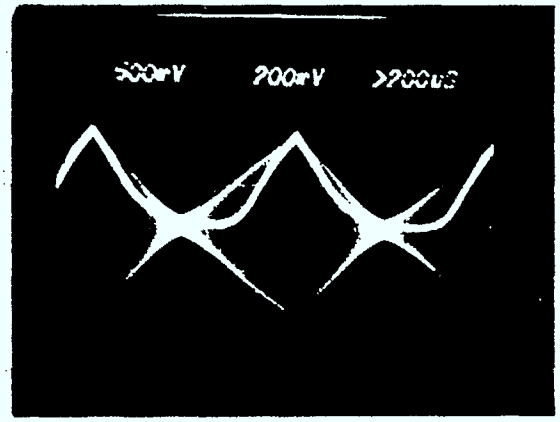

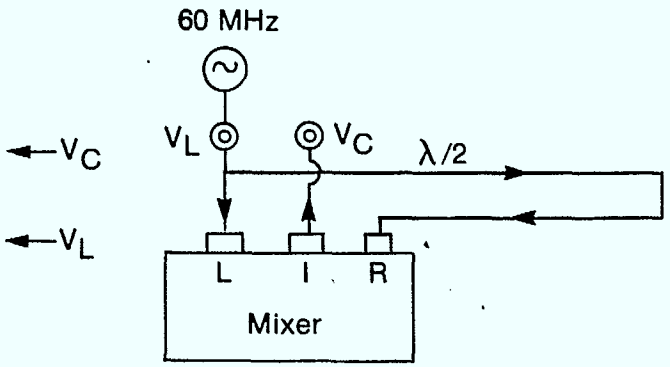

Fig. 4
Control voltage with various error signals

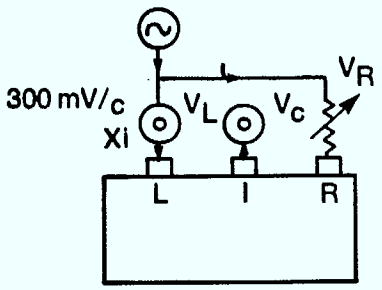

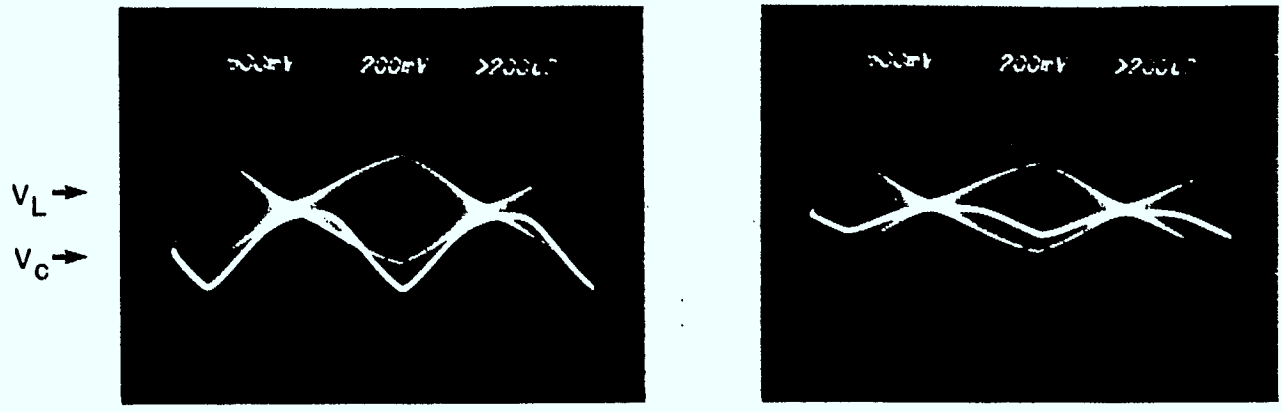

0 dB

10 dB

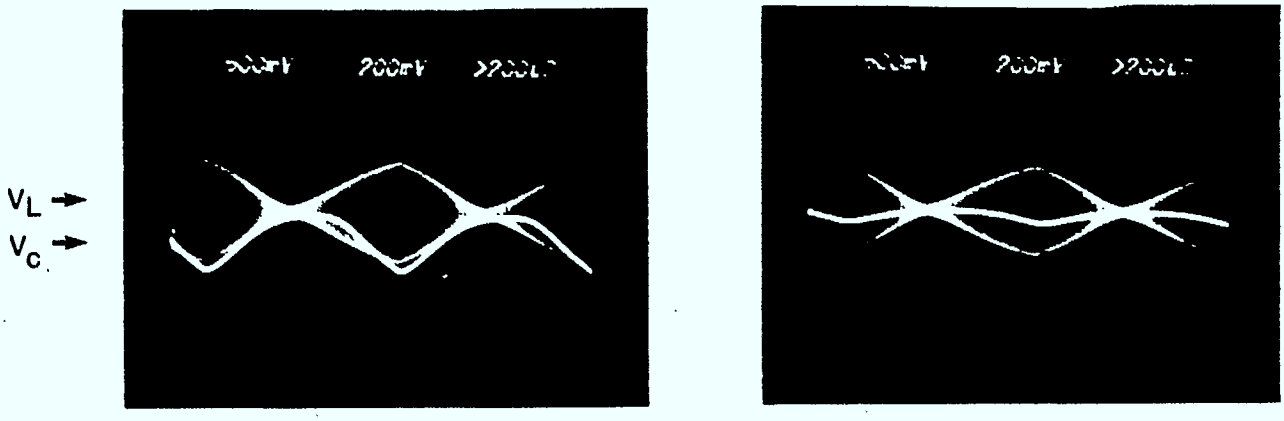

3 dB

20 dB

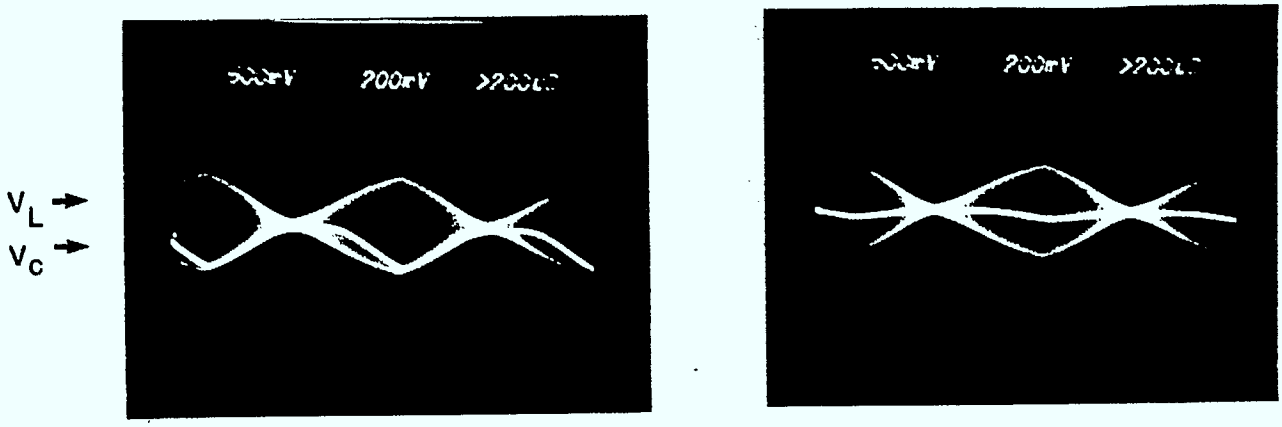

6 dB

42 dB and ∞

Fig. 5
Dynamic range of a Double balanced mixer when used as a voltage controlled attenuator

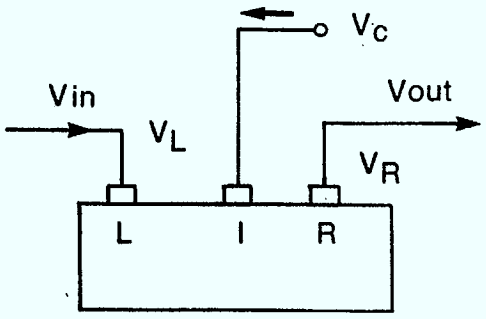

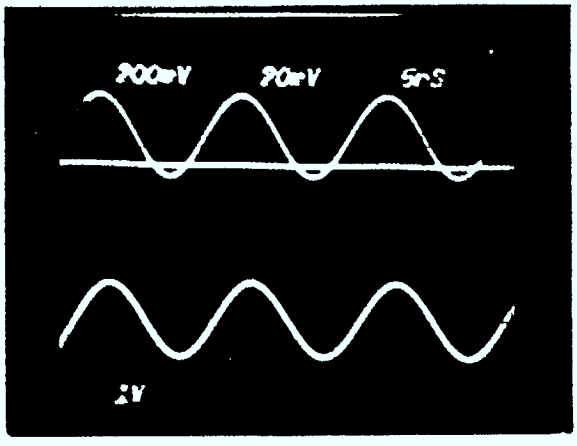

In phase

← Input, V_L
← Vc (+1.5 V)
← 0 line for Vc
← Output (x 1/10) V_R

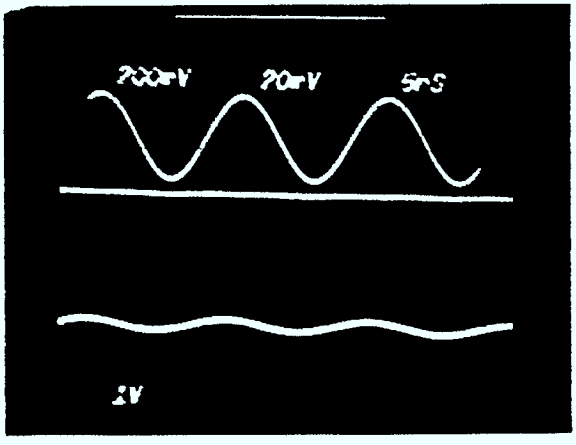

← Input, V_L
← Vc (+0.9 V)
← 0 line for Vc
← Output (x 1/10) V_R

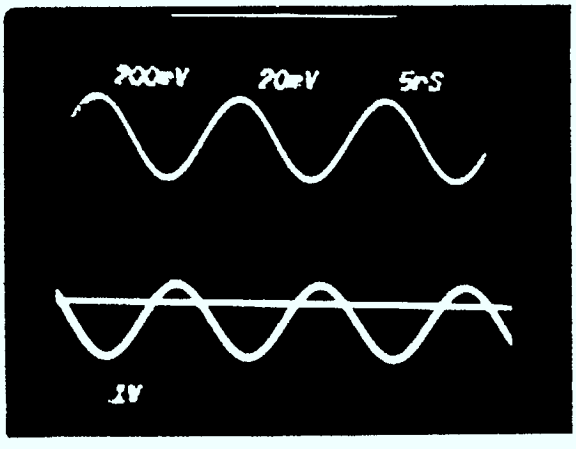

Out of phase

← Input, V_L
← 0 line for Vc
← Vc (-1.5 V)
← Output (x 1/10) x V_R

Fig. 6 Test of feedback loop

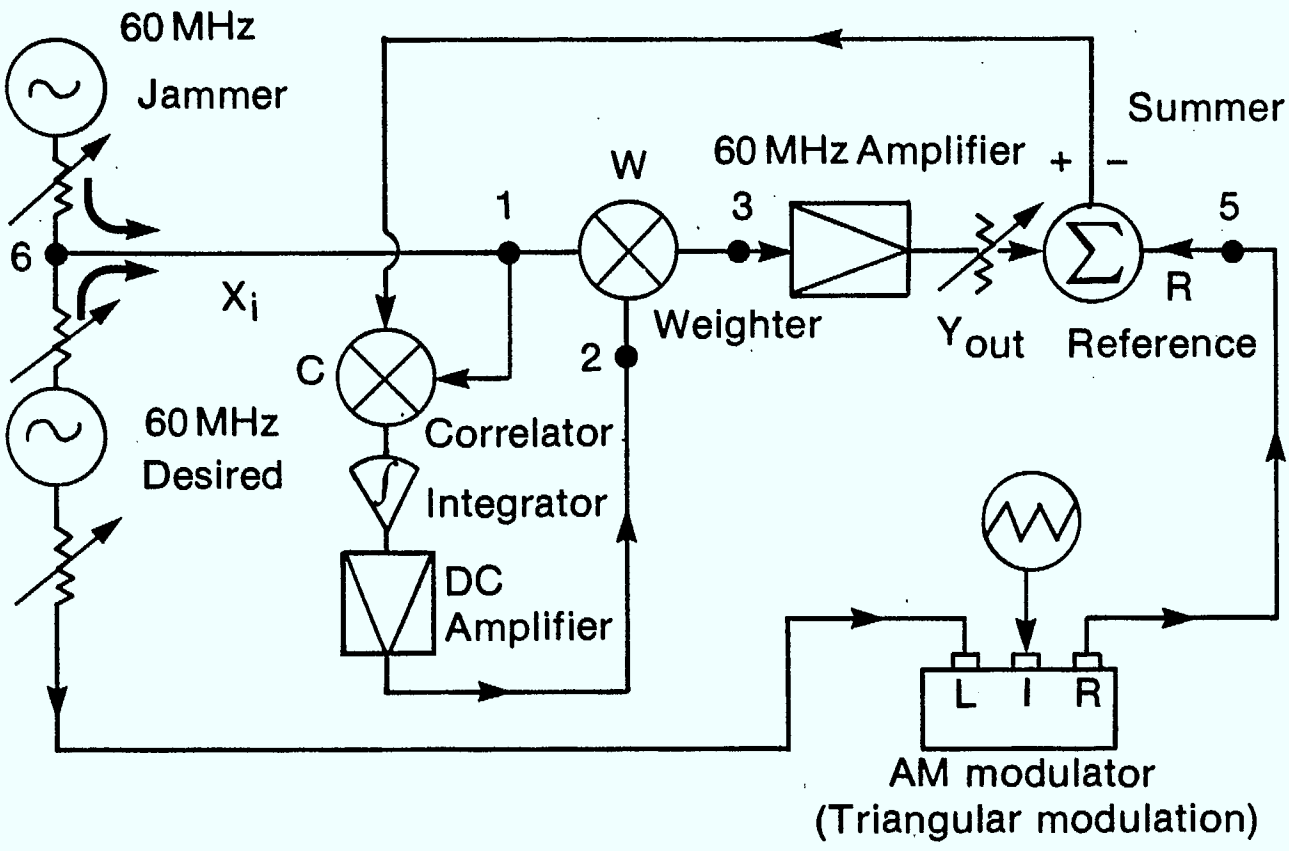

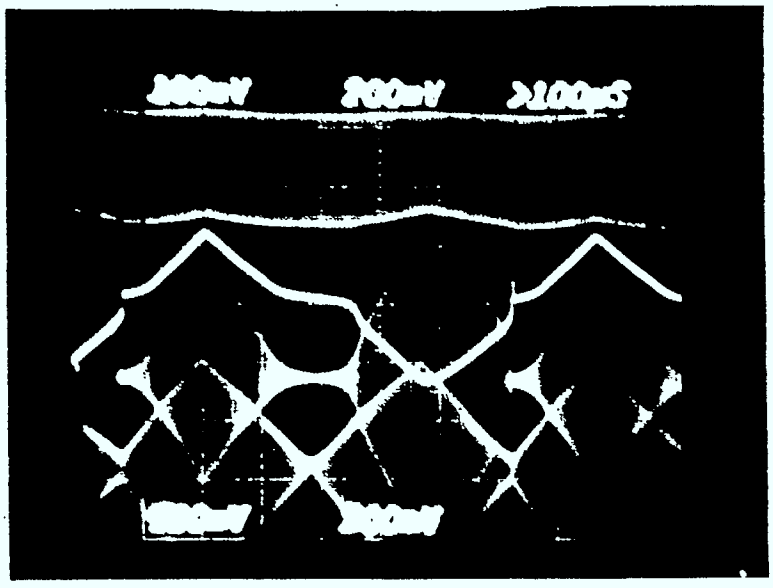

← 1 Input (100 m V/c x 1/10)

← 2 Control V_c (500 m V/c)

← Zero voltage of V_c

← 3 Output (200 m V/c)

← 5 Reference V_d (200 m V/c)

Fig. 7 Test of feedback loop against jamming

(1) Input Xi
(2) Control V_c

(3) Output Y_{out}
(0) Zero for V_c
(5) Reference R

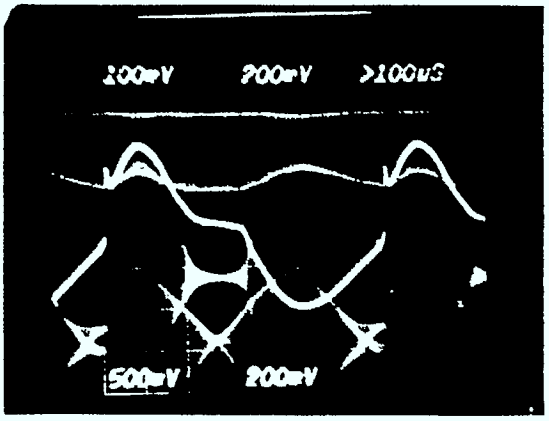

(1)
(2)
(0)
(3)
(5)

(A) No jamming

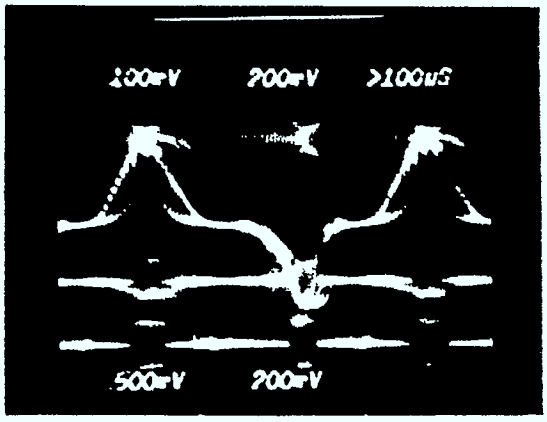

(D) Jamming frequency ≒ reference frequency

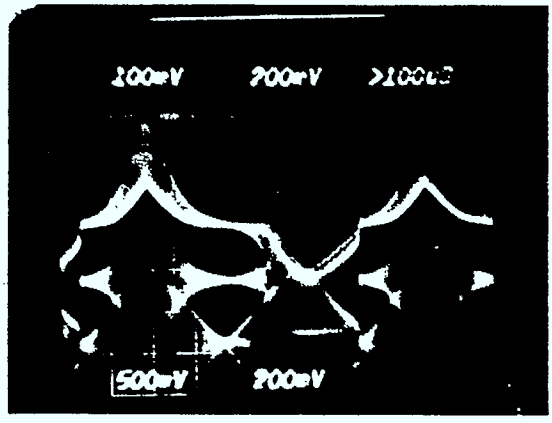

(B) Jamming

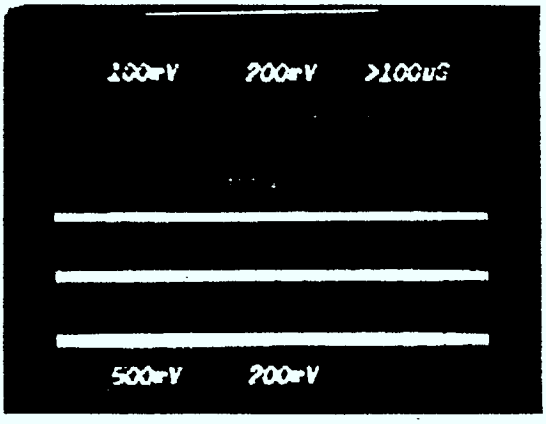

(E) Reference off

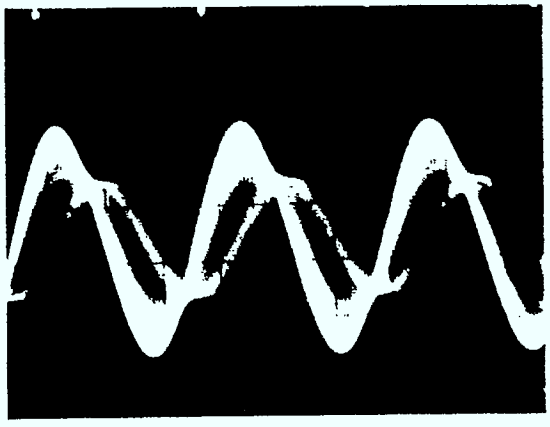

(C) Jamming & signal

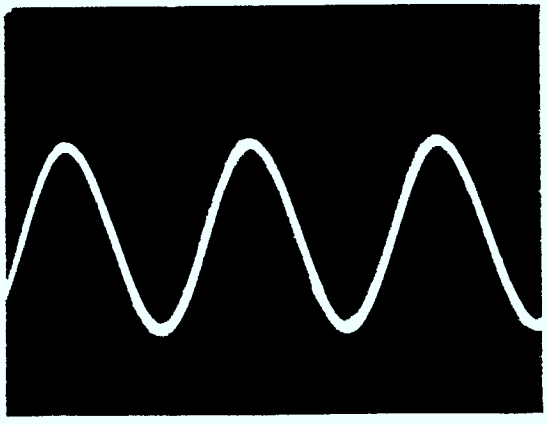

(F) Input (no jamming)

Fig. 8 Test of adaptive array against jamming

(1) Input X_i
(2) Control V_c
(3) Output, Y_i
(0) Zero for V_c
(5) Reference R

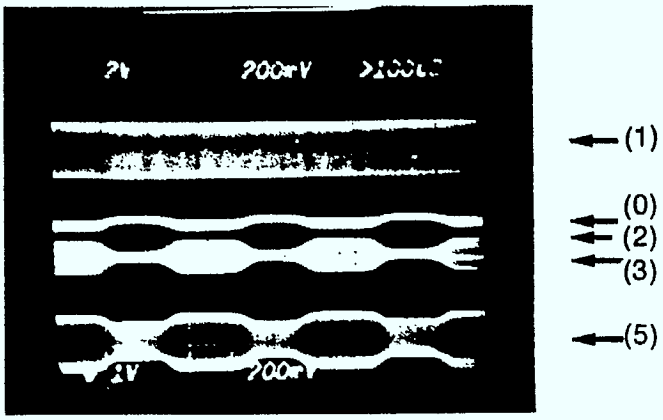

(A) No jamming

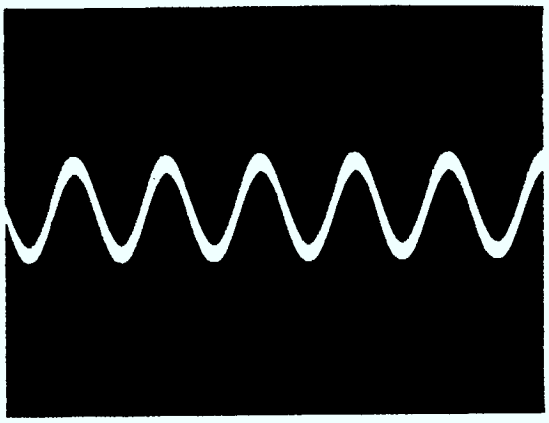

(A)' Signal alone

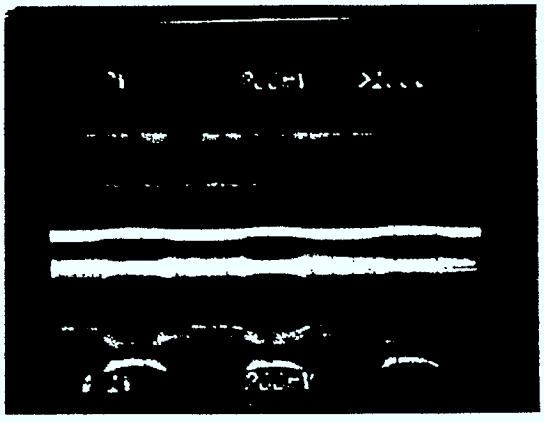

(B) Jamming

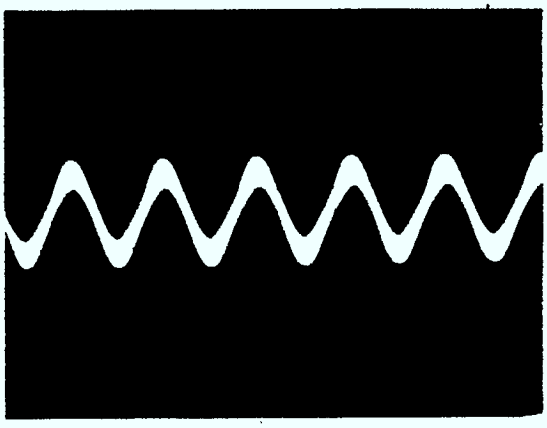

(B)' Signal with jamming

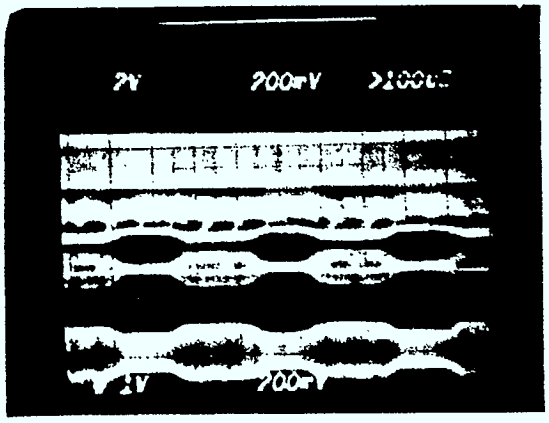

(C) Heavy jamming

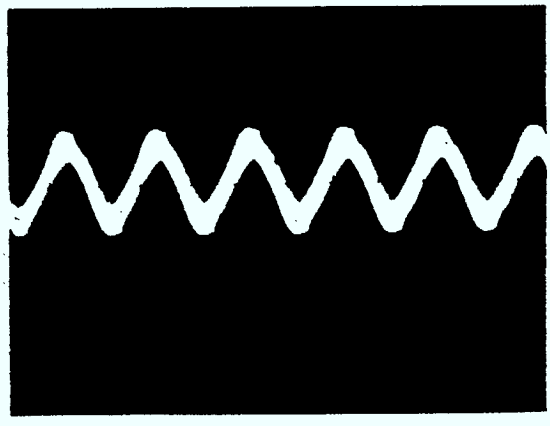

(C)' Signal with heavy jamming

Chapter 8

EHF PHASE AND AMPLITUDE CONTROL ELEMENTS

Tiltek Limited

Summary

An overview is given of ferrite and PIN diode phase shifters. The extension of these to include amplitude control is illustrated. Examples are given of actual phase shifters which have been in use for satellite phased arrays and which might be useful for future millimetre wave antennas.

In addition mention is made of a dielectric guide device which seems to have a good potential for the future.

A section has been included on present day state-of-the-art techniques and data is presented on available off-the-shelf items which may be used at EHF.

1.

General.

The purpose of the present study is to investigate devices and drive circuits for the complex weighting and switching of antenna elements for applications in EHF Controlled-Beam Antennas for SATCOM.

There are two distinct application areas for the EHF Controlled-Beam SATCOM work.

(a) antennas onboard a geosynchronous satellite

(b) antennas for earth terminals.

The emphasis is to be on operation at the frequencies of 30 and especially 44 *GHz* for uplinks and at 20 *GHz* for downlinks. Some consideration may be given to 60 *GHz* crosslinks.

No matter what schemes are used to control the antenna patterns, there are two basic quantities which must be dealt with. These are the amplitude and the phase of the fields in the antenna aperture.

The segment of the study reported herein deals mainly with methods to produce a phase or amplitude change in the RF currents travelling to or from the antenna elements. The methods used depend on the particular transmission medium under consideration.

2.

The Transmission Path Consideration.

In the guided propagation of mm waves one may consider using standard waveguides, microstrip transmission lines, and dielectric waveguides.

2.1.

Standard Rectangular or Circular Waveguide Components.

Such components as couplers, tees, tuners and hybrid rings are available to about 110 *GHz.*

Ferrite isolators, switches, circulators and phase shifters are available to 140 *GHz* with isolations of 15-20 *dB.*

One disadvantage to these components is their increasing loss as the frequency is increased. Perhaps even more important is the fact that they do not lend themselves readily to microwave integrated circuit (MIC) techniques. The latter are more compact, reliable and cost

effective than are discrete waveguide components.

2.2.

Microstrip and Strip Line Techniques.

At sub-millimetre wavelengths MIC components are quite common. Below 100 *GHz* photolithographic techniques are often used to fabricate passive millimetre components. Such items as PIN switches and ferrite circulators and isolators may be conveniently fabricated in a strip transmission system. Several components are now available in the frequency range 35-250 *GHz*.

2.3.

Dielectric Waveguides.

Above the frequency range where strip line techniques can be used successfully ($>$ 250 *GHz*) it is possible that dielectric waveguide techniques will be employed and in fact these techniques may be used at frequencies considerably below this.

Whereas, microstrip lines are about $\lambda/10$ in width, dielectric guides are about one wavelength wide.

In addition, dielectric guides have lower losses at mm wavelengths than do microstrip lines, mainly due to the absence of conductor losses in the former. PIN diode phase shifter techniques for this medium will be discussed later.

One of the few ferrite devices compatible with dielectric waveguide mm wave integrated circuits is a field displacement ferrite isolator for the 50-75 *GHz* band.

The most frequently used dielectric waveguide is the rectangular dielectric rod (Fig. 1).

The basic guide is composed of just a rectangular dielectric rod in free space as shown in Fig. 1a. This structure lacks two quantities which are important in many MIC applications. Firstly there is no heat sink and secondly there is no path for bias currents should they be necessary.

To overcome these difficulties a metallic ground plane may be added as shown in Fig. 1b. This results in the so-called 'dielectric' image guide. Unfortunately an adhesive must be used to keep the dielectric attached to the ground plane and this raises the propagation losses. In addition the ground plane itself adds some conductor losses. A further problem occurs because of bubbles that exist between the ground plane and the dielectric. Some of these difficulties may be overcome by inserting a second (thin) teflon sheet between the alumina or ceramic dielectric rod and the ground plane as shown in Fig. 1c.

Other versions of dielectric waveguides are the strip dielectric (SD) and inverted strip dielectric (IS) guides in which the energy is propagated in a broad thin dielectric layer and a second dielectric rod is used to confine the energy to a localized region of the surface. These are essentially both leaky wave structures.

3.

Phase Shifters - General.

In obtaining electronically controlled phase shifters for phased array and other applications, two widely different techniques have generally been employed, one using ferrites and the other using diodes [3], with neither showing a clear advantage over the other.

Each approach has its own characteristics regarding power handling capability, reciprocity, switching speed, temperature sensitivity and insertion loss.

Keeping in mind that a typical phased array may contain hundreds or even thousands of phase shifters it is evident that a careful comparison should be made of the types available.

White [3] has made a comparison of the differences between diode and ferrite devices which is summarized in the following paragraphs.

Phase shifting with ferrites is usually accomplished by the change in magnetic permeability which occurs with application of a magnetic biasing field. The ferrite is commonly used as a bulk control medium, usually several wavelengths long, which is made to undergo up to one wavelength of phase change with the applied field. The change in relative permeability for the ferrite comes about because of the difference in propagation constants of right and left hand circularly polarized RF magnetic fields (with reference to the direction of an orthogonal magnetic bias field). Reversing the direction of the bias field switches the propagation time and hence the phase delay through the device.

This method of phase control is non-reciprocal. Thus, if the same pointing direction is to be maintained for reception as for transmission then the bias current for reception must be reversed.

PIN diodes on the other hand are very small compared to the operating wavelength and can be easily integrated into the circuits. In order to overcome some of the variable loss characteristics it is common to use PIN diodes as switches, or on-off devices, so that phase shifts have a specified minimum increment. When biased in the forward direction, diode resistances down to 0.5 ohm are possible, while reversed biased diodes have a capacitive reactance of about 1K ohm.

It should be noted that it is possible to obtain reciprocal action from a ferrite phase shifter by use of a so-called "dual-mode" device [4]. Also stepped ferrite phase shifters are possible by means of latching.

In general the advantages of ferrite phase shifters lie in the areas of high power handling capability, low insertion loss and low VSWR.

PIN diodes have the advantage of high switching speeds, simple driving circuitry, reciprocal operation and temperature stability.

Change of permittivity through the use of plasmas, although a possibility, has not proven to be a very useful approach so far.

Next we will consider the properties of ferrite and PIN phase shifters in more detail.

3.1. Ferrite Phase Shifters

Some characteristics of traditional ferrite phase shifts may be found in ref. 5 and are listed below.

Specifications such as those listed above could be met as far back as 1965. Research since that time seemed to show much promise and was carried on extensively until at least 1975 when it seems to have tapered off somewhat, perhaps due to the large amount of effort being expended on diode-type phase shifters.

A survey of the most significant papers on ferrite control devices from 1968-1974 was given by L.R. Whicker and D.M. Bolle [6]. The various types of ferrite phase shifters covered include, waveguide non-reciprocal phase shifters, helical phase shifters, microstrip phase shifters, latching Reggia-Spencer phase shifters, and reciprocal dual mode phase shifters. It is stated (by L.R. Wicker) that, "for array applications the waveguide non-reciprocal phaser and the reciprocal dual mode phaser have proven electrically superior to the other types".

In the dual mode reciprocal phase shifter, linearly polarized EM waves in a rectangular guide are first converted to either left or right-hand polarized waves in a circular guide. The Faraday rotation is used in the circular guide where the phase shift takes place and then the energy is reconverted to linear polarization in a rectangular guide. Dual mode types can be made so that their insertion loss approaches that of the nonreciprocal toroid type. The insertion loss obtainable depends however on the element weight.

Various aspects of the design and manufacture of dual mode reciprocal latching ferrite phase shifters have been reported by Boyd [7]. Since this is one of the important types of

Type Waveguide Ferrite Phase Shifter:

Characteristic	3.9-6.2 GHz	5.2-10.9 GHz	16 GHz
phase shift	360°	360°	360°
insertion loss	0.7 dB	0.5 dB	0.7 dB
max. peak power	20 KW	4 KW	5 KW
temp. sensitivity	6.0°/°F	4.5°/°F	3.0°/°F
freq. variation	0.1°/MHz	0.1°/MHz	0.1°/MHz
drive	250 amp·turn	150 amp·turn	150 amp·turn
switching power	4 W	2 W	1.5 W
switching time	100 μs	100 μs	100 μs
length	12"	8"	5"

Type Co-axial Ferrite Phase Shifter:

Characteristic	1.5-5.3 GHz
phase shift	360°
insertion loss	1 dB
max. peak power	5 KW
temp. sensitivity	3°/°F
freq. variation	0.3°/MHz
drive	300 amp·turn
switching power	7 W
switching time	100 μs
length	25.4 cm

ferrite phase shifters, the main results are given below.

3.2. Dual Mode Reciprocal Latching Phase Shifters.

These types of phase shifters are able to utilize relatively inexpensive lithium-titanium material and have better temperature characteristics than M_gMn ferrites. Their particular advantages are low weight, small size, and low cost.

A disadvantage in some cases is the switching speed which is an order of magnitude slower than that of the non-reciprocal toroid type.

In its simplest form the circular part is made merely by metallizing the surface of a ferrite rod. This single rod is used to contain an efficient non-reciprocal phase shifter at each end of the variable field section which is at the centre. Ferrite yokes, external to the variable field section, are used for latching purposes. A disadvantage to this arrangement is that eddy currents are set up in the thin metal wall.

Matching to the rectangular air filled guide at each end of the ferrite section is obtained by means of a two-section stepped ceramic rod in the rectangular guide. Matching bandwidths of 30 percent of the centre frequency have been obtained.

Return loss and insertion loss curves taken on an experimental dual mode reciprocal latching phase shifter are shown in Figs. 2 and 3 respectively.

Some of the insertion loss with frequency is due to the fact that the non-reciprocal circular polarizers vary faster than $1/f$.

In these devices, conductor losses usually exceed magnetic loss by a factor of 2 or 3.

Some important factors to be taken into account with this type of phase shifter are:

- Insertion phase match from a single batch of ferrite is approximately ± 15 °,
- for the least change of insertion phase with temperature use the longest phase state as the reset point,
- switching speed can be increased by a factor of 5 by incorporating a longitudinal slot in the ferrite rod metallized surface. This leads to switching times of about 34 μs.

It has been stated by Boyd [7] that a considerable amount of random phase error can be tolerated at the element level in a two-axis scanned phased array.

At X band the following specifications were considered [7] to be satisfactory.

Frequency bandwidth:	10 percent
Insertion loss:	1.0 *dB* average, 1.2 *dB* maximum over 80 percent of phase states, 1.5 *dB* absolute maximum.
VSWR	1.2:1 typical, 1.5 maximum
Phase shifter range	500 ° nominal
Phase deviation from command	± 5 ° median deviation ± 10 ° over 80 ° of states ± 20 ° maximum
switching time	50 μs cycle time
weight	28 g

The cost of such units assuming they are made in lots of several thousand at a time was estimated in 1974 to be about $11.00 U.S. each.

3.3. Non-reciprocal Ferrite Phase Shifters.

The phase shift in these devices depends on which direction of propagation is followed through the phase shifter. Early non-reciprocal phase shifters used flat slabs of ferrite material with a DC biasing magnetic field [8]. The relatively slow switching speeds of these devices was due largely to the electro-magnets used. Sub-microsecond switching speeds were later achieved by eliminating the need for holding fields by using digital latching phase shifters.

In these designs a wire running through the centre of a ferrite or garnet carries a positive or negative current pulse that magnetizes the ferrite to saturation (See Fig. 4).

The ferrimagnetic toroids of different lengths are placed along the axis of the waveguide separated by dielectric spacers. The length of each ferrite section determines its phase shift. There are two remanent states of magnetization due to a positive or negative pulse and these have different electrical lengths, that for a forward travelling wave latched to one state being the same as that for a backward travelling wave latched to the other.

There is another type of non-reciprocal phase shifter called a flux-drive phase shifter in which only one length of ferrite is used. This length is chosen to be long enough so that is is possible to get a 360 ° phase shift. By using less flux than the amount required for the 360 ° shift, lesser amounts may be obtained. This may be achieved by using a current pulse, from a constant voltage source, through the toroid for a time duration proportional to the desired flux. Since the ferrite must be driven back to saturation before each net setting, twice as many operations are required with this type as with the digital phase shifter.

An interesting low cost foil-wrapped construction technique has been developed for constructing a low cost non-reciprocal latching ferrite phase shifter [10]. In this process, the ferrite toroid is sandwiched between two low-dielectric constant slabs and wrapped in a thin copper foil as shown in Figs. 5a and 5b. A 3-bit phase shifter with lithium-ferrite material has been constructed [10] having a measured loss of 0.4 *dB*. The phase shift stability with frequency is shown in Fig. 6a while the phase shift with temperature is given in Fig. 6b.

3.4. Microstrip Digital Latching Ferrite Phase Shifter.

Whicker and Jones have reported a construction technique using microstrip which is a development from earlier coaxial line technology [8]. The configurations which they have investigated appear in Fig. 7. The differential phase shift VS frequency appears in Fig. 8a for both garnet and ferrite material. Fig. 8b shows the figure of merit VS frequency relation. The figure of merit is defined as the degrees of phase shift per *dB* of loss. At the high end of the band this figure compares well with waveguide types.

The foregoing has described generally the various types of ferrite phase shifters. Next will be described another and different type called PIN diode phase shifters.

4. PIN Diode Phase Shifters.

PIN diodes are best thought of as on-off devices where phase shift is concerned and this leads naturally into the study of PIN diode digital phase shifters. It is in this operating mode that they have proven so far to be most useful.

A forward biased PIN diode can conveniently be made to have a resistance as low as 0.5 ohm. A back biased PIN diode on the other hand has typically a capacitive reactance of about 1K ohm.

These figures of course vary somewhat with the frequency range being considered.

Various case styles are available. One of the main advantages of PIN diodes is their small size and the fact that they can be conveniently integrated into microstrip and strip line geometries. They lend themselves very well to integrated circuit configurations.

In general they may be said to be used in either of two switching modes, that is in series arrangements or in parallel arrangements, each having its own advantages and disadvantages. These qualities depend upon the particular use to which the switch is to be put, that is for

transmitting or receiving, as stand alone units or in multi-couplers, etc.

One drawback often cited is that of resultant intermodulation distortion from two signals mixing in a diode. This is usually the result of the forward resistance which varies slightly as the RF power fluctuates. While the back biased impedance also varies somewhat with power level, causing intermodulation distortion at low frequencies, it has been found that it is almost negligible at frequencies beyond 100 *MHz*. Therefore parallel PIN diodes may be used to advantage where intermodulation distortion is a problem.

One great advantage of PIN diodes is their short switching time which is typically of the order of a few nano seconds. It should not be thought, however, that this is obtained at no cost since to make the best of these devices regarding switching times they must be driven both "on" and "off" by appropriately designed solid-state drivers. In addition they must be supplied (except for light operated diodes) with bias circuits which interfere to some extent with the RF lines and at the best require at least ground planes for return lines.

For the present, however, we will think of them merely as on-off switches and will present some of the ways in which they may be used in the design of phase shifters, either with or without the need for additional ferrite circulators.

4.1. General Diode Phase Shifting Methods.

4.1.1.
Switched Line Phase Shifter.

There are various traditional ways of accomplishing RF phase switching, many of them using PIN diodes [11, 12 & 13]. Probably one of the most obvious ways of using such a switch for phase shifting is the switched line phase shifter of Fig. 9 in which a section of transmission line may be switched in or out of the transmission circuit. One advantage of this circuit (in principle at least) is that it offers true time delay and hence beam steering which is frequency independent.

As mentioned by White [11] this circuit has several advantages and disadvantages which are:

Advantages:

1) equal diode loss in both paths.
2) planar or microstrip construction is possible.
3) compactness, especially for small bits - line lengths give the required phase shift.

Disadvantages:

1) four diodes per bit.
2) complementary diode signals are required for each bit.
3) phase shift is proportional to frequency.
4) smallest bit has the same diode loss as the largest.

It should be noted with regard to disadvantage number two above that since two bias supplies must be added for every switch position some means must be found for separating them. This leads to extra components and weight.

4.1.2.
Hybrid Coupler Phase Shifter.

The use of a 3 *dB* hybrid coupler reduces the number of diodes per bit to two. The action of this type of coupler can be explained by reference to the branch-line coupler method (Fig. 10a) or the rat-race coupler method of (Fig. 10b). A more broadband type, the backward wave coupler is shown in Fig. 10c.

Referring to the branch-line coupler of Fig. 10a, its behaviour can be explained by writing out the wave matrices, but can also be easily understood by examining the phase diagrams of Fig. 11.

In this diagram two cases are considered. In the first, equal in-phase signals are applied at terminals 1 and 2 of the coupler and terminals 3 and 4 are left open. Phase diagrams for the signals first reaching ports 3 and 4 are next shown as are the resultants at terminals 3 and 4. The sketch on the right then shows the result of waves which are reflected back to terminals 1 and 2.

Next is considered the state of the reflected signals to terminals 1 and 2 which would arise when signals of equal amplitude and opposite phase are fed to terminals 1 and 2.

If the signals from these two cases are added together it will amount to having only an input signal to terminal 1. It will be noticed that there is no reflection at this point, all of the energy in fact having travelled to terminal 2. The phase of this transmitted energy can be varied by adding equal lengths of short-circuited line to terminals 3 and 4. Going back to Fig. 10a, the PIN diode provide the short circuits just mentioned.

To explain the action of the circuit of Fig. 10b, first consider the diode section at terminal 2, and the quarter-wave line and diode at terminal 3, to be removed. Under these conditions ports 1 and 4 will be isolated from one another since the two possible signal paths joining them have a phase difference of 180 °. Then a signal from terminal 4 effectively sees a short circuit at terminal 4. Hence an infinite impedance is seen when looking towards terminal 4 from both terminals 2 and 3.

Should line lengths of equal impedance but having a phase difference of 90 ° be added in parallel at terminals 2 and 3, then the reflected waves from these branches would exit from terminal 4 since they are again in phase at that point. None of this reflected energy is reflected back into terminal 1. Fig. 10b shows such a situation, the PIN diodes providing the short circuit. By adding various lengths of line after the PIN diode, various degrees of phase shift may be obtained.

The action of the coupler in Fig. 10c is similar to those just described except that its bandwidth is somewhat greater due to increased coupler bandwidth. In fact couplers of this type have been built which have an octave bandwidth.

4.1.3.
Loaded Line Phase Shifters

While either series or parallel loads may be used with this type of phase shifter we will review only the parallel type here (Fig. 12a).

These phase shifters work on the principle that if two small equal susceptances are spaced a quarter-wavelength apart along a transmission line, their reflections tend to cancel, resulting in a fairly good VSWR. In addition to this, a phase shift is produced which depends on the susceptance value.

The behaviour of this circuit can be understood by referring to Fig. 12b.

We have

$$\begin{bmatrix} V_1 \\ I_1 \end{bmatrix} = \begin{bmatrix} A & B \\ C & D \end{bmatrix} \begin{bmatrix} V_2 \\ -I_2 \end{bmatrix} \tag{1}$$

If there are equal generator and load impedances Z_0, then the power loss ratio P_0 / P_L (where P_0 is the available generator power and P_L is the power delivered to the load) is given by

$$\frac{P_0}{P_L} = 1 + 1/4\left[(A-D)^2 - \left(\frac{B}{Z_0} - Z_0 C\right)^2\right] \tag{2}$$

For the above network:

$$\begin{bmatrix} A & B \\ C & D \end{bmatrix} = \begin{bmatrix} jZ_0Y & jZ_0 \\ j[Z_0Y^2+\frac{1}{Z_0}] & jZ_0Y \end{bmatrix} \tag{3}$$

Thus

$$\frac{P_0}{P_L} = 1+1/4\left[\frac{Y}{Y_0}\right]^4 \tag{4}$$

It can be seen from eqn. (4) that if the normalized susceptance is left reasonably small then the insertion loss may be made negligible.

When used with a matched load, the voltage transfer function a, of such a network is given by

$$a_1 = j(1+Z_0Y) \tag{5}$$

whereas that for a transmission line, a_2 is given by

$$a_2 = \exp(j\theta) \tag{6}$$

where θ is the electrical length of the line

If $\theta=\frac{\pi}{2}+\Delta\theta$ then

$$a_2 \approx j-\Delta\theta \tag{7}$$

$$\text{Now if} \quad Y = \frac{1}{jX} \tag{8}$$

$$\text{then} \quad a_1 = j+\frac{Z_0}{X} \tag{9}$$

It can be seen from eqns. (7) and (9) that if the shunt elements are capacitive (X is negative) then the effective line length will be increased whereas if the shunt elements are inductive (X is positive) then the effective length will be decreased.

If two elements are used at each end, one causing a phase shift of θ_1 and the other of θ_2 as shown in Fig. 12a, and if we switch between these two elements, then the differential phase shift produced will be [eqn. (5)] equal to the normalized susceptance change in one of the switched elements.

In this type of phase shifter the maximum practical limit of phase shift per pair of elements is 45 °.

When not too much phase shift is required, or high power must be used, this type of phase shifter, with loads distributed down the line, becomes most useful. Otherwise one of the coupler types previously described is a better choice.

Phasers made of T or π sections can also be used [11] when more compactness is needed but this is usually not the case for millimetre waves (Fig. 13).

Although variations occur, particularly in broadbanding the coupler, the types mentioned above cover most of the two-diode-per-bit kinds of PIN diode phase shifters.

4.1.4.

One-diode-per-bit reflection phase shifters.

It is possible to use diodes in conjunction with ferrite circulators to cut the number of diodes in half. This is illustrated in Fig. 14.

Here, energy enters the system from the left. The action of the circulators is such that

any energy entering from the left goes down the next port encountered, the bottom one for each circulator of Fig. 14. When this energy from the latter port is reflected back up it travels to the output port and hence down the transmission line to the next circulator.

With this system 2^M phase may be obtained with M diodes and M circulators.

5. Amplitude variation.

As well as varying the phase distribution across an aperture, it is possible by extending the digital phase techniques given previously to employ digitally controlled amplitude distributions as well.

Foldes [15] reports on a multi-beam spacecraft antenna at C-band which used 16 variable phase horns in the beam forming network (BFN) and a binary power divider tree of 15 variable power dividers (VPDs). This is shown schematically in Fig. 15.

The variable power divider circuit shown in Fig. 15 contains two phase shifters and two hybrids. The first hybrid merely splits the power into the two equal parts for passing through the phase shifters. The phase difference then determines the power split from the two arms of the second hybrid.

The circuit is designed such that the power division ratio P_1 / P_2 for the two outputs is

$$\frac{P_1}{P_2} = \frac{(1+\tan\phi)^2}{(1-\tan\phi)^2}$$

and the transfer phase is independent of this ratio. This particular realization employed ferrite phase shifters. One way to realize such a power splitter is shown in Fig. 16.

Here, $V_2 = jV\cos\theta$ and $V_1 = jV\sin\theta$

The impedance of the quarter-wavelength arms of the hybrid is $\sqrt{2}$ times that of the main transmission line.

6. Distortion and Noise in PIN Diodes.

6.1. Noise.

One of the advantages of PIN diodes is their low noise factor. In fact to quote from a Hewlett-Packard [16] application note: "PIN diodes have an equivalent noise temperature of approximately one; that is, they do not generate noise in excess of an equivalent resistor. Situated in the input of a receiver, the noise figure of a PIN diode switch is equal to the insertion loss. This relationship applies at any bias level".

This means of course that the resistance introduced into the circuit by the diodes must be carefully considered since, although a forward resistance of a fraction of an ohm is possible, it must be kept in mind that several diodes appear in series in any particular transmission path. With cryogenic cooling, switches have been constructed with noise temperatures of 9.8 ° K [18].

6.2. Distortion

Harmonics may or may not be a problem with PIN diodes depending on several factors:

a) power level

b) frequency range

c) degree of suppression desired

d) type of application.

When used as a switch, it is quite reasonable to expect the harmonic generation to be at least 40 *dB* down for frequencies above 4 *GHz* and for RF power levels of up to 0.5 watts through the diode. This is for the case when the diode is biased either full on or full off.

Actually, whenever an RF signal is applied to a PIN diode there is some distortion of the signal [17] caused by the variation of the PIN diode impedance during the period of the RF signal. To minimize this effect the PIN diode should be forward biased to as high a current as feasible (which lowers the resistance in the forward bias case) and should be reverse biased at the highest voltage possible [16]. In addition, if the diodes are connected in a back-to-back manner an additional decrease in distortion can be obtained due to cancellation of the effects of the distortion currents.

When all favourable conditions can be met it is sometimes possible to reduce the distortion to a level about 100 *dB* below the desired signal level.

6.3. Temperature Effects

Temperature effects in PIN diode devices can be made negligible when these devices are used simply as switches. Only a small increase in insertion loss will occur under these conditions. The allowable diode temperature depends upon the lifetime expected. Good practice nowadays to prevent burnout is to keep the diode junctions in the 100 °C to 200 °C maximum temperature range [13].

The final temperature of the diode junction depends on the amount of power dissipated, P_D, the ambient temperature, T_{amb}, and the thermal resistance O_{JA} between the diode junction and the ambient temperature [17].

The Unitrode Corporation rates its $T_{\max}$ as 175 °C (which is conservative). They list the formula for the maximum permissibile power dissipation P_D maximum as:

$$P_D\max = T_J\max - \frac{T_{amb}}{\theta_{JA}} \quad \text{watts}$$

It is important to be able to calculate the quantity θ_{JA}. Means are available for doing this. For instance it is common with many diodes to have in the specification a figure for the thermal resistance between the diode junction and one surface of the diode package. It is usually safe to assume a maximum diode package contact operating temperature of 100 °C [17].

For the applications under consideration here, it is felt that power rating will not be a problem.

6.4. Intermodulation Products in PIN diode Switches.

Intermodulation products arise when two or more signals having different frequencies, mix in the same diode switch to produce sum and difference frequencies. This intermodulation will vary depending upon whether the signals are passing through a series diode biased in the forward direction or whether they are passing by a shunt diode which is back biased.

Most of the effort in determining intermodulation effects has concentrated on the forward bias case.

For the situation where we are dealing with a back-biased shunt PIN diode these nonlinear effects can become severe if the RF signal is greater than the back-bias voltage. If this is not the case, however, then very little intermodulation is said to occur for frequencies above 100 *MHz.*

In the forward-bias case, the intermodulation will depend on the forward-bias current, the effects becoming less as the current is increased [19, 20].

Sicotte and Assaly [20] have carried out intermodulation measurements on a PIN diode in the VHF range. In those experiments one set of data was taken holding the power of 1 signal at 33 watts and varying that of the other from 30 *dBm* to 15 *dBm.* Seventh and ninth order products were measured for various input power variations (from one of the sources) and bias levels. In no case was the intermod level worse than -70 *dBm.* Also this worst level always occured at the point where the peak RF voltage level (in the reverse bias case) was such that the total voltage across the diode goes from negative potential to zero volts. When this was

avoided typical intermodulation values were about -100 *dBm*.

Microwave associates show intermod levels for two 10 *dBm* signals to be down at least 70 *dB* in the forward bias situation when the forward bias current is 5 *mA* or more.

7. Examples of PIN Diodes in Phased Arrays.

A few examples will be given here to show how some of the devices described previously have been used in phased arrays.

7.1. 12 *GHz* PIN Phase Shifter for Satellite Phased Array.

Amitay and Glanee [21] have described a 12 *GHz* PIN shifter and driver module for a satellite communication phased array. The unit is TTL compatible. The phasers are of the two-diode compensated branch coupler type described earlier. The layout for a single phase shifter is shown in Fig. 17.

Some of the characteristics of the unit are listed below:

- longest switching time - 8 *ns*
- maximum driving power - 36 *mW* at 1 *MHz* switching
- RF power handling CW - 800 *mW*
- type of PIN diode - HPND4001
- diode forward resistance - 2 *ohms* at 10 *mA*
- reverse diode capacitance - 0.07 *pF* at -30 *V*

Each 4-bit phase shifter contains four individual units of the type shown in Fig. 17. The RF is kept out of the bias driver port by open-circuited quarter-wave transmission line sections incorporated into the microstrip lines.

The four cells in a phase shifter unit can provide 22.5, 45, 90 and 180 ° of phase shifter, thus allowing 16 phase states from 0 ° to 337.5 °.

The driver circuit used in conjunction with PIN diodes is very important if one is to obtain fast switching.

The driver circuit used in this phase shifter, and shown in Fig. 18, employs a complementary arrangement of a p-n-p transistor in conjunction with a n-p-n transistor.

This circuit efficiently drives the PIN diode both on and off. It is especially important that precautions be taken to drive PIN diodes off quickly if fast switching is required. This is so that when turned off the carriers will be quickly discharged.

Fig. 19 shows the schematic of a complete driver board for one 4-bit phase shifter.

8. Cost Considerations

Although several papers are available which describe the techniques to be used for low cost phase shifters few of them have any real cost data presented [22, 23].

Boyd [7] does comment on the cost of manufacturing dual-mode latching ferrite phase shifters. He estimates that a production rate of 1500 units/working day would be practical. In order to amortize the engineering and start-up costs at the level of $1.00/unit it would be necessary to build 500 antennas each containing 2,000 elements. The estimated production cost was about $11.00/phase shifter, making the total cost of phase shifters about $24,000.00/antenna. These costs are in U.S. dollars for the year of 1974.

Lewis [24] has reported on the cost of PIN diode phase shifters for phased arrays. Again the reporting year was 1974 and prices were in U.S. dollars. The projected production cost at that time of a 3-bit PIN diode phase shifter was $13.00. This would make the total cost of a phased array comparable to a mechanically-gimbaled one. In these units the numer of separate blocks was reduced by printing the hybrids, the chokes and the bias blocks. The couplers were quadrature couplers and two diodes were used per coupler for a total of six diodes per 3-bit

phase shifter.

The costs per unit depended on the number of units. The $13.00 figure assumed a production run of 200,000 units. In addition to the recurring cost of $13.00 there was a non-recurring cost mentioned of $7.11 per unit so that we are really talking of a $20.00 figure when all costs are taken into account.

When the number of units drop to only 4000 the total cost per unit rises to $69.00 being comprised of a recurring cost of $51.00 and a non-recurring cost of about $18.00.

The operational characteristics of the phase shifter were as shown below:

- Frequency - 9.5 to 11.0 *GHz*
- Insertion loss - 1.5 *dB* average
- Phase shift - 0 to 360 °in 45 °steps
- Accuracy - 15 °
- VSWR - 1.5
- Peak power - 130 *W* (150 *ms* pulse)
- Average power - 13 *W*
- Weight - 0.3 oz.
- Size - 0.24 x 2.5 x 0.8 inch

9. Future Developments

It is probable, due to the several advantages that would be achieved, that dielectric millimetre-wave integrated circuits will come into their own.

There are two approaches for incorporating active components into dielectric waveguides to-date [1]. In the first method the components are mounted in a small piece of rectangular guide and mode converters are used to translate from the dielectric E_{11} mode to the waveguide TE_{10} mode.

This is the easiest and most straight-forward approach. The second method entails mounting the components directly on the dielectric guide. This approach is the more difficult one because it requires an understanding of dielectric waveguide effects. Nevertheless, it has great advantages from a production point-of-view.

A possible phase shift mechanism for dielectric waveguide can be illustrated by considering Fig. 20. If the metal plate is removed in Fig. 20 then we have remaining a dielectric guide whose dimensions are '2a' by 'b'.

On the other hand if the metal plate is lowered so as to be in contact with the top face of the dielectric then the field distribution in the dielectric will be the same as that in a dielectric guide whose dimensions are '2a' by '2b'. Since the electrical lengths, for a given physical length of guide, are different in these two cases, a phase shifter can, in principle, be constructed by raising or lowering a metal plate over the surface of a dielectric guide [1]. This of course is a mechanical way of producing the phase shift.

It is also possible to replace the metal plate with a dielectric plate to produce similar results. To accomplish this result electronically, a distributed PIN can be attached to the upper surface. Experiments have shown that with this kind of device, a phase shift varying from 0 to 40 °can be obtained when the DC bias is caried from 0 to 12 *ma*.

The RF frequency used was 70 *GHz* [1]. The radiation losses in these experiments were reported to be 3.5 *dB* and although this is poor, the technology shows great promise.

10. Comparisons

A comparison has been given between various ferrite and PIN diode phase shifters. Although there seems to be no clear cut advantage of one over the other for all purposes (Fig. 21), the PIN structures can be incorporated into MIC devices more easily and therefore will probably come into more and more prominence.

11. Present Capabilities for SATCOM EHF Components.

In any project there are usually several approaches which may be taken in arriving at a solution. In the case of the present SATCOM project the earth station/terrestrial link, shipbourne, airbourne, mobile and satellite links, may be accomplished through a cohesion of discrete components or through the utilization of hybrid circuits. OFF-the shelf hybridized components have usually resulted from the demand to consolidate several recursive discrete component arrangements into a single package. In the K and Q bands, development has been rather limited especially above 18 *GHz*, since there has been relatively little demand in this part of the spectrum. As crowding continues at the lower frequencies < 18 *GHz*, it will become necessary to expand into the higher frequencies. Since this demand is only just starting, there are only a limited number of microwave manufacturers currently geared for production in the bands of interest in this SATCOM project. Hybridization is almost non-existant and there are a limited number of discrete components available. Some of the discrete components which are available are tabulated in Table 1.

The limited number of manufacturers represented is the result of an extensive search. The majority of microwave component manufacturers currently limit their production to 18 *GHz* or below where the demand until recently has been solely located. Discussions held with the New England Microwave Corp., with regards to the limitation of 18 *GHz* on their PIN diode switches and phase shifters indicated that their capability would be increased to 50 *GHz* shortly, depending on the time required for the development of GaAs PIN diodes. The current limitation of PIN diode switches and phase shifters to 18 *GHz* is due to the noise added by the Si PIN diode at higher frequencies, although the Si PIN diodes themselves are useable there.

The capabilities of present waveguide technology with respect to elbows, tees, etc. well exceeds the requirements for SATCOM. Waveguide manufacturers in general are all capable of producing waveguide related components and are not listed exhaustively, in Table 1, due to this fact. Areas where limitations do exist are in related structures and co-axial components. In general, waveguide component are more predominant than co-axial components, although co-axial components lend themselves to hybridization more so than do waveguide ones. Although circuits can be reduced in size through hybridization, the wire bonding which is required tends to keep the cost per circuit high. Discrete devices such as mixers, etc. occupy too large an expanse and are excessively expensive, almost all costing more than $100.00 (1982 dollars) each. In both these schemes the logic is separate from the circuit elements.

The question arises as to whether the components tabulated as well as others not mentioned, could be fabricated on a single chip, thus eliminating the need for wire bonding.

Until recently a major drawback to GaAs fabrication was the rejection rate due to non-uniformity of dopant levels across the wafer and the extra cost associated with rigid process control. A news brief [27] presented in Microwaves, November 1981 indicates that Microwave Associates has developed a process whereby devices can be grown in one continuous flow, without the examination steps that were previously required. This is accomplished by the use of computer control of the process. As a result, the system produces layer thicknesses that are uniform to within ± 5 percent over wafers that are 4 cm^2 or greater. As a result of this development, repeatable, large-scale economical GaAs devices are possible. GaAs however is not the only medium for device fabrication. SoS (silicon on sapphire) has captured attention as has InP (indium phosphide). Gallagher [26] has reviewed the importance of InP as a material for EHF semi-conductors. The main results of the article are summarized below.

InP may be the most important material in the near millimetre range spanning 90-900

Table 1: Available Components from Manufacturers.

values in GHz

		Hughes Aircraft Co. Electron Dynamics Division	Thomson-CSF Ltd.	Narda Microwave	Plessey-Optoelectronics and Microwave Ltd.	Premier Microwave Corp.	EEV: English Electric Valve	Maury Microwave Corp.	Aertech Industries	Aerospace Comm. Device	Aercom Industries Inc.	Electromagnetic Science Inc.	Microwave Associates
AMPLIFIERS:	GaAs FET			2-18	1-10					→ 12.4	→ 18		
	Gunn diode	26.5-110									11.26		
	Impatt diode	26.5-110									→ 18		
	Tunnel diode									4-18	4.26		
ANTENNA:	horn	26.5-220	18-140	1-40									
Coax	fixed			DC-18									
	digital PIN												
	variable PIN			.2-18									
ATTENUATORS:	fixed	26.5-110	18-140	8.2-18									
Waveguide	variable												
	variable ferrite	18-220											
CIRCULATORS:	MIC												
	waveguide	26.5-140					3-34						3-95
	coax						1-18					.3-26	→ 12.5
COUPLERS:	waveguide	26-170	18-140	8-18					1-40	7-18 30-37			
	coax			.1-26			.2-12			1-20			
FILTERS:	coax						.1-10						→ 12.5
	waveguide	26-220	18-50										3-40
	diplexers						.1-10						
ISOLATORS:	coax						1-10					.3-26	→ 12
	waveguide	18-220					2-55			2-40			3-95
KLYSTRONS:								.5-18 30-36					
MAGNETRONS:								1-96					
MIXERS:	waveguide	18-220											
	coax									1-18			
MODULATORS:	waveguide	18-220											3-26
OSCILLATORS:	backward wave tube		67-310					2.5-11.5					
	gunn	18-95	6-40	6-18	5-50								
	crystal												
	solid state									.5-12			
	electrical tunable												
	cavity												
	Impatt.	26-110	6-40		40-140								
	VIG												

Table 1: Available Components from Manufacturers cont'd.

values in GHz

		Hughes Aircraft Co. Electron Dynamics Division	Thomson-CSF Ltd.	Narda Microwave	Plessley - Optoelectronics and Microwave Ltd.	Premier Microwave Corp.	EEV: English Electric Valve	Maury Microwave Corp.	Aertech Industries	Aerospace Comm. Device	Aercom Industries Inc.	Electromagnetic Science Inc.	Microwave Associates
PHASE SHIFTER:	digital PIN												
	ferrite	26-110										3-45	
	analogue PIN												
	varactor												
POWER DIVIDER:	MIC				.5-40								
	waveguide	18-110											
	coax				.5-40						.5-18		
ROTARY JOINTS:							- 18						
SWITCHES:	PIN	26-110			.2-18						2-18		
	transmitt-receive tube							-10 30-35					
	ferrite											3-95	
	waveguide											3-95	
	coax												
	manual waveguide	26-220	27-140									3-60	
TRAVELLING WAVE TUBES:								2-18					
TRANSMITT-RECEIVE TUBES:								-10 30-35					
WAVEGUIDE:	rectangular		18-140				- 325		1-40				
	TEE	18-110	18-140				7-18		1-40				
	taper	18-220	8-140						2-22				
	twists	18-220	18-140						1-40				
	elbows	18-220	18-140						1-40				
	custom												

GHz. In many respects InP is similar to GaAs. Both can be used to design the same types of solid state device such as gunn diodes, impatt diodes and FETs, but with performance differences. Even though existing devices fabricated from silicon (Si) and GaAs can meet system requirements through 60 *GHz*, it is expected that InP might provide performance enhancement within this region as well. InP gunnoscillators will provide higher power than GaAs alternatives through 100 *GHz* and InP diode oscillators are 2-3 times more efficient and have higher peak power capabilities than do GaAs sources. Also, the efficiency of InP impatts is expected to exceed both GaAs and Si up to the region of 90 *GHz*.

Discussions held with the Electron Device Group of Varian indicate that development of InP products has proven to be very successful. Custom products have been manufactured and prototype amplifiers already exist in the 20-44 *GHz* range.

As previously mentioned, it may be desirable to hybridize or manufacture monolithic microwave circuits to further aid in cost reduction and miniturization. The desire to hybridize or process monolithic microwave circuits arises when the function to be performed is identically repeatable. In various scenarios described to implement the uplink/downlink, beam forming arrays consisting of several elements are used in which each element must be controlled separately. Since each element may require control of amplitude and phase, and since these elements may exceed 2000 in number, it is desireable to fabricate these functions in monolithic form. A review of the status of monolithic microwave circuits has been given by Pucel [25]. The main results of this article follow:

The utility of monolithic microwave circuits depends on the availability of a suitable low loss substrate.

Both gallium-arsenide (GaAs), and silicon on sapphire (SoS), are contenders with the former having the edge at present. The carrier mobility of GaAs is about six times that of silicon, making it possible to operate GaAs MESFETS at higher frequencies and powers than silicon MESFETS.

11.1. Numbers of circuits per chip.

With the assumption that lumped components have a linear dimension of approximately a tenth of a material wavelength ($\lambda_g/10$) and that distributed components have a linear dimension of about a quarter wavelength, an estimate can be made of the number of circuits which can be contained per cm^2 of wafer area.

It is possible to produce square GaAs wafers having sides of 5 cm. With the above estimate for circuit size, we could have about 500 circuits per wafer at 20 *GHz* and about 1000 circuits per wafer at 40 *GHz*.

The above illustrates the large potential for packing the various necessary planar passive circuits such as directional couplers, phase shifting lines, meander line inductors, edge coupled capacitors, etc.

In fact much more than this is possible, in particular the incorporation of active circuits based on FET-GaAs technology.

To completely eliminate the need for internal wire bonding on the wafer, two main difficulties must be overcome, one of them due to the desirability of using microstrip construction techniques (both microstrip and coplanar waveguide strip may be used).

The first arises from the need to device low inductance short circuits. This may be achieved by a Via hole process whereby a hole is first etched through the substrate and then plated through. This process results in an inductance of about 50 pH/mm of substrate thickness. Alternatively, with microstrip, a wrap-around ground may be used.

The second difficulty is due to the necessity of having some lines cross over others. One example of this is in the use of spiral inductors where the centre point must cross to the outer edge. The solution here is the use of air bridges in which air bridge interconnecting busses are formed by depositing straps over one or more conductors. The air gap between the strap and

the conductors has a typical dimension of 4 μm.

With the advent of the techniques mentioned, it is possible to incorporate virtually all of the passive and active components in monolithic microwave circuits.

It should be noted that while all the examples given by Pucel [25] had an upper frequency of about 12 *GHz*, this does not seem to be a fundamental constraint. There are however some fundamental limits to size (and hence cost) and component values that one must take into account and these are not peculiar to the use of GaAs.

Regarding the wafer thickness, one would like to keep the wafer thin in order to minimize cost, and to increase the thermal capabilities. On the other hand one would like a thick wafer in order to have lower propagation losses and lower microstrip line tolerances, as well as to minimize the excitation of surface waves.

At a frequency of 30 *GHz*, a thickness of 0.15 mm would be suitable for power amplifiers while 0.6 mm would suffice for low noise amplifiers.

Some typical component values are:

- line width (for microstrip) - 5 μm or $\lambda/8$
- line impedance - 10 to 100 ohms for microstrip
15 - 25 to 125 ohms for coplanar waveguide
- capacitor values - matching 0.1 pf at Q = 50
15 - bi-pass 10-30 pf at Q = 50 - 100
- inductors - 0.5 to 10 nH at Q = 50
- resistors - metal film (various values).

The technology just described seems ideally suited for the production of large numbers of identical circuits such as those used on phased arrays. It overcomes the wire bonding problem inherent in a hybrid approach.

The article by Pucel [25] just described does not mention nor compare the characteristics of InP. The carrier mobility of InP is four times that of Si. There are also subtle advantages of InP in terms of FET design since InP FET's possesses larger dimensions for a given frequency than do GaAs FETS. Even though this implies a reduced chip count per area, a submicron gate for GaAs would be lengthened to a micron gate in InP allowing for easier masking. In terms of FET design, InP is expected to exceed GaAs in both gain and noise even though noise figures of 3.5 *dB* at 18 *GHz* in GaAs material have been achieved by manufacturers like Plessey.

11.2. Microwave Semi-conductors.

Again, as with passive components, there are several manufacturers of microwave semi-conductors. Table 2 summarizes some of these manufacturers and the semi-conductors they manufacture. The list is not exhaustive but illustrates that there are several manufacturers from which devices can be chosen. An attempt has been made to define the bounds within which the varioius semi-conductors can be used. Most microwave equipment manufacturers are also microwave component manufacturers and produce devices for their in-house applications as well as for external sales. As a result, most semi-conductors manufactured do not exceed the 18 *GHz* limit mentioned earlier.

Gunn diodes and impatt diodes form the exception to the 18 *GHz* limit for most microwave semi-conductor manufacturers. It is likely that as the demand for the 18-50 *GHz* region increases, the manufacturers will follow. The advent of GaAs PIN diodes and InP FET amplifiers is an indication of industries commitment towards this spectrum.

Table 2: Microwave semiconductors.

		Frequency Sources GHz Division	NEC Microwave Semi-conductors	Parametric Industries, Inc.	Plessley Optoelectronics & Microwave	MA	
Barrier Mixer	Si		26			X	upper freq. GHz
	GaAs					X	"
schottky	Si						"
schottky	GaAs						"
Fast Switching							
FET	GaAs		.1-15		to 18		useful freq.
	InP						"
Gunn diode	Si						operating freq. GHz
	GaAs	4-24	6-60		4-50	X	operating freq. GHz
	InP						"
Impatt	Si		6-99		40-140	X	freq. GHz
	GaAs					X	"
	InP						"
PIN	Si	.35-2.5	.8-2.5	.25-1		X	series resistance
	GaAs						"
Varactor	Si	1-11	X	X		X	useful freq. GHz
	GaAs	4-31	X	X		X	useful freq. GHz
schottky	Si						"
schottky	GaAs				X		"
harmonic	Si	.15-18		.15-25			useful freq. GHz
harmonic	GaAs						"
harmonic step recovery		60-150		75-350			transit time pS
multiplier	Si		X	X			"
parametric amp	Si			165			cut-off freq.
parametric amp	GaAs	200-750	400-600	150-550		X	cut-off freq. GHz

11.3. Dielectrics

There are several ways to fabricate a microwave system. The system may be constructed from discrete waveguide or co-axial components connected together via the use of waveguide or coax cable. Alternatively, hybrid or microwave monolithic structures may be incorporated into the design. These components usually utilize a dielectric medium. The system itself need not be interconnected via coax or waveguide if it is built on a dielectric substrate, since the substrate itself may be used as the guiding medium. Corporate feeds, power dividers and digital phase shifters are among the components which may be constructed on a microwave dielectric substrate. The decision as to the relative amount of dielectric, microwave monolithics, hybrids, and discrete components is based on a space/weight/cost analysis. Microwave dielectrics therefore constitute an important phase of the component search. A few of the companies which provide microwave dielectric material are listed below:

1) Circuits Systems Group, Rogers Corporation: Duroid
2) Oak Material Group Inc., Laminates Division
3) Millis Corporation
4) 3M
5) Keene Corporation, Chase-Foster Division: Di-Clad
6) Polyflon Corporation, Subsidiary of Resistoflex Corp., a UMC Industries Company.
7) Electronized Chemical Corporation
8) Tek-Wave Incorporated: MIC manufacturer.

Manufacturers and Canadian Representatives.

Manufacturer	Representative
Aercom Industries Inc., Aerospace Communication Device 405 Tasman Drive Sunnyvale, CA. 94086 (408) 744-1320	
Aertech Industries 825 Stewart Drive Sunnyvale, CA. 94086 (408) 732-0880 (800) 538-4406	E.G. Lomas 945 Richmond Road Ottawa, Ontario. K2B 8B9 (613) 725-2177
Circuit Systems Group Rogers Corporation Box 700 Chandler, AZ 85244 (602) 963-4584	
Electromagnetic Sciences Inc., 125 Technology Park/Atlanta Norcross, Georgia. 30092 (404) 448-5770	Datron Canada Ltd., 5150 Dundas Street West Toronto, Ontario. M9A IC3 (416) 239-3025

Manufacturer	Representative
Electronized Chemical Corporation South Bedford Street Burlington, Massacheusett 01803 (617) 272-2850	
English Electric Valve Company Ltd., Waterhouse Lane Chelmford, Essex. CM12QU United Kingdom	EEV Canada Ltd., 67 Westmore Drive Rexdale, Ontario. M9V 3Y6 (416) 745-9494
Frequency Sources Inc., GHz Division 16 Maple Road Chelmsford, MA. 01824 (617) 256-8101	RF Microwave Ltd., 6595 Mackle Road Suite 704 Montreal, P.Q. H4W 2Y1 (514) 489-8213
Hughes Aircraft Co., Electron Dynamics Division 3100 West Lomita Boulevard P.O. Box 2999 Torrance, CA. 90509 (213) 517-6400	Giga-Tron Associates Ltd., 7 Slack Road Suite 205 Ottawa, Ontario. K2G OB7 (613) 225-4090
Keene Corporation Chase Foster Division P.O. Box 308 Bear, Delaware 19701 (302) 834-2100	

Manufacturer	Representative
3M Dielectric Material & System Division Saint Paul, Minnesota. 55101	
Maury Microwave Corporation 8610 Helms Avenue Cucamonga, CA. 91730 (714) 9878-4715	RF Microwave Ltd., 6595 Mackle Road Suite 704 Montreal, P.Q. H4W 2Y1 (514) 489-8213
Microwave Associates South Avenue Burlington, MA. 01803	MA Electronics Canada Ltd., 3135 Universal Drive Mississauga, Ontario. L4X 2E7 (416) 625-4605
Millis Corporation Millis, MA. (617) 376-2611	
Norda Microwave 75 Commercial Street Plainview, N.Y. 11803 (516) 433-9000	Electronetic Systems Ltd., 6420 Victoria Avenue Suite 6 Montreal, P.Q. H3W 2S7 (514) 342-4112
NEC Microwave Semiconductor Japan	California Eastern Laboratories Inc. 3005 Democracy Way Santa Clara, CA. 95050 (408) 988-3500
Oak Material Group Incorporated Lominates Division Franklin, NH 03235 (603) 934-5736	
Parametric Industries Inc., 742 Main Street Winchester, MA. 01890 (617) 729-7333	

Manufacturer	Representative
Plessey Optoelectronics and Microwave Ltd., Wood Burcote Way, Towcester Northamptonshire, NN12 7JN United Kingdom (0327) 51871	GEC Canada Ltd., 766 King Street West Toronto, Ontario. (416) 364-9281
Polyflon Corporation Subsidiary of Resistoflex Corporation 35 River Street New Rochelle, N.Y. 10801 (914) 636-7222	
Premier Microwave Corporation 33 New Broad Street Port Chester, New York. 10573 (914) 939-8900	
Tek-Wave Incorporated 3 Deleware Drive New Hyde Park, N.Y. 11040 (516) 328-0100	
Thomson CSF Division Tubes Electroniques 38, rue Vauthier BP 305 92102 Boulogne-Billonconrt Cedex FRANCE	Thomson-CSF Canada Ltd., 350 Sparks Street Suite 701 Ottawa, Ontario. (613) 236-3628
Varian Electron Device Group Solid State Microwave Division 3251 Olcott Street Santa Clara, CA. 95050 (408) 988-1331	Varian Canada Ltd., 1355 Carling Avenue Ottawa, Ontario. (613) 728-4643

References.

1. K.J. Butler and J.C. Wiltse, "Infrared and millimeter waves." Vol. 4, Millimetre Systems, Academic Press, 1981.
2. V.P. Nanda, *IEEE Trans. Microwave Theory and Tech.*, Vol. MTT-24, pp. 876-879, 1976.
3. J.F. White, "Diode Phase Shifters for Array Antennas." *IEEE Trans. on Microwave Theory and Tech.*, Vol. MTT-22, No. 6, pp. 658-674, June 1974.
4. L.R. Whicker and C.R. Boyd, Jr., "A new reciprocal phaser for use at millimeter wavelengths." *IEEE Trans. on Microwave Theory and Tech.*, Vol. MTT-19, pp. 944-945, December 1977.
5. R.C. Hansen, "Microwave Scanning Antennas." Vol. III, Academic Press, 19XX.
6. L.R. Whicker and D.M. Bolle, "Annotated Literature Survey of Microwave Ferrite Control Components and Materials for 1968-1974." *IEEE Trans. on Microwave Theory and Tech.*, Vol. MTT-23, No. 11, pp. 908-918, November 1975.
7. C.R. Boyd, Jr., "Comments on the Design and Manufacture of Dual-Mode Reciprocal Latching Ferrite Phase Shifters." *IEEE Trans. on Microwave Theory and Tech.*, Vol. MTT-22, No. 6, pp. 593-601, 1974.
8. L.R. Whicker and R.R. Jones, "A Digital Latching Ferrite Strip Transmission Line Phase Shifter." *IEEE Trans. on Microwave Theory and Tech.*, Vol. MTT-13, No. 6, pp. 781-784, November 1965.
9. T.C. Cheston, "Phased Arrays for Radars." *IEEE Spectrum,* pp. 102-111, November 1968.
10. D.A. Charlton, "A Low-Cost Construction Technique for Garnet and Lithium-Ferrite Phase Shifters."
11. J.F. White, "Diode Phase Shifters for Array Antennas." *IEEE Trans. on Microwave Theory and Tech.*, Vol. MTT-22, No. 6, pp. 658-674, June 1974.
12. J.F. White, "Semiconductor Control." Artech House, Inc., 1977.
13. R.V. Garver, "Microwave Diode Control Devices." Artech House, Inc., 1978.
14. F. Ananasso, "Null-Steering Uses Digital Weighting." *Microwave Systems News*, Vol. 11, No. 7, pp. 78-94, July 1981.
15. P. Foldes, "Control Aspects of Multibeam or Multielement Spacecraft Antennas." General Electric Co., Space Division, Valley Forge Centre, Philadelphia, PA. 19101.
16. Hewlett-Packard Company, "Selection and use of Microwave Diode Switches and Limiters." Application Note, AN-932, 19XX.
17. "PIN Diode Designers Handbook and Catalogue." Unitrode Corporation, Book PD-500B, 1981.
18. G.H. Behrens, Jr., "Cryogenically Cooled C-Band PIN Diode Integrated Switch Matrix for Radio Astronomy Applications." *IEEE Trans. on Microwave Theory and Tech.*, Vol. MTT-26, No. 9, pp. 629-635, September 1978.
19. Microwave Associates, Inc., "Microwave Semiconductors for Mobile Communications." November 1979.
20. R.L. Sicotte, R.N. Assaly, "Intermodulation Products Generated by a PIN Diode Switch." *Proc. IEEE*, pp. 74-75, January 1968.
21. N. Amitay and B. Glace, "Switching Performance of a 12 GHz p-i-n phase Shifter/Driver Module for Satellite Communication Phased Array." *IEEE Trans. on Communications*, Vol. 29, No. 1, January 1981.

22. R.W. Burns, R.L. Holden and R.Tang, "Low Cost Design Techniques for Semiconductor Phase Shifters." *IEEE Trans. on Microwave Theory and Tech.*, Vol. MTT-22, No. 6, June 1974.

23. D.A. Charlton, "A Low-Cost Construction Technique for Garnet and Lithium-Ferrite Phase." *IEEE Trans. on Microwave Theory and Tech.*, Vol. MTT-22, No. 6, June 1974.

24. D.J. Lewis, "Inexpensive Phasers Slash Array Costs." *Microwaves,* September 1974.

25. R.A. Pacel, "Design Considerations for Monolithic Microwave Circuits." *IEEE Trans. on Microwave Theory and Tech.*, Vol. MTT-29, No. 6, pp. 513-534, June 1981.

26. J.J. Gallagher, "InP: A Promising Material for EHF Semiconductor." *Microwaves,* Vol. 21, No. 2, pp. 77-84, February 1982.

27. W.J. Bojsza, "MA Reveals Process Details to Audience of Competitors." *Microwaves*, Vol. 20, No. 12, pp. 13-15, November 1981.

28. R.J. Mailloux, "Phased Array Theory and Technology." *Proc. IEEE*, Vol. 70, No. 3, pp. 246-291, March 1982.

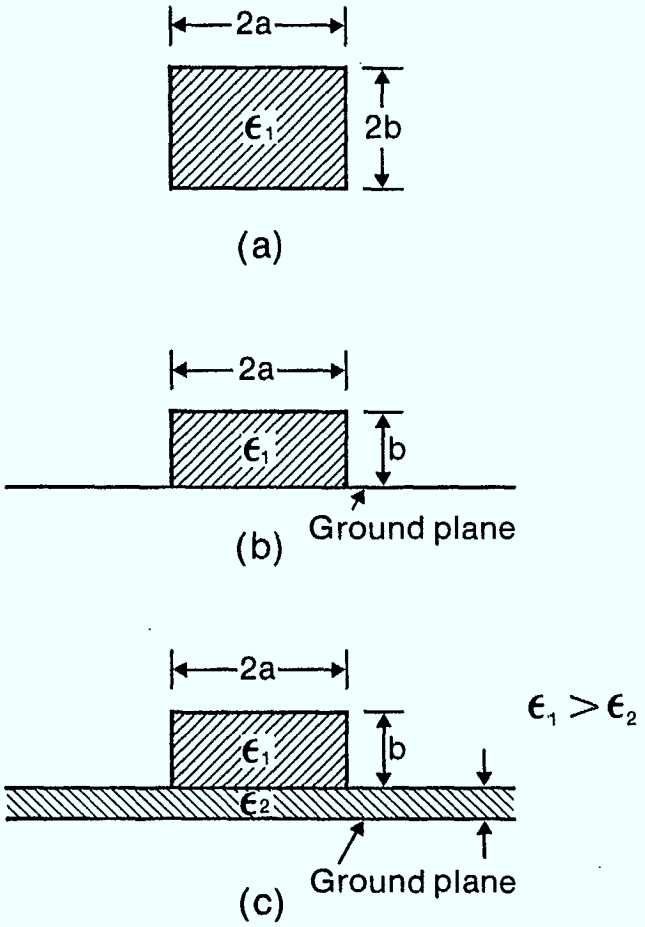

Fig. 1 Cross sections of typical dielectric waveguides for millimeter-wave integrated circuits, (a) rod guide, (b) image guide, (c) insulated image guide.

(From Ref. 1)

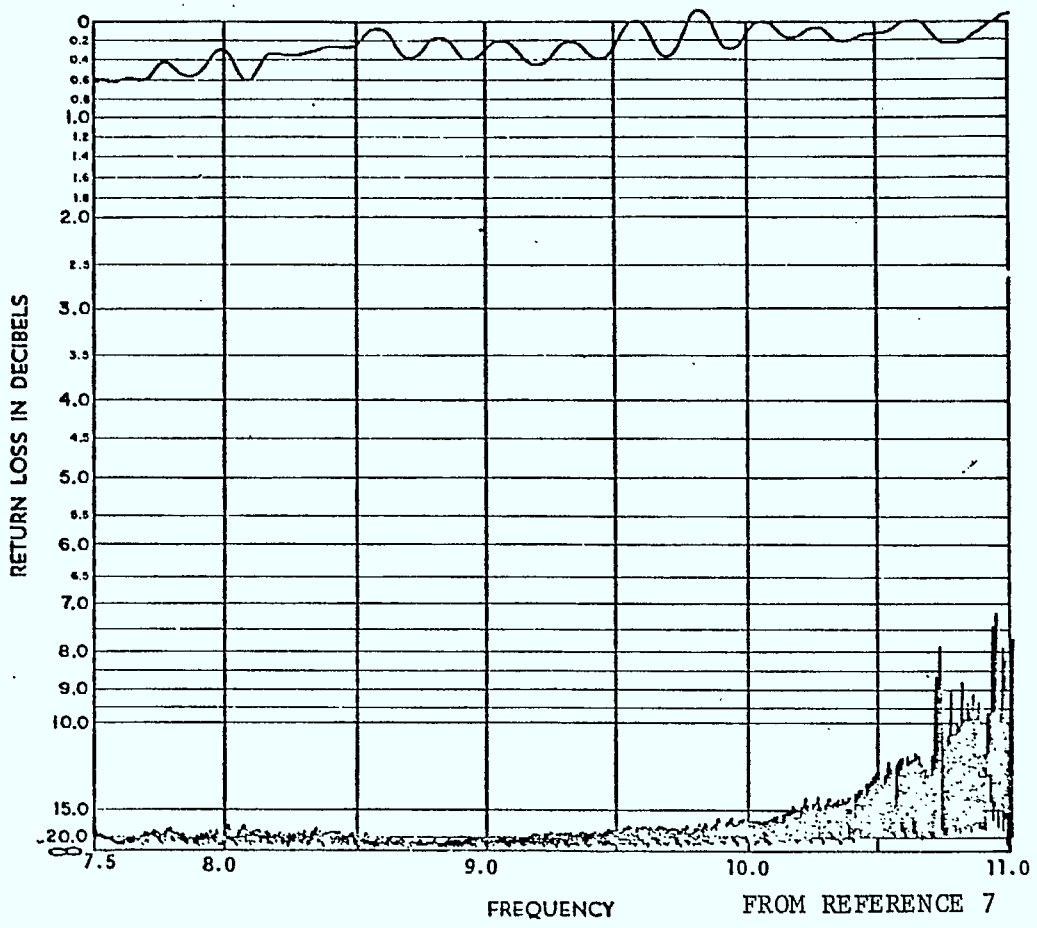

Fig. 2. Return loss trace for a dual-mode phase shifter with broad-band matching.

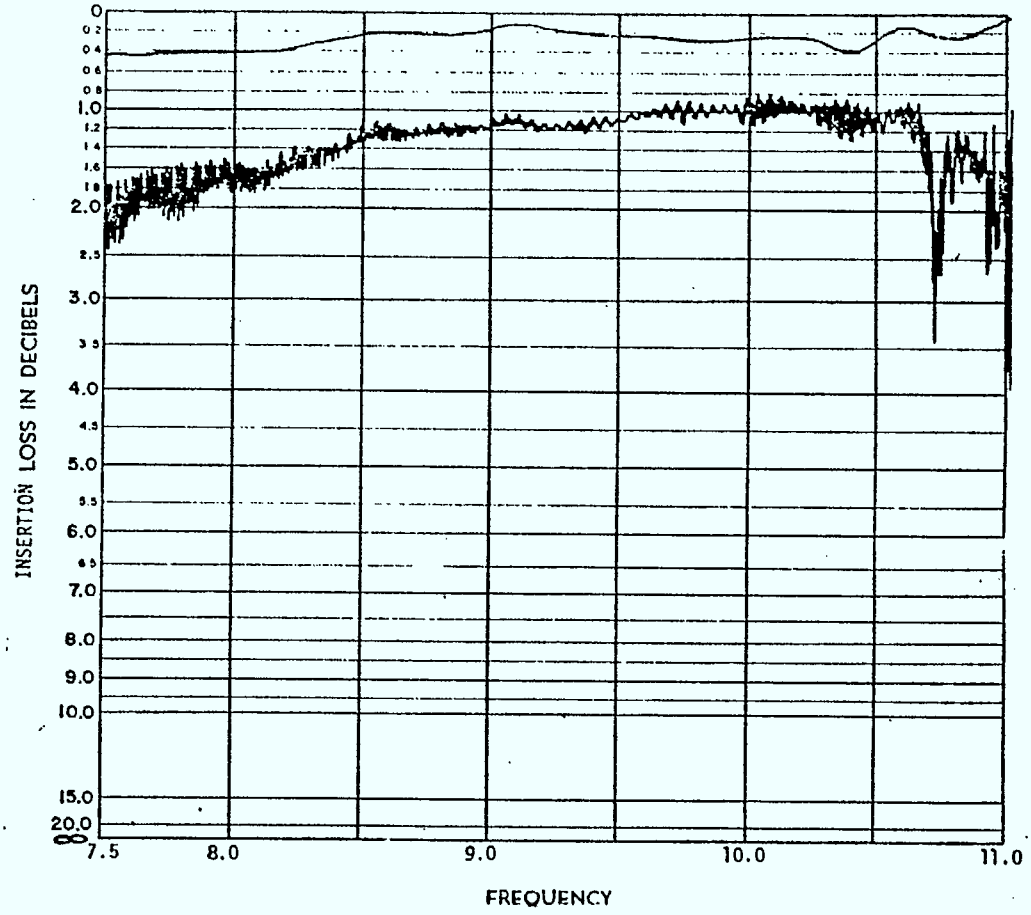

Fig. 3. Insertion loss trace for same phase shifter as in Fig. 2.

FROM REFERENCE 7

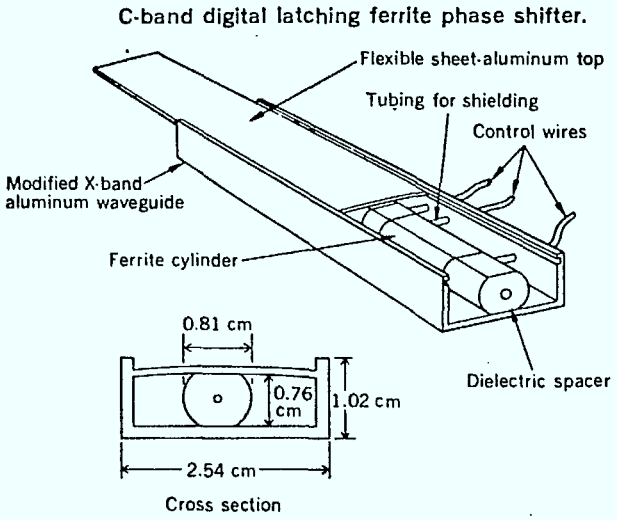

Figure 4 (from ref. 9)

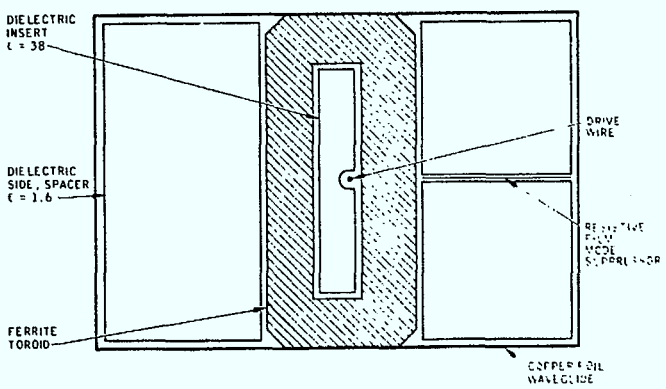

Phase-shifter cross section.

Figure 5 a (from ref. 10)

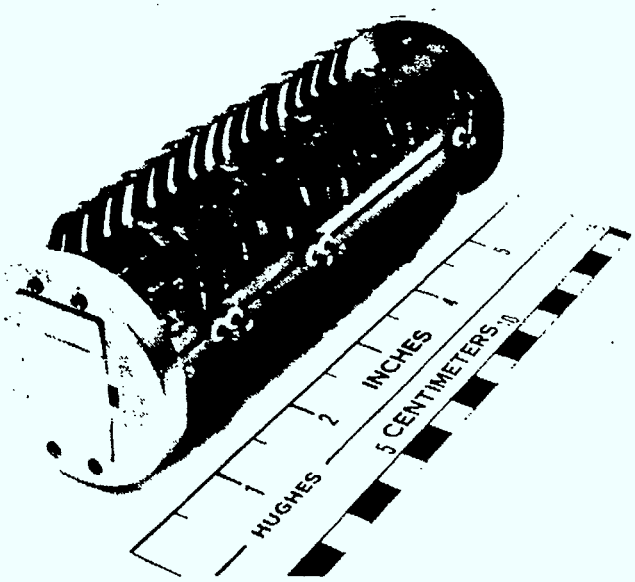

3-bit foil-wrapped phase shifter.

Figure 5 b (from ref. 10)

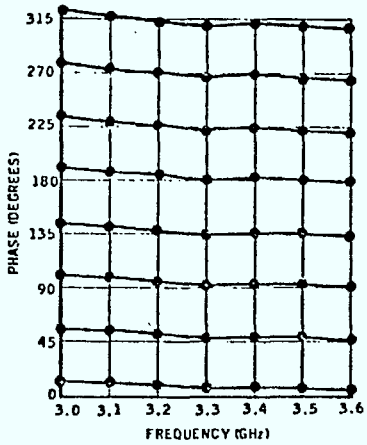

3-bit lithium-ferrite phase shifter. Phase versus frequency.

Figure 6 a (from ref. 10)

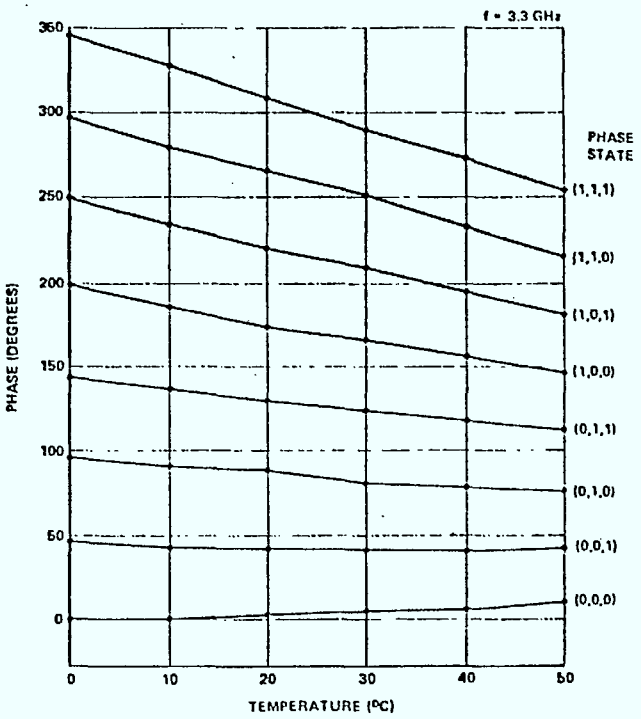

Lithium-ferrite phase shifter. Phase versus temperature with digital drive (the 0,0,0, phase state represents the insertion phase).

Figure 6 b (from ref.10)

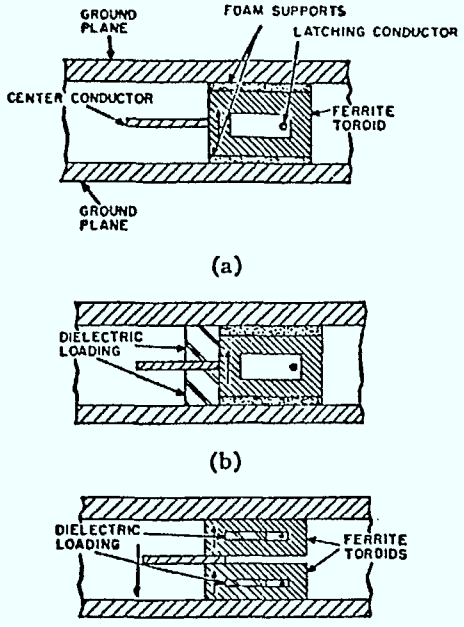

Configurations which have been investigated.

Figure 7 (from ref. 8)

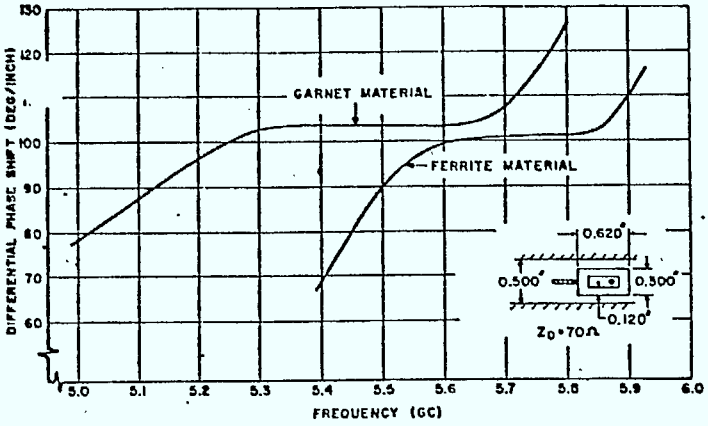

Measured phase-shift data for one toroid configuration.

Figure 8 a (from ref. 8)

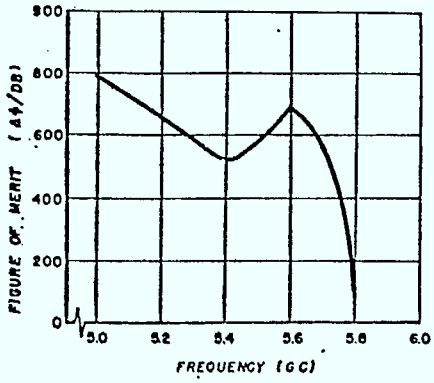

Figure of merit data for one toroid model.

Figure 8 b

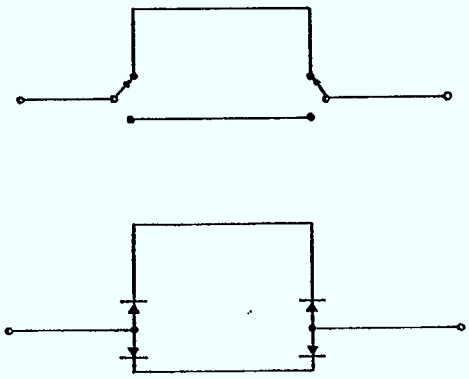

Schematic for switched delay line phase shifter.

Figure 9 (from ref. 3)

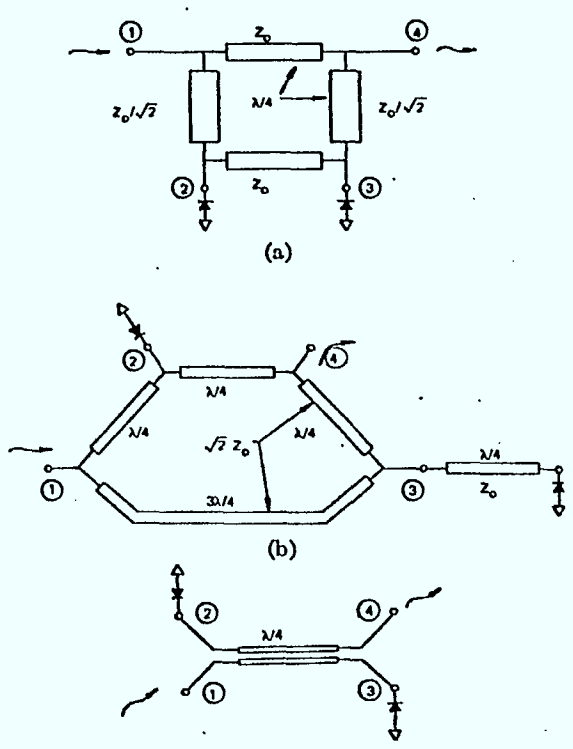

Methods of achieving hybrid coupler properties. (a) Branch line hybrid phase-shifter bit. (b) Rat race bit. (c) Backward-wave coupler bit.

Figure 10 (from ref. 3)

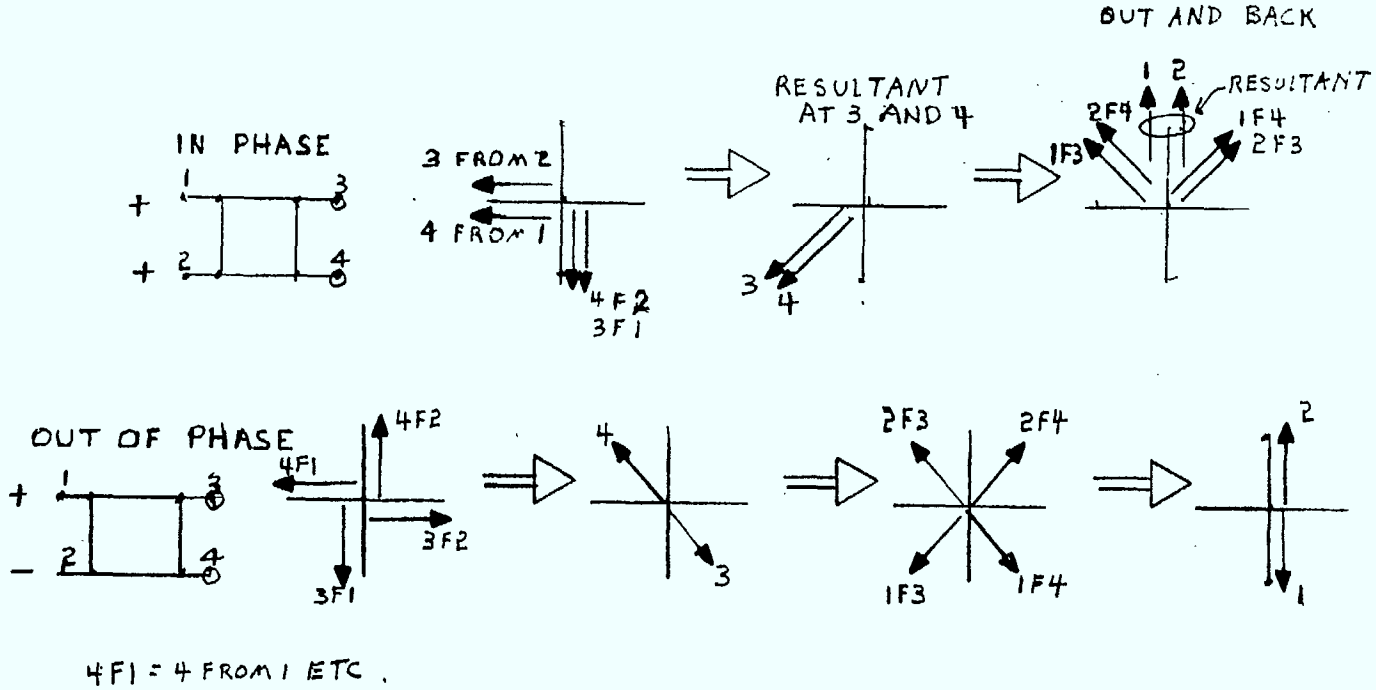

Figure 11.

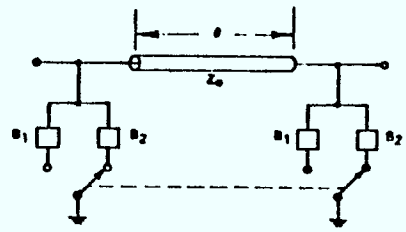

$\Delta\phi = Z_o (B_2 - B_1)$

$Z_o' = Z_o / [1 - (BZ_o)^2 + 2B \cot \theta]^{1/2}$

VSWR $< (Z_o'/Z_o)^2$ or $(Z_o/Z_o')^2$, whichever exceeds 1.

$\theta_{1,2}' = \theta + Z_o B_{1,2}$

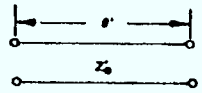

UNIFORM LINE EQUIVALENT

(from ref. 3)

Loaded line phase shifter

Fig. 12 a

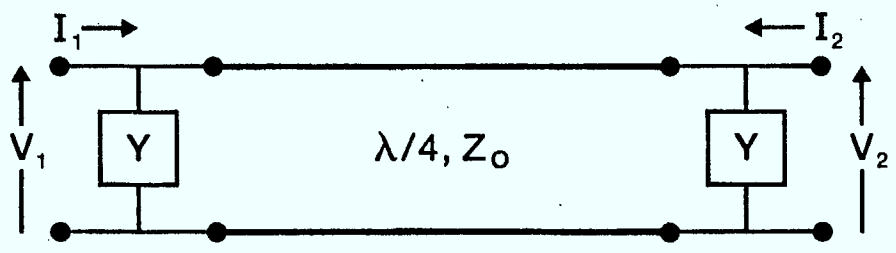

Fig. 12b

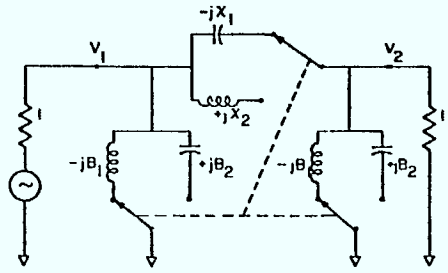

MATCHED TRANSMISSION (IF) $X = \frac{2B}{1+B^2}$

(THEN) TRANSFER PHASE = $\arg(V_1/V_2) = \tan^{-1}\left(\frac{X}{1-BX}\right)$

Three-element π phase-shifter circuit (after Garver

Figure 13 (from ref. 3)

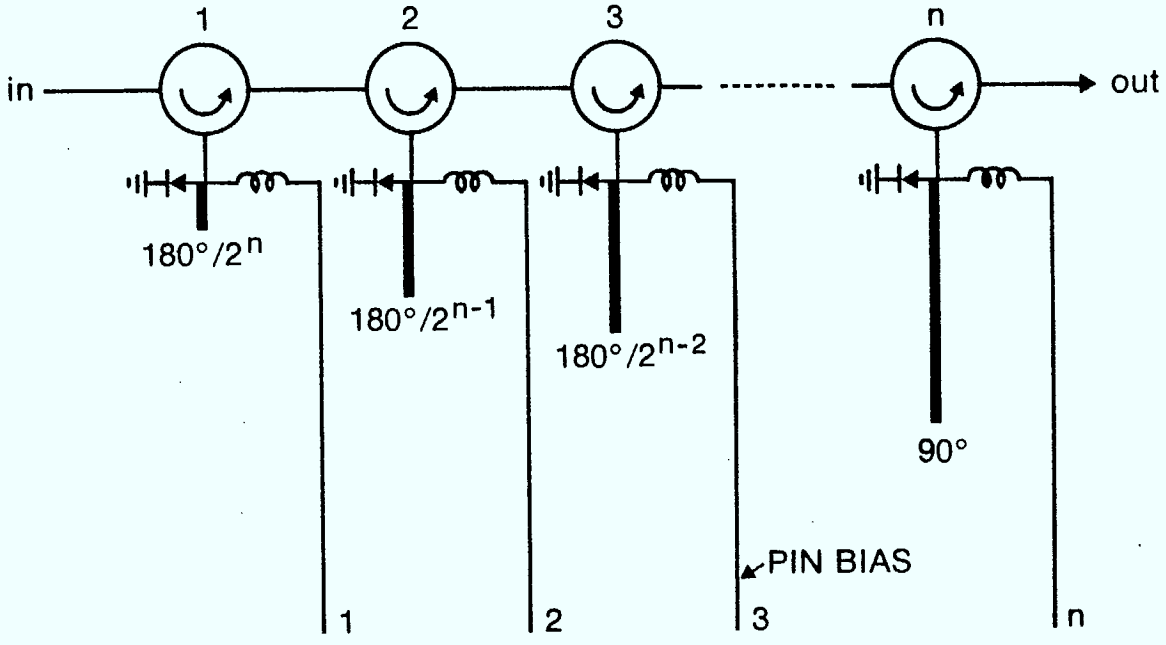

Figure 14 Reflection Phase Shifter

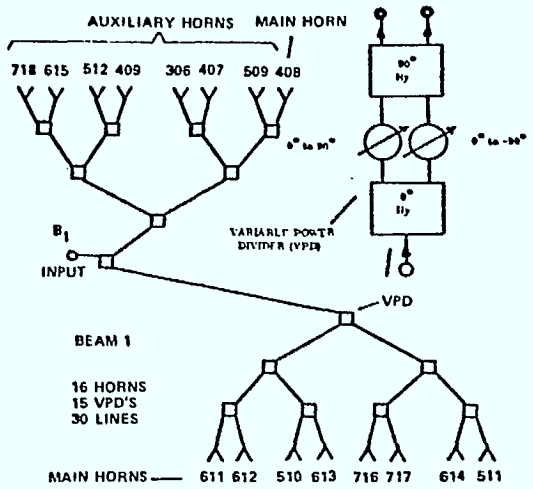

- Layout of beamforming network

Figure 15 (from ref. 15)

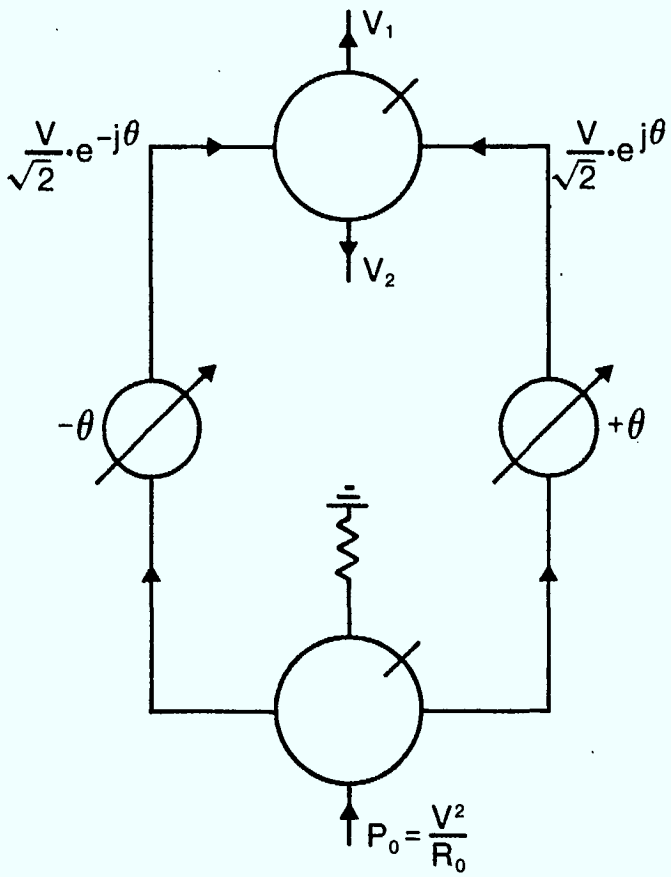

Figure 16 Power splitter

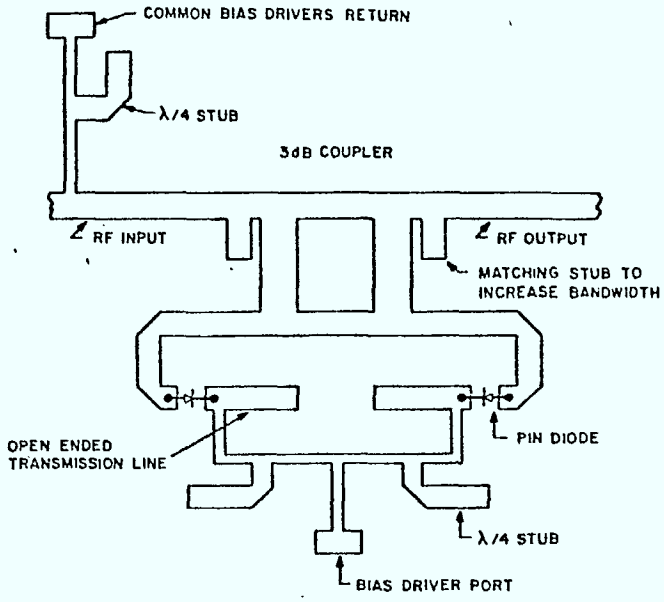

Schematic description of an individual phase shifter cell depicting p-i-n diodes, 3 dB coupler, and biasing circuit.

Figure 17 (from ref 21)

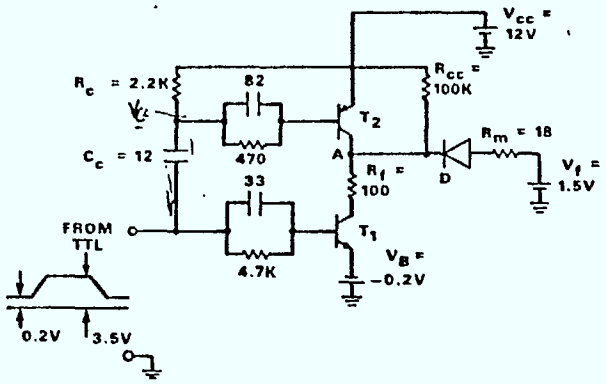

Schematic diagram of an individual bit driver. T_1–HP35824A; T_2–2N4261.

Figure 18

(from ref. 21)

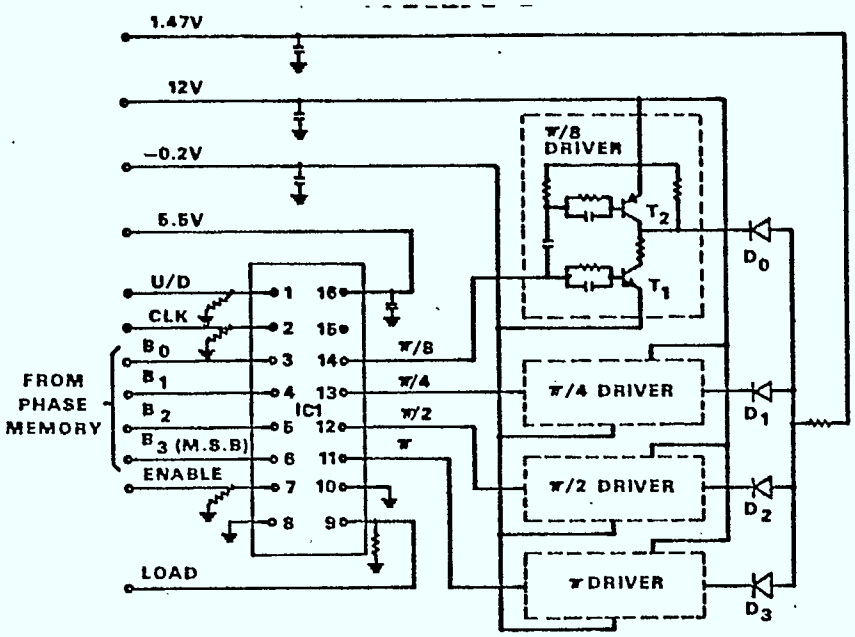

Schematic diagram of the driver circuit board. T_1–HP35824A; T_2–2N4261; IC1–SN74LS669W.

Figure 19 (from ref. 21)

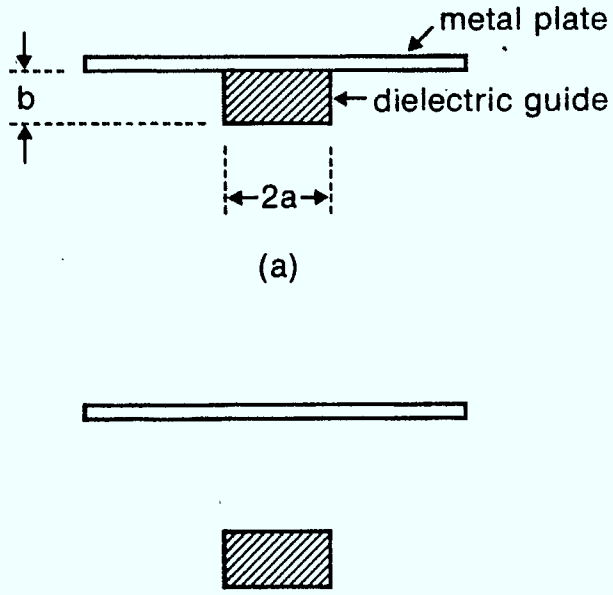

Figure 20

A Comparison of Diode, Ferrite, and Electromechanical Switches.

CHARACTERISTIC	DIODE SWITCHES	FERRITE SWITCHES	ELECTROMECHANICAL SWITCHES
Switching speed	Nanoseconds	Microseconds (low field) Milliseconds (high field)	Milliseconds
Insertion loss	Higher	Low	Low
Isolation	Typ to 80 dB	Typ 20 dB (low field) Typ 60 dB (high field)	Typ 60 dB
Can be used for analog applications	Yes	Yes	No
Lifetime (cycles)	Unlimited	Unlimited	Several million cycles for best quality switches
Size & weight	Least	Greater	Greater
Ability to withstand severe environment	Best	Temperature sensitive	Temperature, vibration, and shock sensitive
Bandwidth	Octaves to multi-decades	Octaves or less	Dc to 18 GHz

figure 21.

(from ref. 16)

Chapter 9

SAMPLE DESIGN: A CONTROLLED-BEAM REFLECTOR ANTENNA SYSTEM WITH HYBRID STEERING.

S. Dmitrevsky and J.L. Yen

In this Chapter we illustrate some of the previous discussions by carrying out a conceptual design of a space segment controlled-beam reflector antenna system with hybrid steering. The basic specifications are taken from the EHF transponder for the proposed Canadian Military Communication Satellite System [1]. The field of view is to be 4 °× 10 °. The downlink is to be at 20 *GHz* with antenna gain of 42 *dB*. The uplink is to be at 44 *GHz* with antenna gain of 48 *dB*. Small amount of electrical beam steering for correction of space vehicle attitude variations is required. The uplink should have capability of nulling a small number of jammers. Fast convergence is necessary for TDMA beam hopping. A dual antenna configuration using reflectors is selected, one for uplink one for downlink. The uplink antenna is a phased-array in either a Y or a centre filled pentagon configuration while the downlink is multi-beam antenna with staggered beams. Hybrid steering in both directions is required for the uplink but only in one direction for the downlink. A recursive sample matrix inversion algorithm with deweighting is proposed for its high convergence. Hybrid analog digital implementation is to be used.

Downlink Antenna.

For a system with given antenna gain and a given number of controlled feed elements Eqn. 2b and 7b of Chapter 3 can be used to determine the scan range. In the case of the multiple beam downlink system the scan range $\alpha\ \beta$ is given as

$$\alpha\ \beta = 5.6N/G$$

Assuming the value of G to be 42 *dB* and that of N to be 7 the scan range $\alpha\beta$ is 4 °× 2 °. Should the scan range be increased to 4 °× 10 ° rectangle the only means thereto is mechanical scanning. Proposed below is a possible realization of a hybrid system of this type.

The first problem that will be considered is the arrangement of the individual feed elements in the feed array. As has been mentioned earlier, the pattern of the centres of the feed elements is the image of the centers of the beams on the target.

Due to the necessary overlap of the beams to assure complete coverage of the scan range there occurs unavoidable spillover of feed beams illuminating the reflector. The need for dense distribution of feed elements, limiting the size of their apertures vanishes if mechanical steering is to be employed, allowing for an increase of the feed element apertures necessary to eliminate the spillover. A possible beam pattern and feed configuration is shown in Fig. 1. A one dimensional rotation of the feed by ±3.25 °will completely cover the scan area of slightly more than 4 °× 10 °.

An important parameter of a reflector antenna system is the ratio of focal length to diameter, f/D. For scan range of 10 ° the ratio must be not less than 2 if coma is to be smaller than the diffraction pattern of the aperture. In the system to be considered below the value chosen for f/D was 2.5. For 42 *dB* gain of 20 *GHz* signal the necessary reflector diameter is from Fig. 4 (Chapter 3), 60 cm. Under these conditions the distance between the reflector and the feed is 1.5 m, which may increase the overall dimension of the system to an undesirable extent.

This may be eliminated by the use of a small planar secondary reflector which may also be employed as a moving element to produce an effective motion of virtual feed, the real feed itself remaining stationary. A sketch of a configuration of this type is shown in Fig. 2. The overall dimensions of the system are approximately 120 cm x 90 cm.

Uplink Antenna.

A similar configuration can be employed for the 44 *GHz* uplink antenna operating in the phased array mode with modifications as listed below. The scan for the desirable gain of 48 *dB* and seven element array is 1.7 °×1.7 ° with the consequence that 4 °×10 ° target will require two dimensional rotation in the range 2.3 °×8.3 ° of the planar secondary reflector. Another difference in the configuration will be the replacement of the feed array of the multiple beam system by a more complicated system consisting of a secondary paraboloid reflector illuminated by a phased array. Fig. 3 shows a system of this type with the diameter D of the main reflector of 50 cm and 125 cm (2.5 D) focal length. The focal length of the secondary reflector shown in one fifth of that of the main reflector rendering the diameter of the feed array 10 cm.

The presence of mechanical scanning elements in the antenna system precludes the use of a signle antenna for real time communication between two earth terminals. Two alternatives are possible if two antennas are to be employed. If the reversal of traffic direction can tolerate delays necessary for re-alignment of mechanical steering elements, the system may employ two single frequency antennas, one for the 44 *GHz* uplink and the other for the 20 *GHz* downlink. Should this not be the case the link will require the use of two antenna systems each operating at 20 and 44 *GHz* with mechanical steering elements.

The design of the uplink controlled-beam phased array begins with the selection of an array configuration. Next to be considered is the prior constraints on beam control. Finally, the control algorithm and implementation are selected. These considerations are discussed separately in the following. Since this is only a conceptual design, no quantitative performance measures are attempted.

Phased Array Configuration.

The uplink adaptive antenna is to be a phased array of between four to seven elements, each illuminating a portion of a single main reflector covering a circular aperture. Beam steering is combined with null steering. The selection of the array configuration is based upon main reflector aperture efficiency, quiescent array pattern which governs signal separation, and baseline distribution which determines scenario analysis. Two simple configurations are considered, a ring with or without a center element. As shown in Fig. 4 the fraction of total aperture illuminated by the elements varies amongst the arrays. The main aperture efficiency, also shown in the Figure becomes small when the element number becomes large. Thinned arrays as discussed in [2] are therefore unsuitable for use with a single main reflector.

The signal separation capability of an array depends to a certain extent on its quiescent pattern. However, it is unclear whether low sidelobe levels or a small main beam is more important. If one considers the case with which sidelobes can be cancelled in adaptive arrays, it may be that for a given number of elements the small main beam criterion lending itself to higher nulling resolution should be used. This conditions was emphasized by Mayhan [2]. This would favour thinned configurations with low main aperture efficiency.

The scenario analysis of an array depends on the baseline configuration as discussed in Chapter 6. Increase in the number of nonredundant baselines implies that more information on scenario is available, hence finer details can be analyzed. Fig. 5 shows the baseline distributions of the arrays of Fig. 4. The fraction of baselines that are nonredundant is included in the figure. Half of the configurations on regular lattices have the most redundant baselines, while the other half have completely nonredundant baselines. The significance of nonredundant baselines on the performance of beam-control, in particular in the presence of thermal noise is not yet understood. Intuitively, one would favour higher capability for scenario analysis if thermal noise does not adversely degrade the behaviour.

Based upon these considerations we emphasize small main beam and redundant baselines and select the four-element array and the six-element pentagonal array as candidates for the present design. The final decision is to be based on the number of jammers to be cancelled. The higher performance system is the six-element pentagon.

Prior Constraints.

Since the antenna employs hybrid steering, information on the desired direction is assumed to be available. In addition, the system is to use spread spectrum with known codes. These two constraints need to be introduced together. How this is to be done is not clear at this time. Detailed mode of operation is required before a proper design can be made. This problem appears not to have been fully investigated. Regardless of how the two constraints are to be applied, fast acquisition for TDMA is necessary. Since referencing using spread spectrum can only be made when the code is acquired, it may be necessary to introduce an additional short code to enable fast slewing for alignment of incoming signal code and local code in the reference loop. Detailed study of acquisition time in the presence of jamming and thermal noise needs also to be undertaken.

Algorithm and Implementation.

The system is to operate in non-stationary environments exemplified by TDMA and blinking jammers. This means the algorithm must have fast convergence. The simple but slow LMS algorithm cannot be used. Among the methods of accelerated convergence based on sample matrix inversion the recursive matrix inversion scheme using exponential deweighting [3] appears to be most suitable for the present application. Using the algorithm on an N-element array, instead iof requiring N^3 operations for sample matrix inversion the optimal weight vector can be obtained using $2N^2$ multiplications for each scenario snap shot. Convergence is often attained within N snap shots. The deweighting of old data is introduced to account for blinking jammers.

The recursive matrix inversion scheme cannot be readily implemented using analog devices. It is therefore necessary to digitize the signal to evaluate the coherence matrix in digital form. LSI fast multiplier chips are necessary to achieve high convergence speed. For an 8-bit multiplier operating at 50 ns the time rquired for convergence is about 6.4 μs for a four-element array and about 22 μs for a six-element array. A possible implementation is to use analog correlators for the measurement of coherence matrix, digital matrix inversion and analog weights.

Conclusions.

The above conceptual design of a controlled-beam reflector antenna system with hybrid steering shows what can be readily achieved and means to do it. Based upon this, detailed quantitative analysis can be carried out and simulations can be performed to arrive at the performance specifications of the system.

References.

1. J.L. Pearce and E.B. Felstead, "Canadian Military Communication Satellite System." Vol. 1 - Concept, Communications Research Centre, May 1981.

2. J.T. Mayhan, "Thinned array configurations for use with satellite based adaptive antennas." *IEEE Trans. on Antennas Propagat.*, Vol. AP-28, pp. 846-856, November 1980.

3. J.E. Hudson, "Sidelobe cancellation using recursive Newton-Raphson and Kalman algorithm." Adaptive Antenna Workshop, Mulrem 1979.

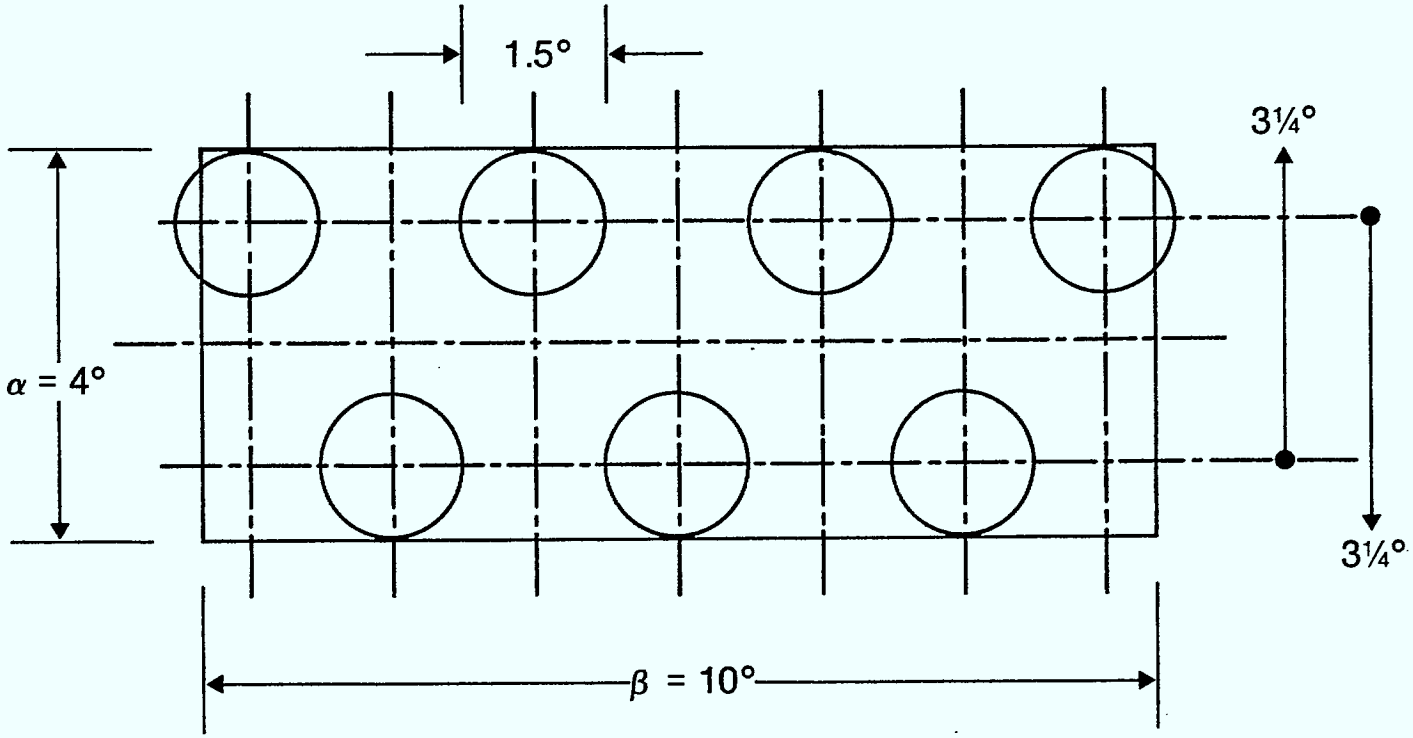

Fig. 1 Pattern configuration in a 7 beam array

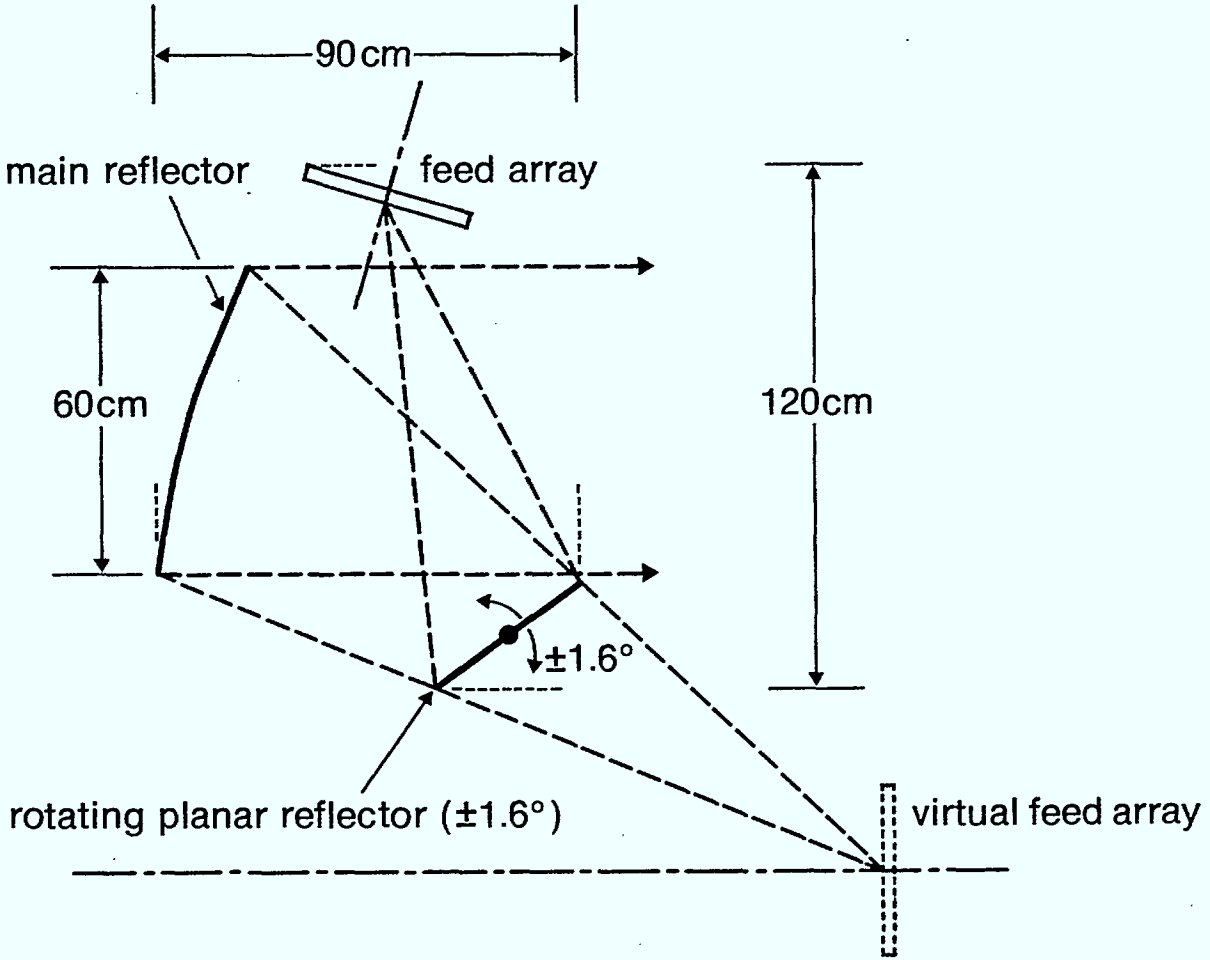

Fig. 2 Offset feed configuration with rotating secondary reflector

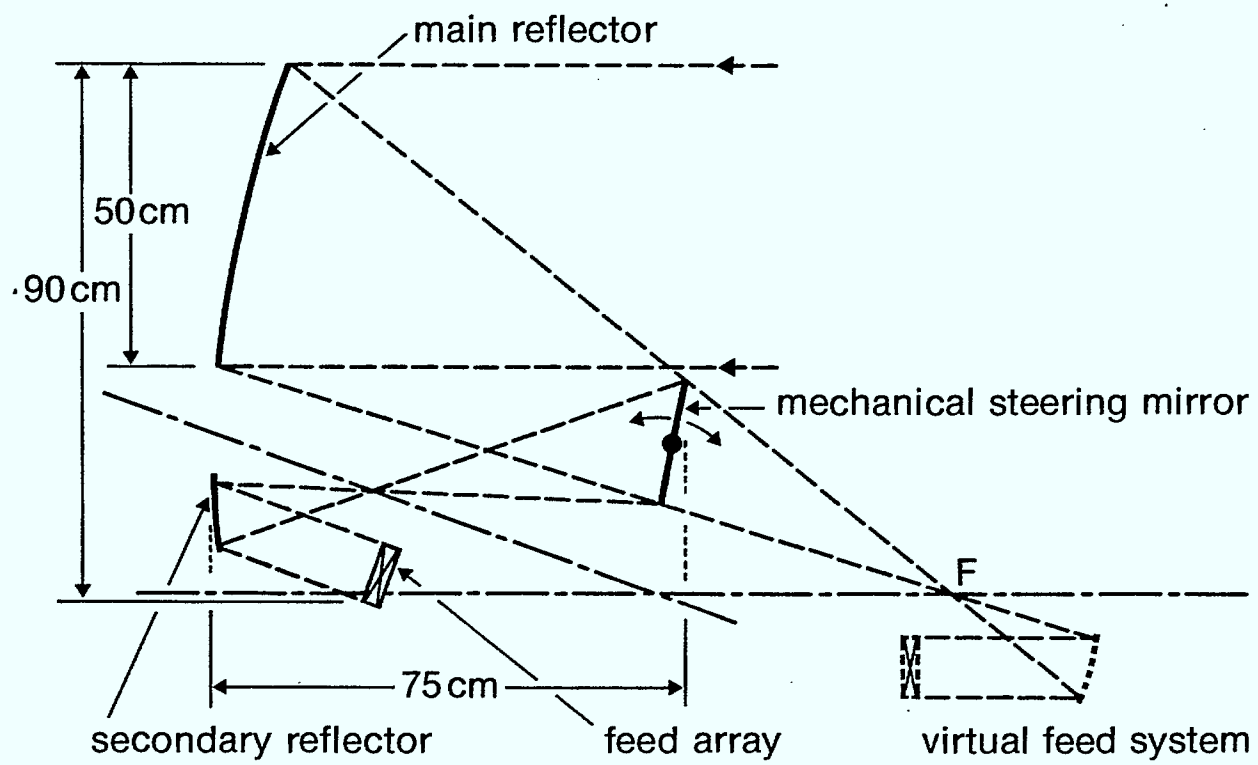

Fig. 3 Phased array antenna system
(magnification ratio of feed optics -5:1)

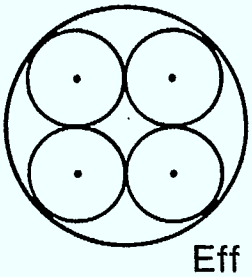

Eff = .69

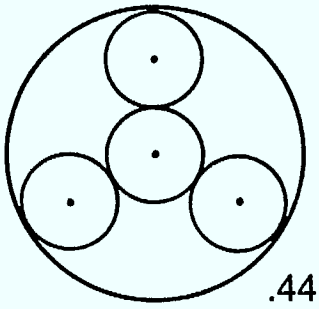

.44

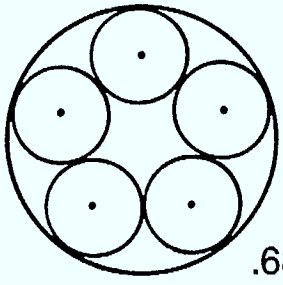

.68

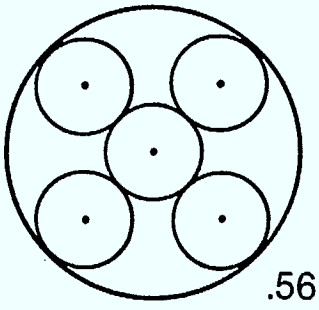

.56

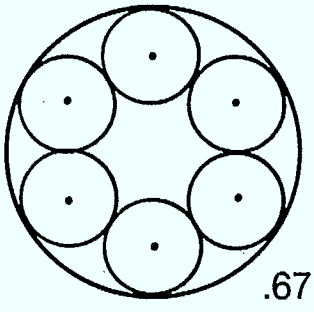

.67

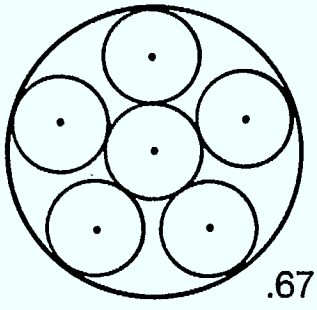

.67

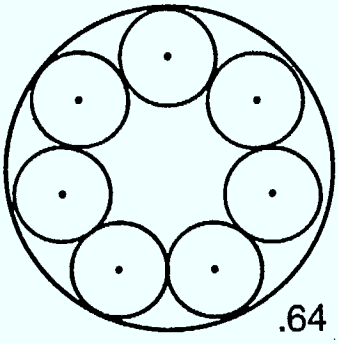

.64

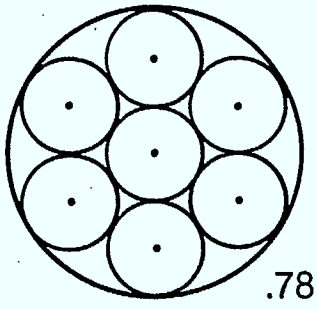

.78

Fig. 4

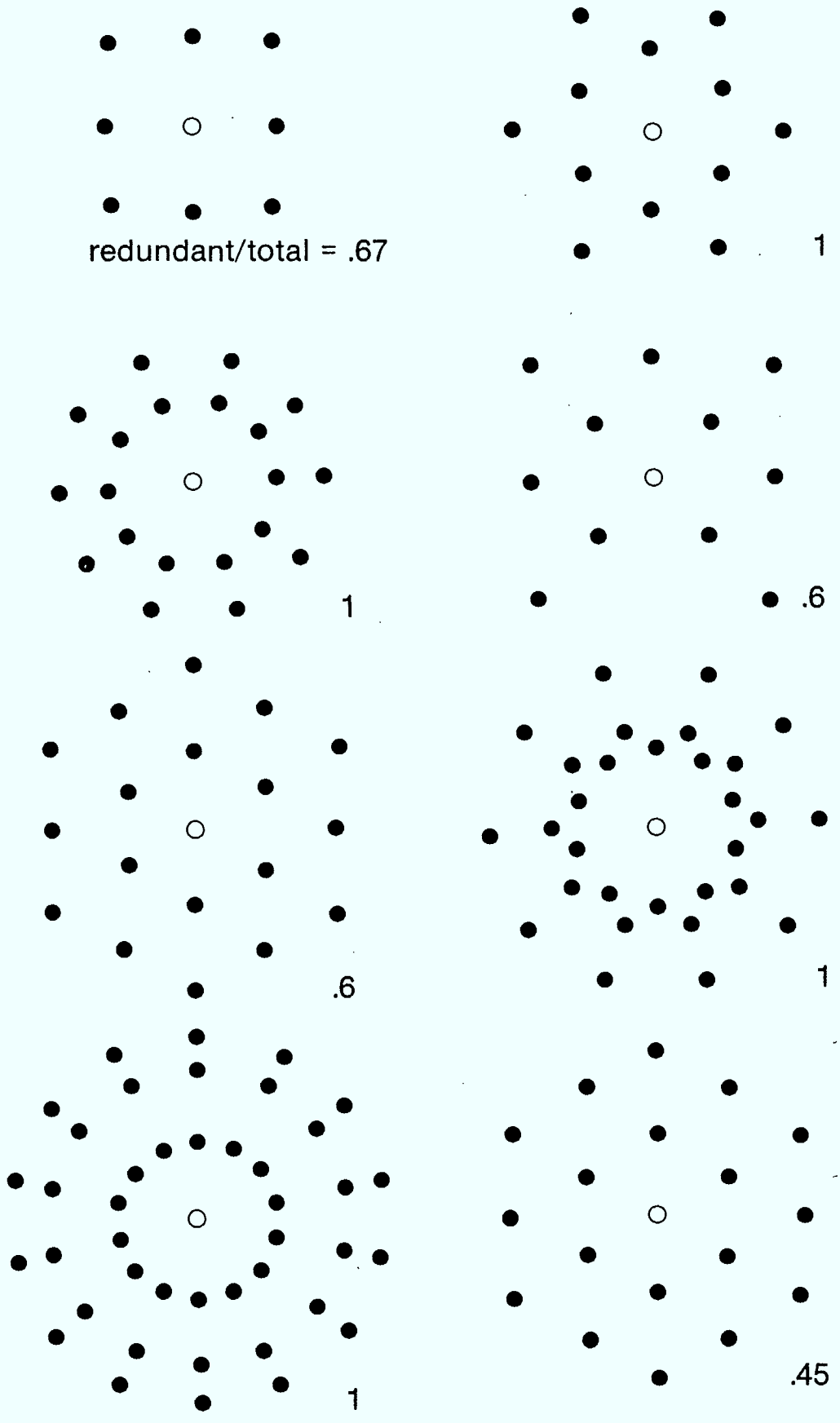

Fig. 5

Chapter 10

RECOMMENDATIONS

From the study of the antenna classes it is evident that reflector antennas are most suitable for the space segment because of easy implementation, light-weight and reasonable versatility. Lens antennas are heavier but appear to have superior multi-beam performance, hence are also promising. Microstrip arrays and reflector arrays appear to be limited by the number of elements, hence cannot be used as the principal antenna in the space segment. They are likely to be used in the ground segment. The following is a list of specific recommendations on promising technologies for detailed investigation and development.

(i) It is recommended that analytical, numerical and experimental investigations on zoned dielectric lens antennas and reflector antennas be carried out. Special attention should be focused on feed systems for large beam scanning angles. Both multi-beam and phased arrays need be considered.

(ii) Single antenna two-frequency system needs to be studied in relation to traffic requirements. Attention on diplexer, intermediate reflectors and feed arrays for wide scan range need be stressed.

(iii) The reflector array antenna shows promise for ground segment applications. Investigations of their theoretical analysis, maximum array cell size, mutual impedance between cells and array elements should be carried out with emphasis on efficiency and costs.

(iv) It is recommended that laboratory simulations of electrostatic charging of dielectric lenses by energetic electrons and ions be carried out in order to evaluate whether or not arc discharges occur and are strong enough to constitute a threat to space systems. Threats to control diodes by discharges on nearby thermal blanket materials or other insulators will have to be assessed.

(v) The effects of array configuration on signal separation and scenario analysis need be investigated analytically by simulation. Possible combinations of sub-arrays to factorize scenario analysis into smaller dimensions leading to reductions in computing burden should be investigated. Optimal hybrid analog-digital implementation using state of art space qualified components needs to be studied.

(vi) Efforts should be made to obtain hard data on costs, delivery and performance of necessary switches and phase shifters. A few of these should be experimentally evaluated.

(vii) In all studies attention should be directed towards optimization methods and trade-offs with respect to performance, cost, weight, power consumption and realiability.

YEN, J.L.

Study of EHF controlled-beam antennas for SATCOM